CHARACTERIZATION OF A TRANSCRIPTIONAL ATTENUATOR IN THE *RPMF-PLSX-FAB* OPERON OF *ESCHERICHIA COLI* K-12

by

Steven P. Solow

Dissertation submitted to the Faculty of the
Virginia Polytechnic Institute and State University
in partial fulfullment of the requirements for the degree of

DOCTOR OF PHILOSOPHY
in
Biochemistry

APPROVED:

_____
Timothy J. Larson, Chairman

_____ _____
Jiann-Shin Chen Dennis R. Dean

_____ _____
Eugene M. Gregory William E. Newton

April 7, 1997
Blacksburg, VA

Keywords:

Escherichia coli, attenuator, fatty acids, phospholipids, s.i.t.k.γ, transcription

CHARACTERIZATION OF A TRANSCRIPTIONAL ATTENUATOR IN THE *RPMF-PLSX-FAB* OPERON OF *ESCHERICHIA COLI* K-12

by
Steven P. Solow
Timothy J. Larson, Chairman
Biochemistry

(ABSTRACT)

Fatty acids are an essential component of the phospholipids of the inner and outer membranes of *Escherichia coli.* The synthesis of both fatty acids and phospholipids is regulated. Synthesis increases when growth rate increases, is inhibited when starvation occurs, and the fatty acid composition of the membrane changes with growth temperature. Several genes encoding enzymes involved in membrane synthesis are located in the *rpmF-plsX-fab* operon. In this operon, a gene encoding a phospholipid synthetic gene of unknown function, *plsX*, lies just downstream of the ribosomal protein gene *rpmF* and upstream of five fatty acid biosynthetic genes, *fabH, fabD, fabG, acpP,* and *fabF*. The operon is also complex; transcription is initiated from at least eight promoters. In addition, some transcripts produced by the operon are cleaved by RNases while others terminate at one of three specific points at the 5' end of *plsX*.

This work demonstrates that a weak transcriptional terminator (an attenuator) lies at the 5' end of *plsX*. The attenuator was localized to a 200 bp segment. Analysis of the secondary structure of the attenuator mRNA has lead to a model which includes four stem-loop structures. In this model, the *plsX* start codon lies within the loop of the second stem. Two tandem stems are located directly upstream of the mapped 3' endpoints. Mutational analysis shows that all four stem-loops play a role in attenuator activity. Regulation of the attenuator and the attenuator's mechanism of controlling downstream gene expression were investigated. Ribosome binding to attenuator mRNA, the PlsX protein, ppGpp concentration, and rate of lipid synthesis all appear to have no effect on attenuator activity. Interestingly, growth temperature appears to have an effect on both attenuator activity and the activity of one or more of the promoters upstream of *rpmF*, P_1, P_2, and P_3. Activity of the three promoters is 4.5-fold higher at 28°C as compared with 42°C. The attenuator also appears to increase expression of downstream genes 2-fold as temperature decreases. Though the attenuator region terminates transcription, growth temperature-regulation of attenuator activity is apparently mediated by a change in stability of the mRNA. These data demonstrate that transcriptional expression of *plsX* is 9-fold higher at 28°C as compared with 42°C. The striking dependence on temperature of *plsX* expression suggests a role for PlsX in the temperature modulation of fatty acid incorporation into the membrane phospholipids.

DEDICATION

To my wife, to my mother, and to the memory of my father.

ACKNOWLEDGEMENTS

I would like to express my deepest appreciation to my advisor, Dr. Timothy J. Larson, for his guidance, support, patience, and consideration throughout my years at Virginia Tech. His dedication to research and the pursuit of knowledge is matched only by his persistance and diligence. My thanks also go to the members of my commitee, Dr. Jiann-Shin Chen, Dr. Dennis R. Dean, Dr. Eugene M. Gregory, and Dr. William E. Newton. I am grateful to Dr. Thomas O. Sitz for his assistance with the secondary structure analysis.

This work was completed in part because the laboratory was always a pleasent place to work and in many ways facillated the exchange of information and the growth of ideas. For this, I would like to thank the former and current members of the lab, Ningyue, Sherry, Sergey, Tsuneo, Krissie, Jason, Andy, Gang, Bing, Keith, Christina, and Matt. I would especially like to thank Ali for assistance in the construction of several of the oligonucleotide-directed deletions, her regular technical advice, and her ability to remember the location of everything in the lab.

Most of all, I would like to thank my wife, Barbara, for her love and support.

LIST OF ABBREVIATIONS

ACP	acyl carrier protein
Ap	ampicillin
bp	base pairs
BSA	bovine serum albumin
CDP	cytosine diphosphate
cpm	counts per minute
CTP	cytosine triphosphate
DEPC	diethylpyrocarbonate
DTNB	5, 5,-dithiobis(2-nitrobenzoic acid)
EDTA	ethylenediamine tetraacetate
glycerol-P	glycerol-3-phosphate
LB	Luria Broth
IPTG	isopropyl β-D-thiogalactopyranoside
MCS	multiple cloning site
MU	Miller Units
nts	nucleotides
ONP	*o*-nitophenol
ONPG	*o*-nitophenol galactoside
PAGE	polyacrylamide gel electrophoresis
PCR	polymerase chain reaction
ppGpp	3',5' guanosine bispyrophosphate
SDS	sodium dodecyl sulfate
rbs	ribosome binding site
RNase	ribonuclease
rRNA	ribosomal RNA
ssDNA	single-stranded DNA
ssRNA	single-stranded RNA
tRNA	transfer RNA
U	units
X-gal	5-bromo-4-chloro-3 indolyl-β-galactopyranoside

TABLE OF CONTENTS

LIST OF FIGURES

LIST OF TABLES

CHAPTER 1: LITERATURE REVIEW

Glycerophospholipids and lipopolysaccharides make up the lipid bilayer portion of the inner and outer membranes of gram negative bacteria such as *Escherichia coli*, creating a permeability layer between the interior of the cell and the outside environment and acting as a support matrix for membrane functions (1,2). Phospholipid production must be coordinated with cell growth in order to maintain a large enough membrane for cell division to take place, while not wasting biochemical energy producing a membrane that is larger than required. Phospholipids are synthesized from various substrates, including fatty acyl-ACPs containing 12 carbons or more. Rock and Jackowski have shown that fatty acyl-ACP intermediates of four carbons or greater are not detectable under normal growth conditions (3). Since fatty acid intermediates appear to be present in the cell in very low concentrations, the individual biosynthetic steps appear to be regulated in a way that prevents intermediates from accumulating. Potential control points include β-ketoacyl-ACP synthase III and enoyl-ACP reductase, which are inhibited by long chain fatty-acyl ACPs (4).

The genes encoding many of the fatty acid biosynthetic enzymes are also probably regulated, though little is known. Some examples include the *acc* genes that encode the subunits of acetyl-CoA carboxylase, the first step in fatty acid biosynthesis. Levels of transcripts containing *accA*, *accBC*, and *accD* have been shown to increase with growth rate (4). Another example is the *fabA*-encoded dehydrase; one of the promoters upstream of *fabA* has been shown to be controlled by an activator (4). A final example involves a cluster of fatty acid biosynthetic genes (Figure 1). At least one promoter upstream of *fabH*, *fabD*, and *fabG* exhibits decreased activity under starvation conditions (5,6). Since these examples do not give a complete picture of the regulation of membrane synthesis; it is likely that there are other points of genetic regulation of fatty acid or phospholipid synthetic genes.

Another purpose for regulation of fatty acid and phospholipid synthetic genes would be to coordinate these two biosynthetic processes. Free fatty acids (those not incorporated into phospholipids) have no structural or enzymatic function in the cell. Fatty acids synthesized by the cell can either be incorporated into phospholipids or degraded and used as a carbon source. Since the degradation of these fatty acids represents a futile cycle, degradation is a waste of cellular energy. The only purpose for synthesizing fatty acids, therefore, is to eventually incorporate them into phospholipids, and any free fatty acids signify wasted cellular energy. For this reason, fatty acid and phospholipid synthesis must be coordinated, not only by control of enzyme activity, but possibly by coordinating the expression of the genes encoding these enzymes. Therefore, to completely understand growth rate-regulation and coordination of fatty acid and phospholipid synthesis, the organization and regulation of operons containing these genes must be understood.

One operon containing several genes for fatty acid and phospholipid synthetic enzymes is the *rpmF-plsX-fab* operon (7, 8) (Figure 1). This operon contains the following genes in order: *rpmF*, encoding the L32 riboprotein (9); *plsX*, encoding a phospholipid synthesis protein with an undefined function (10); *fabH*, encoding the β-ketoacyl-acyl carrier protein synthase III that catalyzes the first condensation reaction of

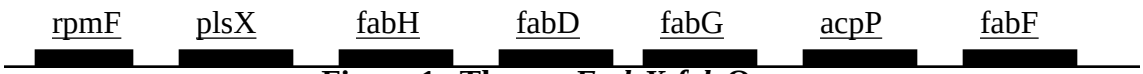

Figure 1. The *rpmF-plsX-fab* Operon

fatty acid biosynthesis (11); *fabD*, encoding the malonyl CoA-acyl carrier protein transacylase which catalyzes the step prior to the condensation cycle (12); *fabG*, encoding the β-ketoacyl-ACP reductase which reduces acetoacetyl-ACP and longer β-ketoacyl-ACPs (13); and *acpP*, encoding the acyl carrier protein which serves as the carrier of the nascent acyl chain in every step in fatty acid synthesis after the transfer of the malonyl group of malonyl-CoA to ACP (13). Downstream of *acpP* is the gene that encodes β-ketoacyl-acyl carrier protein synthase II, *fabF*, which may also lie in the *rpmF-plsX-fab* operon (8,14,15). With genes for a ribosomal protein, fatty acid synthesis, and phospholipid synthesis, the *rpmF-plsX-fab* operon is essential for both protein and cell membrane production. Therefore, understanding the regulatory mechanisms of this operon will shed light on the global controls of cell division, including coordinate regulation of ribosome and cell membrane synthesis and growth rate control of fatty acid and phospholipid synthesis.

FATTY ACID BIOSYNTHESIS IN *E. COLI*

Type I fatty acid biosynthesis, found in eukaryotes, is performed by a large multifunctional protein (1). This large peptide has separate domains which catalyze the separate reactions involved in fatty acid synthesis. On the other hand, fatty acid biosynthesis in *E. coli* is type II, meaning each step is catalyzed by a different enzyme (1). The *accABCD* gene products, subunits of acetyl-CoA carboxylase, catalyze the first step of fatty acid biosynthesis. In this step, acetyl-CoA is carboxylated to form malonyl-CoA (16,17) (Figure 2). The malonyl group is then transfered to the terminal sulfhydryl group of the 4' phosphopantetheine of acyl carrier protein by the *fabD*-encoded malonyl-CoA-ACP transacylase (12). (The acyl intermediate is bound to ACP for the remaining steps of fatty acid synthesis.) β-ketoacyl-acyl carrier protein synthase III, encoded by *fabH*, catalyzes the first elongation step; the acetyl group of acetyl-CoA is added to malonyl-ACP to form acetoacetyl-ACP (11). Synthase III performs only this elongation step (11) and this step is believed to be one of the rate limiting steps in fatty acid biosynthesis (18). The acetoacetyl-ACP is then reduced to β-hydroxybutyryl-ACP by the *fabG*-encoded NADPH-dependent β-ketoacyl-ACP reductase (13). One of two β-hydroxyacyl-ACP dehydrases, encoded by *fabZ* and *fabA*, catalyzes the release of water from β-hydroxybutyryl-ACP to form crotonyl-ACP (19). It has been shown that either enzyme can perform the dehydrase step on fatty acyl-ACP intermediates of up to 10 carbons in length, but that the *fabZ*-encoded dehydrase has a greater affinity for substrates of less then 6 carbons (20). It is also at the dehydrase step that the pathway for the synthesis of unsaturated fatty acids begins. The *fabA*-encoded dehydrase is capable of isomerizing *trans*-2-decenoyl-ACP to *cis*-3-decenoyl-ACP (4). The *cis* isomer cannot be reduced and elongation continues with the double bond intact. In later elongation cycles, the *fabZ*-encoded enzyme performs the dehydrase step on unsaturated intermediates (20), which eventually become *cis*-vaccenic or palmitolenic acid (4).

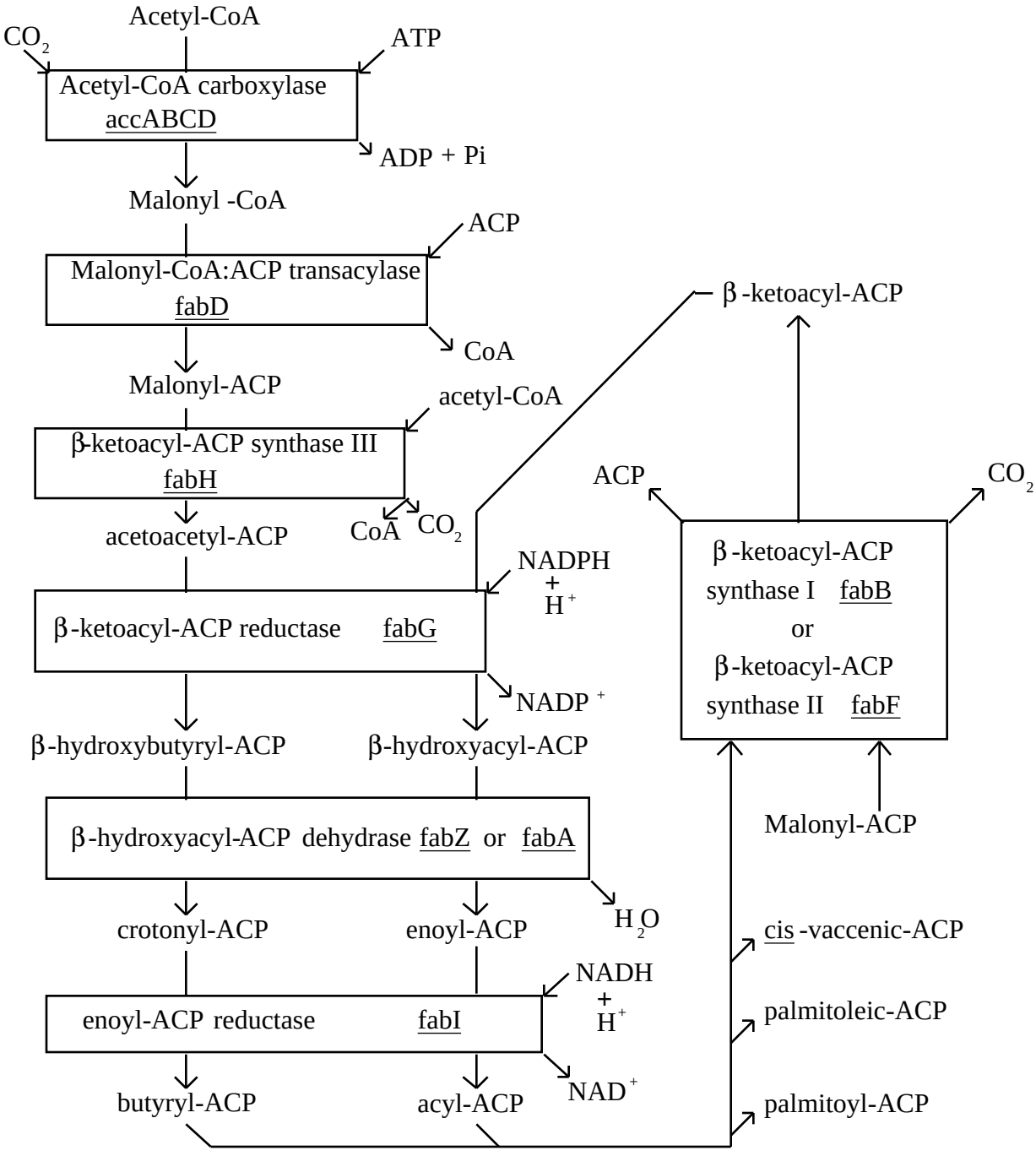

Figure 2. The Fatty Acid Biosynthetic Pathway

The product of the dehydrase reaction, crotonyl-ACP, is reduced to butyryl-ACP by the *fabI* encoded enoyl-ACP reductase (21). The cycle then begins again, with a second malonyl group from malonyl-ACP added to the fatty acyl-ACP. This step cannot be catalyzed by synthase III, but instead the *fabB* encoded β-ketoacyl-ACP synthase I (22) or *fabF*-encoded β-ketoacyl-ACP synthase II (23,24) is used. Synthase I has been shown to catalyze a key reaction in the synthesis of unsaturated fatty acids, believed to be the elongation of *cis*-3-decenoyl-ACP (4). Synthase II has a role in thermal regulation of fatty acid composition and is required for the production of *cis*-vaccenic-ACP (4). The cycles of elongation continue until one of the predominant fatty acids of the membrane, palmitoleic-, *cis*-vaccenic-, or palmitoyl-ACP, is produced.

As stated above, fatty acyl-ACP intermediates of four carbons or greater are not detectable under normal growth conditions (3), implying well controlled synthesis of each intermediate. There is some evidence to show that acyl-ACP may be a key regulatory molecule in the fatty acid synthetic pathway, and that its presence can slow fatty acid biosynthesis. Long chain acyl-ACPs compete with malonyl-ACP for binding at the active site of β-ketoacyl-ACP synthase III (4), and they have also been shown to inhibit reduction of crotonyl-ACP by enoyl-ACP reductase (25). In addition, malonyl-CoA levels are decreased in the presence of long chain acyl-ACPs, though the precise mechanism is not understood.

Besides the enzymatic control described above, there are several mechanisms employed for the regulation of genes involved in fatty acid biosynthesis. For example, transcription of *fabA,* which encodes one of the two dehydrases, is positively controlled by the FadR protein. FadR was first discovered to be a repressor, decreasing the level of transcription of the fatty acid degradation genes of the *fad* regulon. In the abscence of the acyl-CoA inducer, transcription of *fadBA, fadL,* and *fadD* are repressed (4,26). Recently, it was shown that FadR can also act as an activator, increasing transcription from a promoter upstream of *fabA* (27). FadR thus allows the cell to coordinate fatty acid biosynthesis and degradation, preventing a futile cycle. Another example of transcriptional control involves the genes encoding the subunits of acetyl CoA carboxylase, *accA, accB, accC,* and *accD.* The levels of the transcripts of these genes change with growth rate, decreasing as growth rate decreases (4). The final example comes from the *rpmF-plsX-fab* operon. The P_2 promoter, located upstream of *rpmF,* and P_{H1} and/or P_{H2}, located upstream of three fatty acid biosynthetic genes and the gene for ACP (Figure 3), have decreased activity under starvation conditions (5,6).

Fatty acid biosynthesis is also affected by growth temperature (1). Membrane phospholipids of *E. coli* have a higher level of *cis*-vaccenic acid and a lower level of palmitic acid at lower temperatures (28). This change allows the membrane to remain fluid. *fabF* mutant strains lack this temperature control and do not synthesize *cis*-vaccenic acid (1). For a time, it was unknown if FabF activity was required for temperature control or simply the presence of *cis*-vaccenic acid was sufficient. De Mendoza and coworkers showed that overexpression of FabB allowed a *fabF* mutant strain to synthesize large amounts of *cis*-vaccenic acid (29). Since this strain still lacked temperature control, it was concluded that FabF-mediated elongation of unsaturated fatty acids (rather than just the presence of *cis*-vaccenic acid) is required for temperature-mediated incorporation of *cis*-vaccenic acid into phospholipids. Notably, the *vtr* mutation, which causes *cis*-vaccenic acid to be overproduced at all temperatures, has

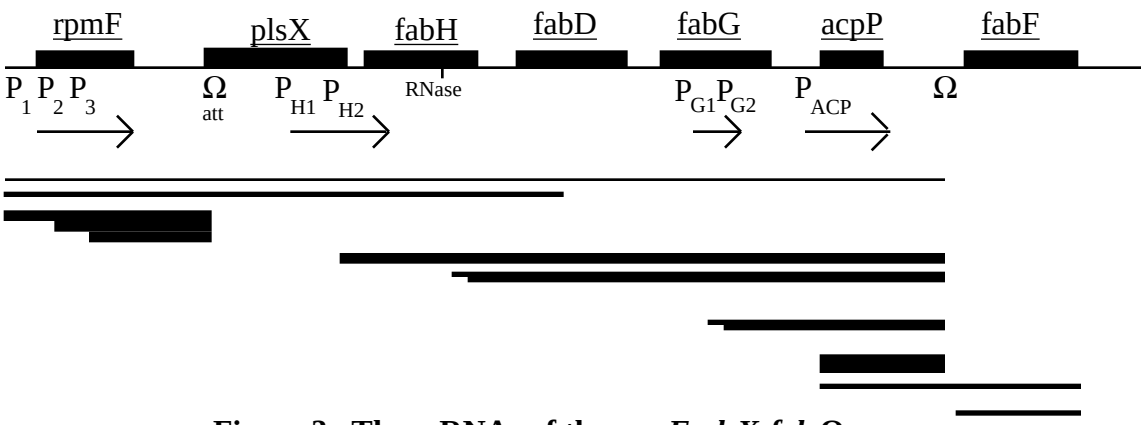

Figure 3. The mRNAs of the *rpmF-plsX-fab* Operon

been mapped near *fabF* (30). Sequencing of *fabF* and *acpP* from *vtr* mutant strains has shown that the *vtr* mutation is not located in either of these genes and its exact location has not been found (31).

A second type of temperature-dependent regulation may also exist. Cells supplemented with both saturated and unsaturated fatty acids preferentially incorporate the unsaturated fatty acids at lower temperatures (32,33). *E. coli* grown in the presence of exogenous fatty acids will express decreased levels of the *fabA*-encoded dehydrase, due to the lack of FadR-mediated activiation of *fabA.* A decrease in FabA activity will reduce the concentrations of its product, *cis*-3-decenoyl-ACP. Since *cis*-3-decenoyl-ACP is a substrate of FabF, the rate of FabF-mediated synthesis of *cis*-vaccenic acid will also drop dramatically. For these reasons, the temperature-dependent incorporation of unsaturated, exogenous fatty acids appears to be independent of FabF (1).

Enzymes involved in three of the first four steps of fatty acid synthesis are encoded by the *rpmF-plsX-fab* operon (Figure 3). *fabH*, *fabD*, *fabG*, and *acpP* lie in the operon in this order and encode β-ketoacyl-ACP synthase III (11), transacylase (12), keto reductase (13), and acyl carrier protein (13), respectively. *fabF,* encoding β-ketoacyl-acyl carrier protein synthase II, is located downstream of *acpP* (15). Interestingly, *fabF* appears to be cotranscribed with other *fab* genes; some transcripts that initiate within the *rpmF-plsX-fab* operon continue downstream into *fabF* (8,14). Since it seems unlikely that these fatty acid biosynthetic genes are located next to one another simply by chance, the mechanisms of coordinate expression of the genes probably lie in the operon. Coordination of fatty acid biosynthesis with temperature changes or cellular division may also be accomplished by genetic regulation of the operon.

FATTY ACID INCORPORATION INTO PHOSPHOLIPIDS

Palmitic acid, a saturated fatty acid, and two unsaturated fatty acids, palmitoleic and *cis*-vaccenic acid, are the major fatty acids found in phospholipids (1). The fatty

acids found in lipopolysaccharides include β-hydroxymyristate, myristate, and laurate (1,34). The first step in phospholipid synthesis is the attachment of the acyl group of acyl-ACP to position one of *sn*-glycerol-3-phosphate (glycerol-P), forming 1-acylglycerol-P (1), as shown in Figure 4. This committed step is catalyzed by glycerol-P acyltransferase, encoded by *plsB* (1). The 1-acylglycerol-P is again acylated to yield phosphatidic acid. 1-acyl-*sn*-glycerol-P acyltransferase, encoded by *plsC*, catalyzes this step (35). After phosphatidic acid is activated by a reaction involving CTP, one of several head groups are added and modified, yielding the major phospholipids, phosphatidylethanolamine, phosphatidylglycerol, and cardiolipin (1).

Glycerol-P acyltransferase, catalyzing the first step in *de novo* synthesis of phospholipids, plays an important role in cell membrane synthesis. Strains carrying the *plsB26* mutation contain a Km-defective acyltransferase (36). The *plsB26*-encoded acyltransferase has a 10-fold lower affinity for glycerol-P, and may have a lower affinity for acyl-ACP as well. Notably, the *plsB26* strain is auxotrophic for glycerol-P only if it also carries the *plsX50* mutation (10). The *plsX50* allele is a one base pair deletion in the *rpmF-plsX-fab* operon that shifts the *plsX* reading frame. The mutation is predicted to place a stop codon in-frame after the sixth codon of *plsX*. Translation will therefore be terminated after a short peptide is synthesized (8). The function of the PlsX protein and how it relates to the acyltransferase is unknown, but a possible role with relation to the transcription of *plsX* was tested.

COORDINATION OF LIPID AND MACROMOLECULAR SYNTHESIS

Phospholipid synthesis must be coordinated with cellular growth rate for orderly cell division to occur. Cell growth and division must also be curtailed if nutrients are in limited. *E. coli* has a complex system for dealing with amino acid starvation, a reaction that has been called the stringent response. A small molecule, guanosine 3', 5'-bispyrophosphate (ppGpp), has been shown to play a key role in the stringent response, with levels of ppGpp increasing dramatically during amino acid starvation (37). At the center of ppGpp synthesis is the *relA* gene product, ppGpp synthetase I (38). This enzyme binds to ribosomes, synthesizing ppGpp when the ribosome binds an uncharged tRNA and stalls (37). This mechanism allows more ppGpp to be synthesized as amino acid levels decrease. Another enzyme, ppGpp synthetase II, encoded by *spoT*, also produces ppGpp (39,40). Synthetase II is different from synthetase I, however, in that its primary activity appears to be the hydrolytic cleavage of ppGpp and that it is not bound to ribosomes (39,40).

Though the full effects of ppGpp have not been explained, studies have shown that ppGpp has various effects on RNA polymerase activity. Artifically elevated levels of ppGpp induce the production of the stationary phase σ factor, σ^S (41), and also repress transcription initiation from some promoters (42). ppGpp slows the elongation rate of RNA polymerase by inducing transcriptional pausing at certain sites on the mRNA that contain secondary structure (43,44). This pausing increases the coupling of transcription and translation, allowing the ribosome to follow very closely behind the polymerase (45,46). Vinella and D'Ari showed that ppGpp mediates the changes in RNA polymerase activity by directly binding to the β subunit (47).

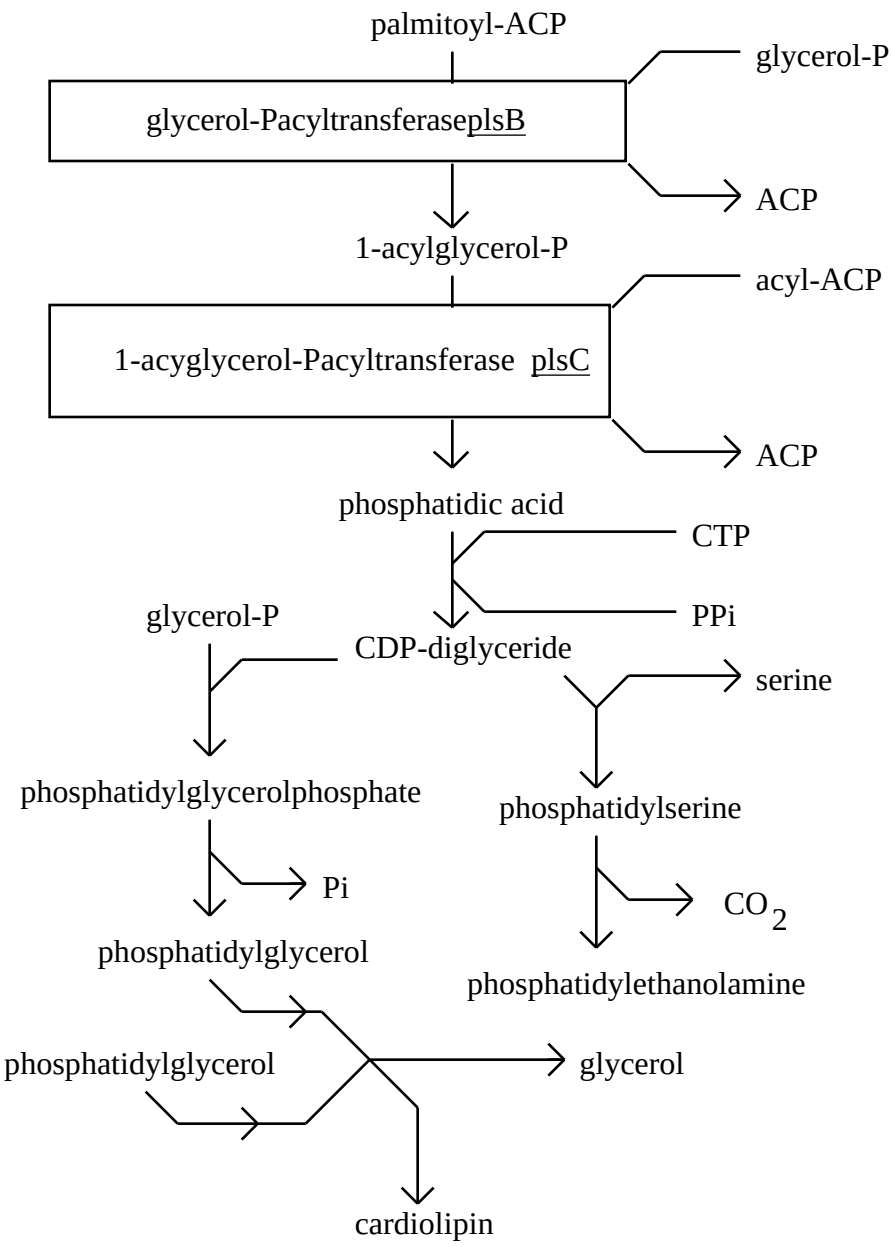

Figure 4. The Phospholipid Synthetic Pathway

Although the stringent response can halt cell division, it appears not to be the only cellular control mechanism regulating growth rate. A promoter upstream of a ribosomal RNA gene, *rrnB* P1, is controlled by the stringent response, though in a mutant strain completely lacking ppGpp, the promoter is still controlled in a growth rate-dependent manner (48). In addition, data from *rrnB* P1 mutants have shown that different sequences within the promoter region are required for either stringent control or another type of growth rate-dependent control (49). Therefore, at least one other regulatory system, which is not reliant on ppGpp, must have a hand in controlling rRNA production and growth rate.

Cell membrane synthesis is coordinated with growth rate and ceases during starvation. Several key points of regulation related to this response have already been demonstrated. Glycerol-P acyltransferase is inhibited by ppGpp (50). The transcription of the *accA, accB, accC,* and *accD*, which encode the subunits of acteyl-CoA carboxylase, have been shown to be growth rate-dependent (51). In addition, at least two promoters upstream of *fabHDG* gene cluster decrease activity during starvation (5,6). Although a mechanism for controlling *fabH*, *fabD*, and *fabG* expression with starvation has been demonstrated, other controls may exist. Importantly, no regulatory mechanism based solely on growth rate has been discovered. As mentioned above, ppGpp can cause RNA polymerase to pause at certain sites and can also increase the coupling of transcription and translation. Notably, RNA polymerase pausing and coupling of transcription and translation have been shown to effect the termination frequency of some attenuators (52,53). The transcriptional termination frequency of the *plsX* attenuator was therefore measured in strains growing at different rates and in strains lacking the stringent response.

Cell membrane synthesis also seems to be regulated in accordance with the protein/lipid ratio of the membrane. When the genes encoding the subunits of fumarate reductase are overexpressed in *E. coli*, the protein is produced in excess, inserted into the membrane normally, and is active (54). Despite the increase in amount of protein in the membrane, the protein/lipid ratio does not change drastically. Instead, more phospholipids are produced by the cell, and a larger, invaginated membrane is made. This effect is also seen when either the membrane-bound ATP synthase (55) or glycerol-P acyltransferase (56) is overproduced. From these experiments, it seems apparent that the cell regulates phospholipid synthesis, in part, based on the protein/lipid ratio of the membrane. Since no regulatory mechanisms have been shown to account for this, experiments were conducted to determine if the *plsX* attenuator is responsive to the protein/lipid ratio of the cell membrane.

THE *rpmF-plsX-fab* OPERON

The basic organization of the *rpmF-plsX-fab* operon has been previously determined (5,7,8,13-15,57), including the locations of many promoters (Figure 3). At least three strong promoters, P_1, P_2, and P_3, are located upstream of *rpmF*. Results of northern analysis suggests that two weaker promoters, P_4 and P_5, lie upstream of *rpmF,* although these have not been characterized (8). A pair of promoters, P_{H1} and P_{H2}, is found within *plsX* (5,6). Recent work has shown that P_2 and one or both of the P_H promoters have decreased activity during starvation conditions (5). No promoters have been found within *rpmF* or just upstream of *plsX.* The absence of a promoter specific for

plsX indicates that *plsX* transcription must be initiated at one of the promoters upstream of *rpmF*. There is also some evidence that an RNase processing site is located in the *fabH* mRNA (6,8). Additional promoters are located within the *fabG* structural gene that appear to promote the transcription of *acpP* and possibly *fabF* (6,8,58). Interestingly, a weak terminator appears to be located between the two genes (8,58). The P_{ACP} promoter, which transcribes both *acpP* and *fabF*, is located in the intergenic region between *fabG* and *acpP* (8,14). Therefore, a large segment of the operon, from the 5' end of *fabH* to the 3' end of *fabD*, appears to have no promoters. In addition, *plsX* can only be transcribed along with *rpmF*, and *fabD* and *fabG* can only be transcribed along with *fabH*. Mechanisms for independent genetic regulation of *plsX*, *fabD*, and *fabG* have yet to be explained.

Previous work has also been done to determine the nature of mRNAs from this operon (8). Northern analysis has shown that most transcripts that initiate from P_1, P_2, or P_3 end at the 5' end of *plsX*, although some run from *rpmF* through *fabD* or *acpP* (Figure 3). Therefore, termination taking place at the 5' end of *plsX* is incomplete. Transcriptional fusions of P_3 to *lacZ* produced higher β-galactosidase activities then did a P_3 - *plsX* - *lacZ* fusion (8). This demonstrates that the 5' end of *plsX* contains either transcriptional terminator activity or this region of mRNA is somehow processed and the downstream mRNA becomes less stable. A conclusive evaluation of whether or not termination at the 5' end of *plsX* takes place therefore cannot be made by northern analysis. Overall, these results show that no *fab* gene in the operon is independently transcribed, and some transcripts run from *rpmF* to *acpP*. The possibility also exists that even more full length *rpmF* to *acpP* transcripts may initially be made, with many of them quickly cleaved and digested by RNases. For my work, the 5' region of *plsX* has been shown to contain a transcriptional terminator and the frequency of termination has been quantitated.

Since no promoter is solely dedicated to *plsX* expression, no upstream promoter could allow the transcriptional expression of *plsX* to be controlled independently. However, if the 5' region of *plsX* contained a transcriptional terminator, and if the termination frequency could be controlled, the level of *plsX* mRNA could be very efficiently regulated. More importantly, regulated antitermination at *plsX* would provide increased levels of full length transcripts, thus increasing expression of not only PlsX, but the *fab* gene products and acyl carrier protein as well. An attenuator at *plsX* could therefore allow a coordinate up- or down-regulation of the enzymes involved in fatty acid synthesis and cell membrane production.

S1 nuclease data show that the 3' ends of the *rpmF* transcripts correspond to three uridine residues (8) (Figure 5) and computer-predicted structures of the 5' end of *plsX* mRNA show that four combinations of stems and loops can form just upstream of these end points (Figure 6). The computer models also show that the rare UUG start codon of *plsX* lies within the region of secondary structure, along with the ribosome binding site. In order to determine the secondary structure of this mRNA in solution, an *in vitro* analysis was performed.

As stated above, PlsX has no known function and the *plsX50* frameshift mutation is not lethal. Interestingly, a *plsX* homologue has been found in at least six other species.

Figure 5. Sequence of the *plsX* Attenuator Region

Pictured above is a portion of the sequence of the *rpmF-plsX-fab* operon with the putative amino acid sequences for the *rpmF*-encoded and the *plsX*-encoded proteins seen in **bold**. The native *HinD*III site located in this region is underlined and marked as HDIII. The relative position of the three mRNA 3' end points mapped by S1 nuclease digestion are marked with a double underline. A *BamH*I site was engineered into this region for cloning purposes; the location of this engineered site is underlined and marked as BHI.

Both *Rhodobacter capsulatus* (59) and *Synechocystis* PCC6803 (60) contain *plsX* upstream of *fabH.* Interestingly, *rpmF* is upstream of *plsX* in *R. capsulatus* but a Na^+-ATPase subunit gene is upstream of *plsX* in *Synechocystis* PCC6803. The *plsX* homologue from *Bacillus subtilis* is also near fatty acid biosynthetic genes, located upstream of *fabD, fabG,* and *acpP* (61). (The region upstream has not been sequenced.) Genomic sequencing of *Mycoplasma genitalium* (62) and *Mycoplasma pneumoniae* (63) uncovered *plsX* homologues, and in both cases they are upstream of *rnc,* which encodes RNase III, and downstream of unidentified genes. *Deinococcus radiodurans* also contains *plsX* (64), but the upstream genes were not identified and the downstream region was not sequenced. It is also interesting to note that *Haemophilus influenzae* Rd contains an operon that is nearly identical to the *rpmF-plsX-fab* operon of *E. coli* (65). The *Haemophilus* operon contains *rpmF, fabH, fabD, fabG,* and *acpP,* but does not contain *plsX*.

REGULATION OF THE TRANSCRIPTION OF OPERONS CONTAINING RIBOSOMAL PROTEIN GENES

The rate of ribosome production and the concentration of ribosomes in the cell increases as growth rate increases (66). At the heart of this growth rate-dependence is the regulated transcription of stable RNAs (tRNA, rRNA). Synthesis of rRNA is controlled in a growth rate-dependent manner (66) and the growth rate-dependent transcription of rRNA allows ribosomal protein production to be regulated with growth rate in a unique fashion. If riboprotein production outpaces rRNA synthesis, free riboproteins (riboproteins not bound in a ribosome complex) accumulate in the cell (66). Some of these free riboproteins can then bind to specific regulatory sites on their own mRNAs, near the Shine-Dalgarno region, causing translation to be repressed. This mechanism of "negative autoregulatory feedback" allows the cell to coordinate the production of rRNA and some riboproteins and plays a major role in the growth rate-dependent regulation of ribosome synthesis.

Many operons containing genes for riboproteins also contain genes for other essential cellular processes. These include the macromolecular synthesis (MMS) operon, which encodes the genes for the riboprotein S21 (*rpsU*), DNA primase (*dnaG*), and σ^{70} (*rpoD*) (67), the *rplKAJL rpoBC* operon, which encodes four riboproteins along with the β and β' subunits of RNA polymerase (68), and the *infC-rpmI-rplT-pheS-pheT* operon, which encodes IF3, two riboproteins, and the large and small subunits of phenylalanyl-tRNA synthetase (69,70). Complex control mechanisms are found in these operons, probably because, in addition to encoding riboprotein genes, they also contain genes for essential enzymes involved in transcription, DNA synthesis and other aspects of translation. For example, the MMS operon has three promoters at the 5' end and an internal promoter (71). Transcription of the genes in this operon is down-regulated during amino acid starvation. In addition, a specific RNase processing site is located in the mRNA between *dnaG* and *rpoD.* An internal terminator is located between *rpsU* and *dnaG* (72,73) and *in vitro* work has shown that antitermination at this site is faciliated by the NusA protein (71).

The *rplKAJL rpoBC* operon contains a regulated attenuator upstream of the *rpoBC* genes encoding the β and β' subunits of RNA polymerase (74). As the cellular concentration of the RNA polymerase holoenzyme decreases, termination at the attenuator has been shown to decrease slightly (75). This attenuator therefore allows increased expression of the RNA polymerase subunit genes when the transcriptional capacity of the cell decreases (75). NusA and NusG also induce antitermination at this attenuator (76). In addition, elevated levels of either the β or β' subunits has been shown to decrease the expression of *rpoB* and *rpoC* at the translational level (75).

The *infC-rpmI-rplT-pheS-pheT* region also contains an attenuator just upstream of the *pheS* and *pheT* genes, which encode the small and large subunits of phenylalanyl-tRNA synthetase (69,70). If the cell does not contain sufficient amounts of phenylalanyl-$tRNA^{phe}$, ribosomes will stall when they reach specific phenylalanyl codons within the *pheS* attenuator. The pausing of a ribosome at one of the specific phenylalanine codons allows transcription to continue and the *pheS* and *pheT* genes to be transcribed. If phenylalanyl-$tRNA^{phe}$ levels are high enough, the ribosome does not stall, and the mRNA upstream of *pheS* can fold in such a way as to cause transcription to terminate. In this way, the attenuator allows expression of the two subunits of phenylalanyl-tRNA synthase only when phenylalanyl-$tRNA^{phe}$ concentrations are low. The three operons mentioned above are similar, not only because they all encode ribosomal protein genes, but they also contain complex transcriptional regulatory mechanisms, such as multiple upstream promoters, internal promoters, and regulated transcriptional terminators. It is also important to note that two of the transcriptional terminators mentioned above appear to be regulated in accordance with a cellular need for the product of the enzymes encoded by the downstream genes.

The *rpmF-plsX-fab* operon of *E. coli* is similar to the operons mentioned above because it contains a transcriptional attenuator between a riboprotein gene and the other genes in the operon. In this case, the downstream genes all relate to the synthesis of fatty acids and phospholipids. Because of the similarity of the *rpmF-plsX-fab* operon to other operons containing riboprotein genes, experiments were conducted to determine if attenuator activity is regulated with a cellular need for fatty acids and phospholipids or if it is regulated by the PlsX protein.

TRANSCRIPTIONAL TERMINATION

In *E. coli*, all known transcription terminators are characterized as either rho-dependent or intrinsic (77). For an mRNA to terminate in a rho-dependent manner, it must contain both a rho utilization (*rut*) site and a transcription stop point (*tsp*) region. Rho initally binds to the *rut* site before causing termination at one of several points within the *tsp* region, which appear to be natural pause sites (78). Rho has been shown to be a homohexamer with RNA-dependent ATPase activity (79,80). It also has RNA-DNA helicase activity, and this activity is required to facilitate termination (81). From these data, two models for rho activity have been proposed, the tracking model and the wrapping model (77). In both, the rho factor initally interacts with the mRNA that will be terminated by binding at the *rut* site. In the tracking model, rho moves along the mRNA in an ATPase-dependent manner, still bound to the *rut* site, eventually reaching the transcribing RNA polymerase. Upon interacting with the *tsp* region, rho causes termination at one of several specific points. The wrapping model is very similar. It, too,

proposes that rho moves toward the RNA polymerase in an ATPase dependent manner, but rho is thought to wrap the mRNA around itself as it moves. As before, termination takes place as a result of rho interaction with the *tsp* region.

Intrinsic terminators are different from rho-dependent terminators in that they depend only upon the DNA (and corresponding mRNA) sequence. Common characteristics of the mRNA of intrinsic terminators include a guanosine/cytosine-rich region with interupted dyad symmetry and a run of uridine residues at the termination site(s) (77). The mRNA transcribed from the region of interupted dyad symmetry is nearly always predicted to form a stable stem-loop structure. Several lines of evidence point to the mRNA stem-loop structure, rather than the DNA sequence, as being essential for termination to take place. Mutations within the symmetric region often dramatically affect the frequency of termination in the region, though the addition of another mutation that would restore stem-loop base-pairing often restores much of the terminator activity (77). The presence of an oligonucleotide complementary to the putative 5' end of the stem has been shown to decrease the rate of termination (82). This is presumably due to an interaction with the mRNA; the interruption of the normal base-pairing inhibits stem-loop formation.

The run of uridine residues is usually within 8 nucleotides downstream of the base of the stem, leaving the mRNA with a series of uridines at the 3' end. It is believed that the uridines are important because of the uniqueness of dA-rU base-pairing. When RNA and DNA interact they form an A-form helix. A repeat of deoxyadenosines are constrained in this helical shape, and the RNA-DNA duplex is unstable (83). For these reasons, it has been theorized that transcription of the adenosines leads the RNA polymerase to pause, and interaction of the stem-loop structure with the polymerase causes the unstable DNA/RNA/RNA polymerase complex to dissociate.

ATTENUATORS AND THE TRANSCRIPTIONAL REGULATION OF OPERONS

Landick, Turnbough, and Yanofsky have stated that, "transcription attenuation allows an organism to regulate gene expression by exploiting RNA sequences and structures, as opposed to information contained in DNA (52)." Attenuators are often regulated transcriptional terminators and a change in the frequency of termination alters the transcriptional expression of downstream genes. The frequencies of termination at some attenuators are indirectly affected by the substrates or products of the enzymes encoded by genes downstream of the attenuator. The *trp* attenuator of *E. coli,* for example, allows increased transcriptional readthrough when tryptophanyl-tRNA^{trp} levels are low, thus increasing the expression of downstream genes involved in tryptophan synthesis (52). The attenuator activity varies this way due to tandem tryptophan codons within a region of mRNA secondary structure. As the attenuator region is being transcribed, the mRNA is also being translated by a bound ribosome. If charged tRNA^{trp} levels are low, the ribosome will stall when it reaches the tryptophan codons. This allows the mRNA to fold into the antiterminator form and the polymerase can continue to transcribe the DNA. If charged tRNA^{trp} levels are high, the ribosome will not stall and transcription and translation will be more tightly coupled. With the ribosome bound to the transcript and following closely behind the polymerase, the attenuator mRNA folds into the terminator form.

The *pyrBI* operon attenuator also involves stalling of the macromolecular synthetic machinery, but in this case, the RNA polymerase activity is slowed (53). This operon contains genes encoding the subunits of transcarbamylase, a pyrimidine biosynthetic enzyme. Upstream of the structural genes lies the attenuator, which encodes several uridine residues followed by a region of secondary structure. The repeated uridines allow the RNA polymerase to stall when the uridine concentration is low, thus increasing coupling of transcription and translation. This increased coupling causes the ribosome to shield the polymerase from mRNA secondary structure and allows transcription to continue. If uridine concentration is high, the polymerase does not stall, transcription/translation coupling is not increased, and termination results. So in both the *trp* and *pyrBI* operons, coupling plays a key role in the attenuation mechanism.

Ribosome binding to attenuator mRNA can also allow gene expression to be controlled in accordance with growth rate. The *ampC* gene encodes β-lactamase, which conveys ampicillin resistance, and expresses it in a growth rate-dependent manner (83). Located 16 bases upstream of the structural gene is the *ampC* attenuator region. This region of mRNA contains one putative stem-loop structure and, 9 bases upstream, a start codon with a weak ribosome binding site that can initiate translation but produce no peptide. Translation from this site yields no product because, although ribosomes bind at this location, the AUG start codon is immediately followed by a stop codon. Studies comparing *in vitro* transcription to *in vitro* transcription and translation show that the presence of ribosomes reduces transcriptional termination at the attenuator four-fold. Other experiments have shown that a single base mutation that weakens the stem base-pairing also eliminates growth rate-dependent expression of the gene. From these experiments, the following model has been postulated (84). As ribosome concentration increases with an increase in growth rate, the number of ribosomes binding at the poor attenuator ribosome binding site would increase. Though a near-consenus Shine-Dalgarno sequence becomes saturated with ribosomes at a low ribosome concentration, the weaker site here does not become saturated, and it is bound more often by ribosomes as growth rate and ribosome concentration increase. It is believed that ribosome binding at the weak binding site disrupts the stem-loop structure, allowing transcription to proceed. As growth rate (and ribosome concentration) increases, binding in the attenuator region would also increase, allowing antitermination to occur in a growth rate-dependent manner. This mechanism may also occur at the *plsX* attenuator, which is preceded by an inefficent ribosome binding site. For this reason, growth rate-dependence of the *plsX* attenuator was tested.

Though the activities of the attenuators described above require only the normal transcriptional and translational apparatus, other attenuators are affected by specific proteins. The activity of the *trp* attenuator of *Bacillus subtilis*, for example, is altered by the *trp* RNA-binding attenuation protein (TRAP) (52). This protein can bind to the mRNA secondary structure of the attenuator mRNA only when TRAP has bound tryptophan (85). With TRAP bound, the terminator form of the attenuator is stablized, and transcriptional termination results. In this way, the *B. subtilis trp* attenuator allows tryptophan levels to control the expression of the *trp* operon. Another example is the *bgl* attenuator of *E. coli*, which lies upstream of several genes involved in β-glucoside metabolism (86). This attenuator can be bound by the BglG protein, but only under certain cellular circumstances. If no glucose is available as a carbon source (and the phosphotransferase system is activated), but β-glucoside is present, the BglF

phosphotransferase dephosphorylates the BglG protein. In this dephosphorylated form, BglG dimerizes and binds to the attenuator mRNA. Unlike TRAP, where protein binding stablizes the terminator form, BglG attachment to the secondary structure stablizes the antiterminator form, allowing transcription to proceed. The attenuator, therefore, increases expression of the β-glucoside enzymes when β-glucoside levels are high and glucose levels are low. These examples demonstrate that some attenuators are controlled by binding of a specific protein, and that binding can stablize either the terminator or antiterminator form.

Other attenuators do not appear to be controlled by either protein binding or transcription/translation coupling, but rather have more unique mechanisms of control. In gram positive bacteria, many operons that contain genes encoding aminoacyl-tRNA synthetases or amino acid synthetic enzymes also contain attenuators that are affected by the uncharged tRNA specific for that operon (for review see ref. 87). The mechanism is as follows. If the cell cannot acylate a specific tRNA as quickly as the tRNA is made, uncharged tRNA will begin to accumulate. Each specific tRNA molecule (free of aminoacylation) is able to bind to the secondary structure of its respective attenuator mRNA, with specific base pairing taking place. In *B. subtilis* for example, *tyrS*, the gene that encodes tyrosyl-tRNA synthetase, is controlled this way. The mRNA upstream of *tyrS* contains a region of secondary structure, and within this region lies a UAC triplet termed the "specifier sequence." The anticodon loop of an uncharged $tRNA^{tyr}$ can base pair with this triplet, but not as the function of any translation activity. Another portion of the $tRNA^{tyr}$, the acceptor stem, which is normally acylated with tyrosine, can base pair to a sequence of the mRNA called the T-box. These two regions of binding stablize the mRNA-tRNA complex (88). This stable RNA duplex maintains the mRNA in an antiterminator form, allowing transcripion of *tyrS* to proceed.

Another example of an unusual regulatory mechanism is the *rpoB* attenuator of *E. coli*, which is located upstream of the genes encoding the β and β' subunits of RNA polymerase (*rpoBC*) (75). Though the precise mechanism of the attenuator is not understood, it is known that the frequency of termination at this attenuator increases as the concentration of the RNA polymerase holoenzyme increases (75). By doing this, the expression of the β and β' subunits decreases as the transcription capacity of the cell increases. From examining these various attenuators, it can be seen that attenuator activity can be altered by coupling of transcription and translation, by tRNA or protein interaction with the attenuator mRNA, or by some aspect of transcription that has yet to be explained.

With fatty acid and phospholipid production increasing with an increase in growth rate, an increase in expression of the *fabHDG* and *acpP* genes of the *rpmF-plsX-fab* operon is also very likely. The *plsX* attenuator, positioned upstream of all of the *fab* genes, is in a unique position to provide regulatory control of these genes. Experiments were conducted to determine if the attenuator is regulated by a mechanism similar to those employed by any of the attenuators mentioned above. Attenuator activity was measured with varying amounts of upstream promoter activity and changes in the level of ribosome binding. In addition, the possibility that an attenuator binding protein is present was investigated.

CHAPTER 2: EXPERIMENTAL PROCEDURES

MATERIALS

Restriction endonucleases were purchased from various sources, including: Amersham Life Sciences (Arlington Heights, IL), Promega (Madison, WI), New England Biolabs (Beverly, MA), Pharmacia Biotech (Piscataway, NJ), and Boehringer Mannheim (Indianapolis, IN) and used with the buffer supplied by the manufacturer. Vent (exo$^-$) DNA polymerase, T4 polynucleotide kinase, and T4 DNA ligase were purchased from New England Biolabs and used with the buffers from the supplier. Shrimp alkaline phosphatase and the appropriate buffer were acquired from Amersham Life Sciences. 5-bromo-4-chloro-3 indolyl-β-galactopyranoside (X-gal) and isopropylthio-β-D-galactopyranoside (IPTG) were also obtained from United States Biochemical. The radiolabelled nucleotides for sequencing, [α-^{35}S]dATP (1000-1500 mCi/mmol), and 5' end labelling, [γ-^{32}P]ATP (3000 mCi/mmol), were purchased from DuPont-New England Nuclear (Boston, MA). Difco Laboratories (Detriot, MI) supplied yeast extract, tryptone, casamino acids, and bacto agar. Other chemicals such as glucose, glycerol, chloroform, isopropanol, isoamyl alcohol, phenol, agarose, acylamide, and various salts were bought from Fisher Scientific (Fair Lawn, NJ). Oligonucleotides for both sequencing and PCR were made on an Applied Biosystems model 381A DNA synthesizer and purified with oligopurification cartitridges from Cruachem (Glasgow, Scotland).

MICROBIOLOGICAL TECHNIQUES

Bacterial strains and growth media

The strains of *E. coli* K-12 used for this work are listed in Table 1. Cultures were routinely grown in LB medium (89) and, when required, the medium was supplemented with the appropriate antibiotics at the following concentrations: ampicillin, 100 μg/mL; chloramphenicol, 50 μg/mL; kanamycin, 50 μg/mL; spectinomycin, 50 μg/mL; or tetracycline, 12.5 μg/mL. AB minimal media (89) was used in some experiments and, if required, supplemented with one or more of the following: 0.2% glucose, 0.4% glycerol, 0.4% succinate, 0.5% casamino acids, 0.005% thiamine, or 0.001% tryptophan. A glycerol/fumarate medium (90) was also used; it contained 0.4% fumarate, 0.4% glycerol, M9 salts (91), 0.005% thiamine, 0.01 M $MgSO_4$, 0.001 mM $CaCl_2$, 0.05% casamino acids, 0.001% tryptophan. Both MacConkey-lactose agar and LB agar supplemented with 0.2% X-gal were used as indicator plates to test for the expression of β-galactosidase.

Transduction using bacteriophage P1

P1 transductions were performed essentially as described by Silhavy *et al.* (101).

Maintenance of strains

Stationary cultures of *E. coli* grown in LB medium were stored frozen at -70°C after the addition of 15% glycerol.

Table 1: Strains of *E. coli* K-12

(1) DHαF derivitive with *lacI*^{q} and *tetR* on a spectinomycin resistance cassette inserted at the λ attachment site, constructed by R. Lutz and T. Larson

Strain	Genotype	Derivation, Reference or Source
RZ1032	Hfr KL16PO/45 [*lysA(61-62)*] *dut1 und1 thi1 relA1 zbd-279*::Tn*10 supE44*	(92)
BW13745	DE3(*lac*)X74 Δ*phoA*532	(93)
RR1	BW13745 *tetR lacI*^{q} *Sp*^{R}(1)	P1(RL22) x BW13745, selection for Sp^R
SP2	BW13745 *pcnB recA1 srl*::Tn*10*	(94)
JM109	(F' *traD36 proAB lacI*^{q}*Z*ΔM15) *endA1 recA1 gyrA96 thi hsdR17* (r_K^-, m_K^+) *relA1 supE44* λ$^-$ Δ(*lac-proAB*)	(95)
DH5αF'	(*F'ϕ80 ΔlacZΔM15*) *endA1 recA1 hsdR17*	(96)
RL22	DH5αF *tetR lacI*^{q} *Sp*^{R}(1)	R. Lutz
MG1655	λ$^-$ *rph-1*	(97,98)
TL504	MG1655 Δ(*lac-ZYA-argF*) *U169 zah-735*::Tn*10*	P1(SH205) x MG1655 This laboratory
MC4100	*F*$^-$*araD139 Δ(argF-lac)U169 rpsL150 deoC1 relA1 rbsR ptsF25 flhD5301*	(99)
TL157	MC4100 *glpD3 glpR2 zce-727*::T*n10 plsX50*	(10)
AB201	MC4100 *plsX50 zce-727*::Tn*10*	P1(TL157) x MC4100 This laboratory
SH205	HfrC *phoA8 glpD3 glpR2 relA1 spoT1 pit-10 fhuA22 ompF627 fadL701* (λ) [Δ(*argF-lac*)*U169 zah-735*::Tn*10*]	(100)
TL125	HfrC *phoA8 glpD3 glpR2 relA1 spoT1 pit-10 fhuA22 ompF627 fadL701* (λ) *glpK*^{i} *plsB26 plsX50 gyrA zce-727*::Tn*10*	(10)
SS36	λSS36 lysogen of TL504	This work
SS77	λSS77 lysogen of TL504	This work
SS90	λSS90 lysogen of TL504	This work
SS144	λSS90 lysogen of TL504	This work
SS36R	λSS36 lysogen of RR1	This work
SS77R	λSS77 lysogen of RR1	This work
SS36X$^+$	λSS36 lysogen of MC4100	This work
SS36X50	λSS36 lysogen of AB201	This work
SS77X50	λSS36 lysogen of AB201	This work
SS36Xwt	SS36X$^+$ *zce-727*::Tn*10*	P1(TL125) x SS36X$^+$
SS77Xwt	SS77X$^+$ *zce-727::Tn10*	P1(TL125) x SS77X$^+$

Table 1: Strains of *E. coli* K-12 continued

Strain	Genotype	Derivation, Reference or Source
SS194	λSS170 lysogen of TL504	This work
SS196	λSS171 lysogen of TL504	This work
SS198	λSS172 lysogen of TL504	This work
SS231	λSS231 lysogen of TL504	This work
SS231F	λSS231F lysogen of TL504	This work
SS239	λSS239 lysogen of TL504	This work
SS239F	λSS239F lysogen of TL504	This work
SS241	λSS241 lysogen of TL504	This work
SS241F	λSS241F lysogen of TL504	This work
SS243	λSS243 lysogen of TL504	This work
SS243H	λSS243H lysogen of TL504	This work
SS244	λSS244 lysogen of TL504	This work
SS244G	λSS171 lysogen of TL504	This work
SS245	λSS245 lysogen of TL504	This work
SS245H	λSS245H lysogen of TL504	This work
SS247	λSS247 lysogen of TL504	This work
SS247E	λSS247E lysogen of TL504	This work
SS250	λSS250 lysogen of TL504	This work
SS250H	λSS250H lysogen of TL504	This work
SS250E	λSS250E lysogen of TL504	This work
SS260	λSS260 lysogen of TL504	This work
SS260H	λSS260H lysogen of TL504	This work
SS261	λSS261 lysogen of TL504	This work
SS261G	λSS261G lysogen of TL504	This work
SS262	λSS262 lysogen of TL504	This work
SS262N	λSS262N lysogen of TL504	This work
SS262L	λSS262L lysogen of TL504	This work
SS262H	λSS262H lysogen of TL504	This work
SS263	λSS263 lysogen of TL504	This work
SS263F	λSS263F lysogen of TL504	This work
SS264	λSS264 lysogen of TL504	This work
SS264D	λSS264D lysogen of TL504	This work
SS312	λSS312 lysogen of TL504	This work
SS312G	λSS312G lysogen of TL504	This work
SS333	λSS333 lysogen of TL504	This work
SS333H	λSS333H lysogen of TL504	This work
SS350	λSS350 lysogen of TL504	This work
SS350H	λSS350H lysogen of TL504	This work

Table 1: Strains of *E. coli* K-12 continued

Strain	Genotype	Derivation, Reference or Source
SS361	λSS361 lysogen of TL504	This work
SS361E	λSS361E lysogen of TL504	This work
SS370	λSS370 lysogen of TL504	This work
SS370F	λSS370F lysogen of TL504	This work
SS410	λSS410 lysogen of TL504	This work
SS410G	λSS410G lysogen of TL504	This work

Transformation of *E. coli* with plasmid DNA

Competent *E. coli* cells were made by a standard procedure using $CaCl_2$ and $MgCl_2$ described by Sambrook *et al.* (102). Approximately 150 µl of competent cells and 0.1 pmol of DNA were used for each transformation. A 30 minute incubation at 4°C and 2 minutes at 42°C were sufficient to allow the plasmid to enter the cell. The culture was then grown in LB for 1 hour at 37°C and plated on LB agar containing the appropriate antibiotic.

Transfection of *E. coli* with M13 RF DNA

M13 RF DNA was transfected into competent *E. coli* cells as follows. DNA and competent cells were combined and incubated at 4°C for 30 minutes and 2 minutes at 42° C. The transfected cells were then mixed with LB top agar before plating on LB agar plates.

Preparation of M13 RF DNA for cloning

M13 RF DNA was prepared for cloning using the large scale isolation procedure described by Maniatis *et al.* (103).

Homologous recombination between plasmid and λ DNA

Deriviatives of pRS415 (104) (see Table 4) were recombined with the phage λRS45 (see Table 6) as follows. A strain carrying the appropriate plasmid was used as the host for preparation of a 2-ml liquid lysate of λRS45 (101). Dilutions of this lysate were plated on a lawn of strain BW13745 (Δ*lacZ*) (see Table 1) on LB X-gal plates. When recombination events occurred at both the homologous *bla* sequences of the the plasmid and phage DNA and the homologous *lacZ* sequences of the plasmid and phage DNA, the promoter - *lacZ* fusion or promoter - attenuator - *lacZ* fusion was transfered to the phage DNA. The recombinant phage appeared as blue plaques and were selected. These phage were purified and propagated as high titer lysates. In most cases, for each

recombinant λ sought, two independent (but identically constructed) recombination lysates were made and used in the construction of λ lysogens.

Construction of single-copy λ lysogens

Lysogens were constructed using the recombinant λ phage described above. Briefly, 10 μl of λ lysate was plated on a lawn of host cells in which the lysogen was to be made. After 12 hours of growth at 37°C, surviving cells were picked from the lysed area and streaked on LB X-gal plates. Colonies were restreaked until they were found to be pure blue. For each strain, eight lysogens were selected and the β-galactosidase activities measured. (When two independent recombination lysates were made, four lysogens from each lysate were used.) In all cases, multiple-copy lysogens were identified because they had β-galactosidase activities several-fold higher than the majority of the lysogens. Multiple-copy lysogens were discarded. Lysogens created from the two identical recombinant phage lysates always had β-galactosidase activities that deviated from one another by no more than 10%.

MOLECULAR BIOLOGICAL TECHNIQUES

Dephosphorylation of linear DNA

Linear DNA to be used in cloning procedures was often dephosphorylated. Five units of Shrimp alkaline phosphatase was used in each reaction, according to the manufacturer's instructions.

Fill-in reaction

When required, the 5' overhang product of restriction enzyme digests was filled-in to create a blunt end. This was done using 13 U of Sequenase Version 2.0 from Amersham Life Sciences in the recommended buffer supplemented with 33 μM of each dNTP. The reaction was incubated for 5 minutes at room temperature.

Ligation reaction

For ligation reactions, 0.1 pmol of digested vector and 0.4 pmol of insert were usually used. T4 DNA ligase was used as suggested by the manufacturer's instructions.

Agarose gel electrophoresis

DNA was analyzed by electrophoresis on 0.8% to 2.0% agarose gels in 0.05 M Tris, 0.05 M boric acid, 0.01 M EDTA (TBE) buffer containing 0.5 μg/ml ethidium bromide, essentially as described by Sambrook *et al.* (105).

Extraction of DNA fragments

DNA was extracted from low melting agarose gels with the reagents found in either the Wizard PCR preps kit from Promega or the Qiaquick gel extraction kit from Qiagen (Chatsworth, CA) following the instructions provided by the manufacturer.

Isolation of DNA

Plasmid DNA was isolated using the materials in the Wizard Minipreps kit from Promega following the instructions provided by the manufacturer. M13 ssDNA was isolated for sequencing using a standard procedure described in the the Sequenase Version 2.0 DNA Sequencing kit protocol from Amersham Life Sciences.

Table 2: Oligonucleotides

(1)The pair of oligonucleotides served as a linker to construct pRS415L
(2)The pair of oligonucleotides was used in the cloning of the attenuator for the construction of pGA010
(3)The pair of oligonucleotides was used in the cloning of P_{N25} from pUHE2PN25tet040*01
(4)The pair of oligonucleotides was used in the cloning of P_{lacUV5} from λRS74
(5)Used in the sequencing of pRS415 derivitives
(6)The pair of oligonucleotides was used in the cloning of T_0 from pUHE2PN25tet040*01
(7)Used in the construction of M13XA117
(8)Used in the construction of M13XA111
(9)Used in the construction of M13XA110
(10)Used in the construction of M13XA112
(11)Used in the construction of M13XA114
(12)Used in the construction of M13XA115
(13)Used in the construction of M13XA113
(14)Used in the construction of M13XA116
(15)Used in an unsuccessful mutagenesis reaction

Number	Sequence(21)	Positions of Endpoints (if used in attenuator region)
105277	AATT*CCCGGG*AAAGCTTGAGTGGCCAGAGG(1)	
105431	GATCCCTCTGGCCACTCAAGCTTTCCCGGG*G*(1)	
05232	TTATGGATCCATGGCGTCGGAATTGCCGA(2)	1975-1947
91568	ATGAAGATCTGACCGCAGTCACCAGCC(2)	1641-1659
224495	CTGTCGAATTCAGAAATCATAAAAAATTTATTTGC(3)	
96291	CTTTAAAAGCTTCCCAATTCTGTGTGAAATTCT(3)	
224450	GATCGGAATTCTCACTCATTAGGCACCC(4)	
223891	GTTGTAAGCTTCCTGTGTGAAATTGTTATC(4)	
104362	TGGCGGCTGTGGGATTAACTGCG(5)	
207202	GGATTTTGGCGCCGACTAGTGCTTGGATTC(6)	
224389	TGGGGCTCGAGAGCTCGCTTGGACTCCT(6)	
336877	TGGCCCTTCCGTGACCAGGCACTGAATTC(7)	1891-1906
162570	CCAAACCGGGGGAGGACGATACCATGACACGTCTA(8)	1809-1843
162526	CCAAACCGGGACGTGACGATACCTAGACACGTCTA(9)	1809-1843
192071	CACGTCTAACCCGGCGTTAGATGT(10)	1836-1860
329732	AAGCTTAGTGAGGATGACCAAACCGGGCGG(11)	1770-1821
329933	TAACCCTGGCCTATCTGCTCATGGAGG(12)	1842-1869
333408	CGGCCAGTGCCAAGCTTTTCCCCAGGCAAC(13)	3' end 1798
336822	CTGGCGTTAGATGTCGACAGTGCCTGCAGC(14)	1847-1902
333532	CACGTCTAACGGGCCCGTTAGATGTC(15)	1836-1861
386446	ACCAAGCTTCGTCTAACCCTGGC	1829-1851
C300	ATCGGATCCGCCCGGTTTGGTC(	1828-1807
372689	ACGGGATCCTTAGACGTGTCAAGG	1853-1830
386243	CCAGGATCCCCTCCCATGACATC	1878-1858
386480	TAAAGATCTCCTAGGTGCCGCGCCCC	
258763	AGAGGATCCTAACTAACTAGCGAT)	

DNA sequencing

Plasmid DNA or M13 ssDNA was used as templates for the dideoxynucleotide chain termination sequencing method first described by Sanger *et al*. (106). Sequencing was done using Sequenase Version 2.0 and DNA sequencing reagents from Amersham Life Sciences by the method described in the manufacturer's instructions. The reactions were analyzed by electrophoresis on 6% polyacylamide gels with 7 M urea in TBE buffer.

Polymerase chain reaction

Approximately 100 ng of plasmid DNA was used as a template for DNA amplification. The reactions were done using the reagents from the GeneAmp PCR kit and a GeneAmp PCR 9600 thermocycler (Perkin Elmer Cetus, Norwalk, CT) following the manufacturer's instructions. Primers used in these reactions are listed in Table 2. PCR fragments were purified from an agarose gel as described above.

Site-directed mutagenesis

All site-directed mutations within the attenuator region were constructed using the method first described by Kunkel and co-workers (92). M13XA100 (see Table 3) ssDNA was used as a template for all reactions. The first step was to enrich the M13 DNA with uridine. This was done by first infecting log phase RZ1032 cells (see Table 1) with 20 µl of M13XA100-containing supernatant in LB media containing 250 ng/ml of uridine. Since RZ1032 (*dut ung*) is deficient in dUTPase and uracil *N*-glycosylase, uridine will occasionally be incorporated into the M13XA100 DNA in the place of thymidine. The culture supernatant from this infection was harvested, and this "uridine-enriched" M13 was used to repeat the infection of RZ1032. This process was repeated until plate titering of the uridine-enriched M13 on RZ1032 cells showed 10^6-fold more phage then titering on DH5αF' cells. This difference in titer is a reflection of the fraction of M13 DNA in the supernatant that contains uridine, and can therefore not infect DH5αF' cells.

The next step was to create M13 dsDNA that carried a specific mutation. Single-stranded M13 DNA was isolated from the uridine-enriched lysate by the procedure described above. Eleven picomoles of the desired phosphorylated oligonucleotide (see Table 2), 500 ng of ssDNA, and 2.0 µl Sequenase buffer (Amersham Life Sciences) were combined in a final volume of 10 µl. The mix was heated to 65°C for 5 minutes and annealed by cooling to 25°C over a two hour time period. The reaction to synthesize the complementary strand of DNA was then carried out by adding each of the four dNTPs to a final concentration of 50 µM, ATP to a final concentration of 1 mM, 13 U of Sequenase (Amersham Life Sciences), and 800 U of T4 DNA ligase (New England Biolabs). The mix was incubated for 15 minutes at 37°C, 5 minutes at 65°C, then placed on ice. The newly synthesized dsDNA was then transfected into competent DH5αF' cells.

One strand of this dsDNA contained uridine (the uridine-enriched template) and the other did not (the strand synthesized *in vitro* that contained the mutation). After infection into DH5αF', uridines from the uridine-containing strand were released by uracil *N*-glycosylase, producing apyrimidinic sites. Since DNA containing apyrimidinic sites is biologically inactive, the majority of the progeny phage from this transfection

came from the *in vitro* strand that contained the mutation. Sequencing was used to find phage clones containing the expected mutations.

M13 phage derivatives

All M13 phage constructed for this work are listed in Table 3. The *Hin*dIII to *Bam*HI fragment of pGA010 was cloned into the same sites of M13mp19 or M13mp18 (95) to form M13XA005 and M13XA100, respectively. This fragment encodes bases 1770-1965 of the *rpmF-plsX-fab* operon. This region contains the "*plsX* attenuator region" and will be referred to by this name throughout this manuscript. The base numbers for the operon are the same used by Won Oh (8). In her system, the first base of the *Pst*I site upstream of *rpmF* is 1, the first base of the *rpmF* reading frame is 1578, and the first base of the *plsX* reading frame is 1832.

M13XA110 through M13XA117 contain the *plsX* attenuator region with various mutations. All mutations were made using M13XA100 as a template for the site-directed mutagenesis procedure described by Kunkel and co-workers (92). Oligonucleotides used to make each mutant are listed in Table 3, along with the mutation. For describing mutations in the attenuator region, a base and number are used. The first base of the attenuator region is the first adenosine residue of the *Hin*dIII site at 1770, and is called A-1. The C-50G mutation denotes that the C at base 50 is changed to G. Deletions are signified by a Δ. This notation method is used throughout this manuscript.

Plasmids - General

All plasmids that are not derivatives of pRS415 are listed in Table 4. The plasmid pGA010 was constructed by PCR amplification of the attenuator region using primers 05232 and 91568 (see Table 2) with pWO603 as a template. The product was digested with *Hin*dIII and *Bam*HI and cloned into the same sites of pGEM3Z.

Plasmids - Derivatives of pRS415

Table 5 contains all plasmids derived from pRS415 used in this study. To expand the versatility of the multiple cloning site of pRS415, pRS415L was constructed by annealing oligonucleotides 105277 and 105431 to one another (see Table 2) and cloning them into the multiple cloning site of pRS415 between the *Eco*RI and *Bam*HI sites. The multiple cloning site of pRS415L contains *Eco*RI, *Sma*I, *Hin*dIII, *Msc*I, and *Bam*HI sites.

The plasmid pDYA015 was constructed by cleaving pRS415L at the *Sna*BI and *Nru*I sites. An *Xho*I linker from Promega (Madison, WI) was cloned in by the method described by the manufacturer. This procedure deleted a third of *lacY* and all of *lacA*, thus eliminating any problems that may occur due to expression of the *lacY*- and *lacA*-encoded proteins from the plasmid.

Table 3: M13 phage deriviatives

[(1)]M13XA100 was used as a template for site-directed mutagenesis (92)

Phage	Method of Construction	Change in *plsX* Attenuator Region (if any)
M13XA005	*Hin*dIII to *Bam*HI attenuator region from pGA010 cloned into M13mp19	
M13XA100	*Hin*dIII to *Bam*HI attenuator region from pGA010 cloned into M13mp18	
M13XA110	Primer 162526 used[(1)]	C-50A, G-51C, C-53T, T-64A
M13XA111	Primer 162570 used[(1)]	C-50G, G-52A, C-53G, T-63A
M13XA112	Primer 192071 used[(1)]	ΔT79
M13XA113	Primer 333408 used[(1)]	ΔT5-A14
M13XA114	Primer 329732 used[(1)]	ΔT16-A37
M13XA115	Primer 329933 used[(1)]	G-83C, T-84A, T-85A, A86-T, G-87C, A-88T, T-89G, G-90C
M13XA116	Primer 336822 used[(1)]	ΔA93-T118
M13XA117	Primer 336877 used[(1)]	ΔA122-G137

High levels of transcription into the origin of replication of a plasmid can decrease copy number of the plasmid, making preparation of large amounts of the plasmid difficult. For this reason, the plasmid pSS1 was constructed as follows. The t_o terminator was amplified using primers 207202 and 224389 (see Table 2) with pUHE2PN25tet040*01 (see Table 4) as the template. The product of this reaction was digested with *Nar*I and *Xho*I and cloned into pDYA015 at the same sites. This terminator halts transcription from *lacZ* into the origin of replication.

Table 4: Plasmids - General

(1) The plasmid was acquired from Lutz and Bujard, and the sequence of P_{N25} is found in the reference. This promoter is semi-synthetic, containing the -10 and -35 sequences of wild-type P_{N25} and TetR binding sites.

Plasmid	Description and/or Reference
pGEM3Z	Promega (Madison, WI)
pGA010	*Hind*III to *Bam*HI attenuator fragment in pGEM3Z
pUHE2PN25tet040*01	(107), R. Lutz, H. Bujard(1)
pALS10	wild-type *relA* (108)
pALS14	truncated *relA* (inactive) (108)
pBAD22	Control vector for pHC122 (109)
pHC122	Truncated thioesterase gene (*'tesA*) in pBAD22 (110)
pBR322	Control vector for pFRD84 (111)
pFRD84	*frdABCD* in pBR322 (112)
pTL61T	RNase III site derived from this vector (113)
pWO632	*Hind*III to *Nsi*I fragment (1770-3319) of *rpmF-plsX-fab operon* in pGEM4 (8)
pWO603	*Xho*I to *Nsi*I fragment (1215-3319) of *rpmF-plsX-fab operon* in pGEM4 (8)
pMS421	Encodes *lacI*^{q} and spc^R, SC101 origin of replication (114)
pWO401	*Sal*I to HindIII fragment (711-1770) of *rpmF-plsX-fab operon* in pGEM4 (8)

Table 5: Plasmids - Derivatives of pRS415

Plasmid	Method of Construction or Reference
pRS415	(104)
pRS415L	Oligos 105277, 105431 used as linker in MCS
pDYA015	pRS415L with region between *Sna*BI and *Nru*I removed, replaced by *Xho*I linker
pSS1	pDYA015 with *Xho*I to *Nar*I removed, replaced by t_0 terminator from pUHEPN25tet040*01
pSS20	P_{lacUV5} in MCS of pSS1
pSS63	*Hin*dIII to *Bam*HI attenuator fragment in pSS20
pSS160	*Eco*RV to *Bam*HI deleted from pSS20
pSS161	*Eco*RV to *Bam*HI deleted from pSS63
pSS36	P_{N25} promoter in MCS of pSS1
pSS77	*Hin*dIII to *Bam*HI attenuator fragment in pSS36
pSS90	*Sal*I to *Hin*dIII *rpmF* fragment (containing $P_{1,2,3}$) in pSS1
pSS144	*Hin*dIII to *Bam*HI attenuator fragment in pSS90
pSS170	Attenuator fragment from M13XA110 in pSS36
pSS171	Attenuator fragment from M13XA111 in pSS36
pSS172	Attenuator fragment from M13XA112 in pSS36
pSS231	Attenuator fragment with A-75G mutation in pSS36
pSS239	Attenuator fragment with C-50T mutation in pSS36
pSS241	Attenuator fragment with A-88G, T-128C mutations in pSS36
pSS245	Attenuator fragment with A-161G mutations in pSS36
pSS244	Attenuator fragment with T-9C, C-62G mutations in pSS36
pSS243	Attenuator fragment with A-60G mutation in pSS36
pSS247	Attenuator fragment with G-47T mutation in pSS36
pSS260	Attenuator fragment from M13XA113 in pSS36
pSS261	Attenuator fragment from M13XA114 in pSS36
pSS262	Attenuator fragment from M13XA115 in pSS36
pSS263	Attenuator fragment from M13XA116 in pSS36
pSS264	Attenuator fragment from M13XA117 in pSS36
pSS312	Attenuator fragment with ΔA1-C69 mutation in pSS36
pSS350	Attenuator fragment with ΔC53-T196 mutation in pSS36
pSS361	Attenuator fragment with ΔC76-T196 mutation in pSS36
pSS370	Attenuator fragment with ΔG101-T196 mutation in pSS36
pSS333	pSS36 with RNase III site downstream of attenuator
pSS410	pSS77 with RNase III site downstream of attenuator
pSS421	*Hin*dIII to *Bam*HI attenuator fragment in pSS1

The *lacUV5* promoter was cloned into pSS1 to form pSS20, as described below. Amplification of P_{lacUV5} was achieved using primers 224450 and 223891 (see Table 2), with λRS74 (see Table 6) DNA as the template. This PCR product was digested with *Eco*RI and *Hin*dIII and cloned into pSS1 at the same sites. A similar method was used to construct pSS36, where the P_{N25} promoter was cloned into pSS1. Amplification of P_{N25} was done using primers 224495 and 96291 (see Table 2) with pUHE2PN25tet040*01 (see Table 4) as the template. Again the product was digested

with *Eco*RI and *Hin*dIII and cloned into pSS1 at the same sites. In both cases, a promoter - *lacZ* transcriptional fusion was made.

The plasmid pSS90 was also constructed by cloning a promoter region into pSS1, but in this case *rpmF-plsX-fab* operon promoters were used. P_1, P_2, and P_3 of the operon are located between *Sal*I (711) and *Hin*dIII (1770). There is some evidence that two other promoters, P_4 and P_5, may also lie in this region (8), though they have not been mapped. This 1059 bp region was cloned from pWO401 (see Table 4) by digesting with *Sal*I and *Hin*dIII. The 5' overhang of *Sal*I site was filled-in and the promoters cloned into pSS1 between *Sma*I and *Hin*dIII. Again, a promoter - *lacZ* transcriptional fusion was made. The operon promoters in this fusion will be referred to as "$P_{1,2,3}$," although additional promoters may be present in this construct.

The *plsX* attenuator fragment was cloned into plasmids pSS20, pSS36, and pSS90 as follows. The attenuator region was cloned out of pGA010 using *Hin*dIII and *Bam*HI and this fragment was cloned into the same sites of pSS20, pSS36, and pSS90, to yield pSS63, pSS77, and pSS144, respectively. In each construct, a promoter - *plsX* attenuator - *lacZ* transcriptional fusion was created. It is important to note that pSS90 carries bases 711 to 1770 of the operon and pSS144 carries bases 711 to 1965. By comparing the levels of β-galactosidase in these strains, the effect of the region between 1770 and 1965 on transcriptional expression can be determined.

The pSS160 and pSS161 plasmids were constructed in similar ways. Both pSS20 and pSS63 were digested with *Eco*RV and *Bam*HI, and the 5' overhangs filled-in and ligated, yielding pSS160 and pSS161, respectively. This procedure deletes 1200 bp from the 5' end of *lacZ* (including the ribosome binding site), eliminating expression of β-galactosidase. Attenuator mRNA is expected to be expressed at high levels from pSS161, while pSS160 is the control plasmid.

The *Hin*dIII to *Bam*HI attenuator fragments from M13XA110, M13XA111, and M13XA112 (see Table 3) were cloned into the same sites of pSS36 to form pSS170, pSS171, and pSS172, respectively.

Eight different mutations in the attenuator region were constructed by mutagenic PCR (described below in the section entitled **Random mutagenesis by PCR and phenotypic screening of the products**). The PCR fragments containing potential mutations were digested with *Hin*dIII and *Bam*HI and cloned into the same sites of pSS36. The specific mutations were identified by sequencing, and the mutations for pSS231, pSS239, pSS241, pSS245, pSS250, pSS244, pSS243, and pSS247 are listed in Table 5.

The *Hin*dIII to *Bam*HI attenuator fragments from M13XA113, M13XA114, M13XA115, M13XA116, and M13XA117 (see Table 3) were cloned into the same sites of pSS36 to form pSS260, pSS261, pSS262, pSS263, and pSS264, respectively.

Transcriptional fusions with small portions of the *plsX* attenuator were also made. Amplification of a downstream portion of the attenuator was done using primers 386446 and 05232 (see Table 2), with pSS77 as the template. The product was digested with *Hin*dIII and *Bam*HI and cloned into the same sites of pSS36, forming pSS312. Three

constructs were also made with one of three upstream portions of the attenuator. Amplification was done using primer 224495 and C300, 372689, or 386243 (see Table 2), with pSS77 as the template. Each of the PCR products encode both the P_{N25} promoter and an increasingly larger portion of the attenuator. They were digested with *Eco*RI and *Bam*HI and cloned into pSS1 at the same sites. The product from primer C300 was used to make pSS350, the product from primer 372689 was used to make pSS361, and the product from primer 386243 was used to make pSS370. Each of these constructs was checked by sequencing to ensure the proper sequence was intact, and the mutations are listed in Table 5.

Two constructs were made with an RNase III site just downstream of the attenuator region. Using pTL61T (see Table 4) as a template, primers 258763 and 386480 (see Table 2) were used to amplify the DNA coding for an RNase III site. The PCR product was digested with *Bam*HI and *Bgl*II and cloned into the *Bam*HI site of pSS36 and pSS77, forming pSS333 and pSS410, respectively. Both constructs were checked by sequencing to ensure a single RNase III site was cloned in the correct direction.

The *Hin*dIII to *Bam*HI attenuator region from pGA010 (see Table 4) was cloned into pSS1 at the same sites to form pSS421. This fused the attenuator region to *lacZ* and was used to determine if there is a promoter in this region.

Lambda phage derivatives

All λ phage used in this work are listed in Table 6. The homologous recombination between plasmid and phage DNA was done as described above. In most cases, the homologous recombination was done in duplicate cultures, ensuring that two independently created phage were isolated (i.e. λSS231 and λSS231F).

Strains of *E. coli* K-12

All strains used for this work are described in Table 1. P1 transductants and λ lysogens were made as described above. In most cases where λ lysogens were isolated, two identical (but independently created) recombinant phage were constructed (i.e. λSS231 and λSS231F). When this was done, single-copy lysogens using each of the lysates where made and yielded strains with β-galactosidase activities within 10% of one another. This helped to ensure that no phage construct was the result of contamination or of a random recombination event. Data reported in the Results section is an average of assay data from both identical lysogens (i.e. SS231 and SS231F) and listed under the first strain name (i.e. SS231).

***In vitro* transcription**

The transcript for *in vitro* secondary stucture analysis of the *plsX* attenuator region was synthesized using pWO632 (8) (see Table 4) as a template for *in vitro* transcription. This plasmid carries a portion of the *rpmF-plsX-fab* operon from the *Hin*dIII site at 1770 bp (the upstream end of the attenuator) to the *Nsi*I site at 3319 bp. In addition, a T7 RNA polymerase promoter on pGEM4 initiates transcription 10 bp upstream of the *Hin*dIII site of the attenuator region. The template plasmid was linearized with *Eco*RI cleaving the plasmid once at the native *Eco*RI site within *plsX*, located one base downstream of the

Table 6: Lambda phage derivatives

Phage	Method of Construction or Reference
λRS45	(104)
λSS74	(104)
λSS36	Homologous recombination between pSS36 and λRS45
λSS77	Homologous recombination between pSS77 and λRS45
λSS90	Homologous recombination between pSS90 and λRS45
λSS144	Homologous recombination between pSS144 and λRS45
λSS194	Homologous recombination between pSS170 and λRS45
λSS196	Homologous recombination between pSS171 and λRS45
λSS198	Homologous recombination between pSS172 and λRS45
λSS231	Homologous recombination between pSS231 and λRS45
λSS231F	Homologous recombination between pSS231 and λRS45
λSS239	Homologous recombination between pSS239 and λRS45
λSS239F	Homologous recombination between pSS239 and λRS45
λSS241	Homologous recombination between pSS241 and λRS45
λSS241F	Homologous recombination between pSS241 and λRS45
λSS243	Homologous recombination between pSS243 and λRS45
λSS243H	Homologous recombination between pSS243 and λRS45
λSS244	Homologous recombination between pSS244 and λRS45
λSS244G	Homologous recombination between pSS244 and λRS45
λSS245	Homologous recombination between pSS245 and λRS45
λSS245H	Homologous recombination between pSS245 and λRS45
λSS247	Homologous recombination between pSS247 and λRS45
λSS247E	Homologous recombination between pSS247 and λRS45
λSS250	Homologous recombination between pSS250 and λRS45
λSS260	Homologous recombination between pSS260 and λRS45
λSS260H	Homologous recombination between pSS260 and λRS45
λSS261	Homologous recombination between pSS261 and λRS45
λSS261G	Homologous recombination between pSS261 and λRS45
λSS262	Homologous recombination between pSS262 and λRS45
λSS262H	Homologous recombination between pSS262 and λRS45
λSS263	Homologous recombination between pSS263 and λRS45
λSS263F	Homologous recombination between pSS263 and λRS45
λSS264	Homologous recombination between pSS264 and λRS45
λSS264D	Homologous recombination between pSS264 and λRS45
λSS312	Homologous recombination between pSS312 and λRS45
λSS312G	Homologous recombination between pSS312 and λRS45
λSS333	Homologous recombination between pSS333 and λRS45
λSS333H	Homologous recombination between pSS333 and λRS45

Table 6: Lambda phage derivatives continued

Phage	Method of Construction or Reference
λSS350	Homologous recombination between pSS350 and λRS45
λSS350H	Homologous recombination between pSS350 and λRS45
λSS361	Homologous recombination between pSS361 and λRS45
λSS361E	Homologous recombination between pSS361 and λRS45
λSS370	Homologous recombination between pSS370 and λRS45
λSS370F	Homologous recombination between pSS370 and λRS45
λSS410	Homologous recombination between pSS410 and λRS45
λSS410G	Homologous recombination between pSS410 and λRS45

last predicted stem-loop structure of the attenuator region. The transcript produced from this linearized vector ends two nucleotides from the 3' end point of the native mRNA, as mapped by S1 nuclease analysis (8). The transcription reaction was performed using 1 μg of linearized template DNA plus T7 RNA polymerase and other reagents for *in vitro* transcription from Ambion (Austin, TX), following the manufacturer's instructions. The transcript made corresponded to the predicted size, 159 nts; RNA transcribed from the *rpmF-plsX-fab* operon comprised 149 nts, while the first 10 nts of the 5' end were encoded by the vector.

Radiolabeling of RNA

In vitro RNA transcripts were radiolabeled with ^{32}P phosphate on the 5' end. This was accomplished by first dephosphorylating the 5' end of approximately 35 pmols of transcript using 5 units of shrimp alkaline phosphatase. The reaction proceded for one hour at 37°C. The enzyme was then denatured at 65°C for 30 minutes. The dephosphorylated RNA was precipitated with one-tenth volume of 3 M sodium acetate in DEPC-treated water and four volumes of ethanol. The 35 pmol of dryed RNA were mixed with 10 units of T4 polynucleotide kinase and 525 μCi of [γ-^{32}P]ATP (150 mCi/mL) in a final volume of 35 μl. This reaction was incubated for one hour at 37°C before 1 volume of load buffer (5 mM Tris, 5 mM Boric Acid, 1 mM EDTA, 0.01% xylene cyanol, 0.01% bromophenol blue and 10 M urea) was added and the reaction placed at -70°C.

The next step was to purify the labeled RNA, in order to ensure that only full-length transcripts were used in the secondary structure analysis. The labeled RNA/load buffer solution was electrophoresed on a 6% polyacrylamide gel containing 7 M urea and TBE buffer. The gel was then covered with plastic wrap and marked several times with iridescent paint. Full-length labeled RNA was located by placing a piece of x-ray film on the plastic wrap covered gel. After a 30-second exposure, the film was developed and the location of the RNA was determined, using the paint spots as reference points. The RNA was cut from the gel and the slice crushed in an microfuge tube using a pestal. Approximately 300 μl of elution buffer (1 mM Tris-HCl (pH 7.3), 1 mM EDTA, and 150 mM NaCl in DEPC-treated water) was then added and the mix was frozen and thawed at least three times (115). After centrifugation, the RNA-containing supernatant was removed and precipitated with one-tenth volume of 3 M sodium acetate in DEPC-treated

water and four volumes of ethanol. The dried RNA was resuspended in DEPC-treated H_2O.

Analysis of RNA secondary structure

The secondary structure of the *plsX* attenuator mRNA was determined by performing RNA sequencing reactions and comparing them to the cleavage bands resulting from various treatments with ribonucleases. Four individual sequencing reactions were done using RNases T1, U2, PhyM, or *B. subtilis*, from Pharmacia Biotech. Sequencing reactions using RNase T1 or RNase PhyM were performed using 3 µl of Buffer 1 (33 mM sodium citrate pH 5.0, 1.7 mM EDTA, 0.04% xylene cyanol, 0.08% bromophenol blue, 1 mg/ml carrier tRNA and 7 M urea). For sequencing reactions using RNase U2, 3 µl of Buffer 2 (33 mM sodium citrate pH 3.5, 1.7 mM EDTA, 0.04% xylene cyanol, 0.08% bromophenol blue, 1 mg/ml carrier tRNA and 7 M urea) was used. Finally, for reactions containing RNase *B. cereus*, 3 µl of Buffer 3 (33 mM sodium citrate pH 5.0, 1.7 mM EDTA, and 1 mg/ml carrier tRNA) was used. Also included in each of the reactions was 1 µl of labelled *plsX* attenuator mRNA (100,000 cpm/µl), which was made as described above. Before any RNase was added, the labelled RNA/buffer mix was incubated at 55°C for 7 minutes. After the addition of 1 µl of diluted RNAse, the reaction was incubated at 55°C for 12 minutes. Three microliters of load buffer (5 mM Tris, 5 mM boric Acid, 1 mM EDTA, 0.01% xylene cyanol, 0.01% bromophenol blue and 10 M urea) was then added before the reaction was placed at -70°C. The amount of each RNase needed to give partial digestion of the labelled RNA substrate was determined emperically. For the sequencing reactions in this study, 0.14 U of T1, 0.67 U of U2, 0.125 U of *B. cereus*, and 15 U of PhyM were used. Since the sequencing reaction is not clear at every base, two alkaline hydrolysis ladders were also prepared, facilitating the interpretation of the cleavage pattern. Alkaline hydrolysis reactions contained 2 µl of labelled *plsX* mRNA (100,000 cpm/µl), 1 µl of 5 mg/ml carrier tRNA, and 1 µl of alkaline hydrolysis buffer (150 mM $NaHCO_3$, 150 mM Na_2CO_3, and 1 mM EDTA). This reaction was incubated at either 2.5 or 4 minutes at 95°C, then set on ice, where 3 µl of load buffer was added.

Reactions were performed in a similar way to analyze secondary structure, with one of four RNases used in each reaction. RNases T1, PhyM, and *B. cereus*, described above, all cleave only single-stranded RNA. On the other hand, RNase V1, acquired from Phamarcia Biotech, cleaves predominately at double-stranded RNA. These RNases were used in reactions consisting of 1 µl of buffer (60 mM Tris pH 7.3, 60 mM $MgCl_2$, 300 mM KCl), 2 µl of 5 mg/mL carrier tRNA, 1 µl of labelled *plsX* mRNA (100,000 cpm/µl), and 1 µl of dilute RNase. Before any RNase was added, the labelled RNA/carrier RNA/buffer mix was incubated at 55°C for 7 minutes, 37°C for 4 minutes, and 4°C for 2 minutes. After the addition of the diluted RNAse, the reaction was incubated at 37°C for 12 minutes (and 95°C for 3 minutes to denature the RNase). Three microliters of load buffer (5 mM Tris, 5 mM boric Acid, 1 mM EDTA, 0.01% xylene cyanol, 0.01% bromophenol blue and 10 M urea) was then added. In order to locate all possible cleavage sites, two different amounts of each RNase were used (with the exception of PhyM). Again, the appropriate amount of each RNAse was determined empirically; 0.1 U and 0.2 U of T1, 0.1 U and 0.2 U of B. cereus, 0.007 and 0.0035 U of V1, and 15 U of PhyM were used for this work.

All reactions performed for sequencing or secondary structure analysis were co-electrophoresed on either a 10 or 15% polyacylamide/ 7 M urea gel in TBE. After electrophoresis was complete, the gel was covered with plastic and placed on x-ray film for 24 hours. By comparing the cleavage specificity of single-stranded and double-stranded RNases to computer generated mRNA folding patterns, the RNA secondary structure could be predicted.

Random mutagenesis by PCR and phenotypic screening of the products

Random mutations in the *plsX* attenuator region were made by the modified polymerase chain reaction initially described by Leung and coworkers (116). The template for this reaction was pWO603 (8) (see Table 4) and primers 05232 and 91568 (see Table 2) were used to amplify and mutagenize the attenuator region. Three different PCR reactions were done: one with a five-fold higher concentration of G than A (1000 μM versus 200 μM), another with 500 μM $MnCl_2$, and a third with both the higher G concentration and $MnCl_2$. Both uneven nucleotide concentrations and Mn^{2+} ions decrease the fidelity of *Taq* DNA polymerase.

The products from these reactions were digested with *Hin*dIII and *Bam*HI and cloned into the same sites of pSS36 (see Table 5). (Each of the three PCR products was used in a separate ligation reaction.) These constructs were then transformed separately into the strain RL22 (see Table 1). All of the transformants were grown in single cultures, and plasmid DNA was isolated. These plasmid preparations, potentially containing many different mutations, were then transformed into SP2 (see Table 1) for screening. Both of these transformations were necessary because, while DNA is easily transformed into RL22, the strain cannot be used to do the phenotypic screening because plasmid copy number is too high. Alternatively, SP2 (*pcnB*) carries fewer copies of plasmids and is therefore suitable for screening, but it cannot be used to transform a ligation reaction. Colonies carrying mutated attenuators were identified by plating on MacConkey-lactose plates. The most intensely red colonies, presumably expressing elevated β-galactosidase due to increased transcription through the attenuator and into the *lacZ* gene, were selected. Elevated β-galactosidase activity was confirmed by enzyme assays and the attenuator mutations were characterized by DNA sequence analysis.

BIOCHEMICAL TECHNIQUES

Denaturing gel electrophoresis

Proteins were electrophoresed on 15% SDS-polyacrylamide gels as described by Laemmli (117).

Determination of protein concentration

The method first described by Bradford (118) was used. A standard curve using 0 to 3.0 μg of bovine serum albumin was routinely made.

Assay of thioesterase activity

Thioesterase activity was determined in the same basic way as described by Barnes (119). A sufficient amount of log phase cells was lysed by sonication and resuspended in 60 mM potassium phosphate, pH 7.4. Each assay consisted of cell extract, 14 μM palmitoyl-CoA, 80 μg/ml BSA, and 100 μM 5,5'-dithiobis(2-nitrobenzoic acid) (DTNB), in 60 mM potassium phosphate, pH 7.4. Assays were conducted for 2.5

minutes at 25°C using three different amounts of cell extract. The change in absorbance at 412 nm was measured in order to follow the reduction of DTNB and concentration was calculated using a molar extinction coefficient of 13,600 $M^{-1}cm^{-1}$. A control was also done in which palmitoyl-CoA was excluded, in order to measure the contribution of cell extract to the reduction of DTNB.

Assay of β-galactosidase activity

β-galactosidase activity was determined essentially as described by Miller (120) with the considerations proposed by Giacomini *et al*. (121). Overnight cultures were regularly diluted 1/100 into the same medium used in the overnight and grown into log phase. The production of ONP by β-galactosidase was quantitated by measuring absorbance at 420 nm, using an extinction coefficient of 4500 $M^{-1}cm^{-1}$. For some experiments, the log phase cultures were lysed by 1.5 minute sonication and enzyme activity is expressed as nmol of *o*-nitrophenol produced per min per milligram of lysate protein (U/mg). Protein concentration was determined as described above. In other experiments, the activity is expressed as Miller Units (MU). In this case, cells were lysed with 10 µl of 0.1% SDS and 20 µl of chloroform for 10 minutes at 30°C. Protein concentrations were estimated by measuring culture optical density at 578 nm. Duplicate assays were always done with incubation times of between 10 and 20 minutes on at least two different days.

The following formulas were used to calculate U/mg:

$$\text{Specific Activity} = \frac{\text{nmols of ONP}}{t \times \text{vol} \times [\text{protein}]}$$

t = time (minutes)
vol = volume of cell extract in assay (µL)
[protein] = protein concentration (mg/µl)
nmols of ONP described below

The amount of ONP produced was determined by measuring A_{420} and using the formula below.

$$A_{420} = \varepsilon \times c \times l$$

$$\text{mols} = \frac{A_{420} \times \text{vol}}{\varepsilon \times l}$$

A_{420} = Absorbance of assay at 420 nm
ε = extinction coefficient = 4500 $M^{-1}cm^{-1}$
c = concentration of ONP (M)
l = length (cm)
mols = mols of ONP
vol = assay volume (L)

The formula below was used to determine Miller Units of activity:

$$\text{MU} = \frac{A_{420} \times 800}{OD_{578} \times t \times \text{vol}}$$

A_{420} = Absorbance of assay at 420 nm
OD_{578} = Opitcal density of resuspended cells at 578 nm
t = time (minutes)
vol = volume of cell extract (ml)

Using approximations for cell optical density, protein, and A_{600} suggested by Miller *et al.* (120),

10^9 cells = 150 μg protein OD_{600} of 1.4 = 10^9 cells

1 nmol of ONP/mL = 0.0045 A_{420} $OD_{600} = OD_{578}$

Miller Units can be converted to Specific Activity.

$$U/mg \approx 3.5\ MU$$

CHAPTER 3: RESULTS

LOCALIZATION OF THE *PLSX* ATTENUATOR

Messenger RNAs encoding the ribosomal protein L32 have 3' endpoints that lie within the 5' end of *plsX*. Data from S1 nuclease analysis show the 3' ends correspond to bases 1918, 1919, and 1921 of the operon and that some transcripts read through the terminator located in this region (8). Since transcription termination is inefficient at this site, termination may be regulated, and so this region is refered to as a transcriptional attenuator. The *Xho*I (1215) to *Pst*I (2009) region of the *rpmF-plsX-fab* operon has a lower promoter activity than the *Xho*I (1215) to *Hin*dIII (1770) region (8). These data imply that at least a portion of the attenuator lies between bases 1770 and 2009, but do not address the possiblity that a region between bases 1215 and 1770 influences attenuator activity. To determine the location of the attenuator, transcriptional fusions containing different portions of the region were constructed and the β-galactosidase activities of strains carrying these fusions were measured.

The first step was to quantitate the effect of the attenuator on the transcriptional expression of downstream genes. Transcriptonal fusions of the operon promoters, P_1, P_2, and P_3, (with or without the attenuator) to *lacZ* were constructed, integrated into the chromosome as single-copy lysogens, and the β-galactosidase activities were measured (Figure 7). "Percent Expression" is a quantification of the effect of the attenuator on expression of downstream genes. This decrease in expression could potentially be due to transcriptional termination or mRNA instability caused by the attenuator region. Percent expression is calculated by dividing the β-galactosidase activity from the strain containing the promoter-attenuator-*lacZ* fusion (in this case SS144) by the activity of the strain containing the control fusion (in this case SS90) and multiplying by 100. This method of expressing the effect of the attenuator is used throughout the Results section. To determine if any operon sequences upstream of base 1770 are needed for the attenuator to function normally, strains containing either P_{N25}-*lacZ* or P_{N25}-attenuator-*lacZ* transcriptional fusions were used. The results are also listed in Figure 7.

The above results show cultures of SS144 (encoding bases 711 to 1965) and SS77 (encoding bases 1770 to 1965) both expressed β-galactosidase at a level that is 26% of the control strains. No change in attenuator activity was seen when the bases between 711 and 1770 were replaced by P_{N25}. The data for SS36, SS77, SS90, and SS144 therefore show that the attenuator region lies between bases 1770 and 1965 and that it mediates a 3.8-fold decrease in expression of the downstream *lacZ* gene.

SECONDARY STRUCTURE ANALYSIS

The secondary structure of the *plsX* attenuator region mRNA was probed using both single-stranded (ss)-specific and double-stranded (ds)-specific ribonucleases. RNases T1, U2, *B. cereus,* and PhyM were used to identify regions that are single-stranded under native conditions while RNase V1 was used to identify regions that are double-stranded under these conditions. In the digestions, two amounts of each enzyme were used, in order to probe all possible cleavage sites. Samples were electrophoresed

Strain	Region of the Operon (bases)	β-Galactosidase Activity (U/mg)	Percent Expression
SS90 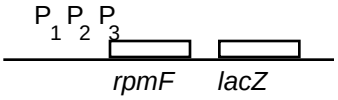	711-1770	6900 +/- 717	--------
SS144 	711-1965	1800 +/- 319	26%
SS36 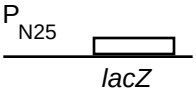	-------	2800 +/- 259	-----
SS77 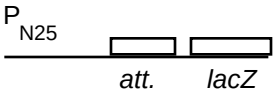	1700-1965	740 +/- 43	26%

$$\text{Percent Activity} = \frac{\text{Promoter-att-}\ lacZ}{\text{Promoter-}\ lacZ} \times 100$$

Figure 6. β-galactosidase Activities of Strains Carrying Different Portions of the Attenuator Region

Cultures were grown at 37°C in LB. The region between bases 711 and 1770 may also encode two other promoters, P4 and P5, though evidence they exist is not concrete.

for longer or shorter periods of time to achieve resolution of large and small fragments (Figure 8).

The data in Figure 8 were compared to structures predicted by the mFOLD program (Figure 6) and a folding model is proposed in Figure 9. The attenuator nucleotides in Figures 8 and 9 are numbered by the method described in the Experimental Procedures section. The first nucleotide (A-1) of the attenuator region corresponds to the first base of the *Hin*dIII site at base 1770 of the operon. The last two nucleotides seen in Figure 9 (U-149 and U-150) correspond to the first two of the three termination points (at bases 1918 and 1919 of the operon) in this region.

Examination of the data in Figure 8 shows several regions of secondary structure. All sites between A-14 and C-22 were sensitive to cleavage by the ds-specific RNase V1,

as are the sites between U-30 and A-36. No ss-specific RNase cleavage was detected in these regions. Importantly, three sites sensitive to ss-specific RNases were located between these regions; cleavage by RNase T1 at G-25 and C-26 and cleavage by *B. cereus* RNase at G-25, C-26, and A-27 was detected. These data suggest the presence of a stem-loop structure between U-15 and G-38 (Figure 8). The region upstream of this putative stem-loop contained cleavage sites for both ss- and ds-specific RNases. Six sites in this region were cleaved by RNase V1 (G-3, C-4, U-5, U-6, G-8) and 11 sites were cleaved by either RNases T1, *B. cereus,* or both (G-3 through G-13). Single-stranded- and double-stranded-specific RNase cleavage sites were interspersed in this region, implying that only a portion of the bases in this region are involved in base pairing. The region downstream of the putative stem also contained several RNase V1 cleavage sites. Between nucleotides C-40 and G-51, the ds-stranded specific RNAse cleaved at 8 sites. These dispersed sites also imply that only selected bases in this region pair to other bases. Since one of the mFOLD structures predicted this region formed a stem with three bulges, the entire region between G-3 and C-50 is predicted form Stem I (Figure 9).

Two regions further downstream, C-53 to G-57 and A-68 to U-73, contained mutiple cleavage sites for RNase V1. Sites between these two regions, U-59, C-61, U-63, and G-65, A-66, and C-67, were all cleaved by ss-specific RNAses. For these reasons, the portion of the mRNA between G-54 and C-72 is predicted to form Stem II. Notably, some of the cleavage sites seen in Figure 7 contradict this portion the model. RNase V1 cleaved five sites at the top of the predicted loop, U-59, C-61, C-62, U-63 and U-64. These bases are not predicted to lie in a region of secondary structure for two reasons. First, RNase V1 is not strictly ds-specific and occasionally cleaves at stacked helical residues (122,123). Second, no model was found that predicted these nucleotides were involved in a stem structure (Figure 6).

The proposed model in Figure 9 predicts the region between U-73 and G-90 to be unstructured, though again some of the data in Figure 8 contradicts this. Cleavage data showed digestion by RNase V1 at nucleotides C-77 to U-79, G-83 to U-85, and G-87 implying that this region may form a stem structure. This possibility seems unlikely for several reasons. The sites in this region cut by the ds-specific nuclease, produced very light bands, suggesting weak cleavage. Also, as mentioned above, RNase V1 can cleave at stacked helical residues (122,123). On the other hand, strong cleavage sites for RNases *B. cereus* or T1 were seen at all bases between C-76 and G-81, plus G-87. In addition, no model was found that predicted all of these nucleotides were involved in a stem structure (Figure 6).

The 3' end of the *plsX* mRNA contained several regions of very intense cleavage by either ss-specific or ds-specific nucleases. Strong RNase V1 cleavage was seen in two regions, G-97 to G-101 and C-112 to G-117. Between these regions were strong cleavage sites for the ss-specfic nucleases. All sites between G-102 and G-109 were cleaved well by one or more of the RNases with ss-specificity. For these reasons, the region between U-91 and A-120 is predicted to form Stem III. Some weak cleavage by ss-specific nucleases were seen at sites between G-96 and G-101. This may have been due to a second cleavage of transcripts initially cut by a ss-specific nuclease in the loop region between G-102 and G-109.

The final predicted stem-loop structure (Stem IV) lies immediately downstream of the third (Figure 9). Again, the usual cleavage pattern for a stem-loop is seen. Two

regions cleaved by RNase V1 (U-124 to C-126 and C-138 to G-141) suround a region cleaved by ss-specific nucleases (G-129 to U-136). The cleavage data support the predicted model of two adjacent stems; no cleavage by ss-specific RNases was seen at sites between the final two stems.

The secondary structure seen in Figure 6D is most consistant with the cleavage data presented above. Stems I, III, and IV appear to be stable, although the data relating to Stem II and the unstructured region downstream is not as conclusive. The structure in Figure 6C may therefore be transiently present in solution.

MUTATIONAL ANALYSIS

Point Mutations

Secondary structure analysis shows that the 140 nucleotide region upstream of the mRNA 3' end is capable of forming stem-loop structures *in vitro*. To determine if these structures, or the bases in them, are required for attenuator activity *in vivo*, random and site-directed mutagenesis was performed, as described in the Experimental Procedures section. Random mutagenesis was followed by phenotypic screening and the mutageneized attenuators that allowed increased expression of *lacZ* were selected. One site-directed mutation was designed to test the effect of the *plsX50* mutation on downstream gene expression. This mutation, the deletion of T-79, is located just downstream of the second predicted stem (Figure 10). The deletion shifts the *plsX* reading frame, placing a stop codon in-frame after the seventh codon of *plsX*. As stated previously, strains carrying both the *plsB26* mutation, which encodes a Km-defective acyltransferase, and *plsX50* are auxotrophic for glycerol-3-phosphate. It seemed plausible that *plsX50* could cause a change in termination frequency at the attenuator. If *plsX50* has this effect, the *plsB26 plsX50* auxotrophy could be in part due to decreased expression of *fabH, fabD, fabG,* and *acpP* in addition to the elimination of *plsX* expression. To quantitate the effects of the point mutations, the β-galactosidase expression of strains carrying altered attenuators in single-copy transcriptional fusions to *lacZ* was measured (Table 7).

Although these mutations lie well upstream of the two stems nearest the 3' end of the mRNA, all have an effect on attenuator activity. Interestingly, the mutations in Stem I carried by SS247 and SS239 lie only three bases apart, but there is a two-fold difference in expression. This suggests that either a specific sequence in, or the structure of, Stem I is necessary for wild-type attenuator activity. The results for SS231 and SS243 suggest that the same is true for the region containing Stem II. The *plsX50* mutation also appears to have an effect on the attenuator, with expression increasing from 30% to 48%. These results make it unlikely that the *plsB26 plsX50* phenotype is caused by an attenuator-mediated decrease in *fabH, fabD,* and *fabG* expression.

Multiple Mutations

The mutant screen resulted in identification of several isolates that carry more than one mutation in the attenuator region (Figure 11). As with the point mutations, these were tested to determine what portions of the attenuator region are essential for normal activity. All of the mutations listed in Table 8 were produced by random mutagenesis, except the attenuator fragment in SS262. The substitutions in SS262 were made by site-directed mutagenesis; this construct was designed to determine if the sequence of the

Table 7. The Effect of Point Mutations on *plsX* Attenuator Activity

Cultures were grown at 37°C in LB. Results for the wild-type attenuator control strain, SS77, are listed here for comparison. SS198 carries the *plsX50* deletion. The locations of the mutations listed in this table are shown in Figure 10.

Strain	Mutation	β-Galactosidase Activity (MU)	Percent Expression
SS36	----------	810 ± 51	--------
SS77	----------	240 ± 19	30
SS198	ΔT-79	390 ± 16	48
SS231	A-75G	460 ± 34	57
SS239	C-50T	430 ± 34	53
SS243	A-60G	330 ± 27	41
SS247	G-47T	190 ± 16	23

unstructured region downstream of Stem II is important for attenuator function. (This region could transiently form part of the alternate stem-loop structures in Figure 6B and C.)

Since all of these mutations contain multiple sequence changes, no firm conclusions concerning an individual base can be made. Instead, these mutations show the importance of various portions of the attenuator. The results for strain SS241 demonstrate that the downstream portion of the attenuator region is essential for wild-type activity. The three substitutions in SS250 are all located in Stem I, again demonstrating that changes at bases in this portion can dramatically affect attenuator activity. The results from strain SS244 also show that the upstream half of the attenuator region plays a role. Interestingly, the mutations in SS262 decreased expression of the downstream gene, implying a role for the region between Stems II and III.

Stem-Loop Deletions

The point mutations described above demonstrate that sequence changes throughout the attenuator region affect attenuator activity. In order to determine which of the proposed stems are necessary for normal attenuator activity, individual deletions affecting the three most stable stem-loop structures were made (Figure 12). SS260 and SS261 carry attenuators with deletions in the first stem, while Stems III and IV are deleted in strains SS263 and SS264, respectively. Another construct was designed to create substitutions at every base between C-77 and G-81 (Figure 9), but several attempts to isolate this construct were unsuccessful. The efforts may have failed because one end of the mutagenic oligonucleotide that was designed to anneal within the Stem II region was unable to do so due to folding of the M13 ssDNA template. Results from these deletion strains are listed in Table 9.

Though the deletions in SS260 and SS261 both alter Stem I, they appear to have very different effects on attenuator activity. The elimination of the top portion of Stem I allowed an increase in expression, while deletion of a portion near the base appeared to decrease expression slightly. This demonstrates the importance of all of Stem I for normal attenuator function. The results from SS263 and SS264 are also notable. As

Table 8. The Effect of Various Mutations on Activity of the *plsX* Attenuator

Cultures of these strains were grown at 37°C in LB. Results for the wild-type attenuator control strain, SS77, are listed here for comparison. The locations of the mutations listed in this table are shown in Figure 11.

Strain	Mutations	β-Galactosidase Activity (MU)	Percent Expression
SS36	----------	810 ± 51	--------
SS77	----------	240 ± 19	30
SS241	A-88G, T-128C	430 ± 28	53
SS244	T-9C, C-62G	550 ± 43	68
SS250	T-9C, T-16C, A-43G	430 ± 26	53
SS262	G-83C, T-84A, T-85A, A-86T, G-87C, A-88T, T-89G, G-90C	112 ± 4	14

Table 9. The Effects of Stem-Loop Deletions on *plsX* Attenuator Activity

Cultures were grown at 37°C in LB. Results for the wild-type attenuator control strain, SS77, are listed here for comparison. The locations of the mutations listed in this table are shown in Figure 12.

Strain	Mutation	β-galactosidase Activity (MU)	Percent Expression
SS36	----------	810 ± 51	--------
SS77	----------	240 ± 19	30
SS260	Δ5-T16	150 ± 16	19
SS261	Δ16-A37	530 ± 28	65
SS263	Δ93-T118	160 ± 13	20
SS264	Δ122-G137	190 ± 12	23

stated above, a stem-loop structure is usually adjacent to the termination points of an intrinsic terminator and one would expect to find that Stem III and/or IV is essential for attenuator activity. However, the results from these experiments show that either of the two stems near the 3' end can be eliminated with little effect on function. This implies the possibility of an unusual mechanism of termination.

Deletions at the 5' and 3' Ends of the Attenuator

S1 nuclease mapping identified three 3' end points just downstream of Stem IV (8), suggesting transcription through this region may result in termination. However, the mapping data do not exclude the possibility that termination takes place further upstream as well. If the attenuator region did encode a pair of tandem terminators, this would

Table 10. The Effect of Deletions at the 5' and 3' Ends of the Attenuator on *plsX* Attenuator Activity

Cultures were grown at 37°C in LB. Results for the wild-type attenuator control strain, SS77, are listed here for comparison. The locations of the mutations listed in this table are shown in Figure 13.

Strain	Mutation	β-galactosidase Activity (MU)	Percent Expression
SS36	----------	980 ± 20	--------
SS77	----------	290 ± 4	30
SS312	Δ1-C69	380 ± 5	39
SS350	Δ53-T196	2180 ± 50	220
SS361	Δ76-T196	1300 ± 115	130
SS370	Δ101-T196	1330 ± 46	140

explain why Stem I mutations influence transcriptional expression (SS260 and SS261, Table 9). For this reason, deletions made so that only the upstream or downstream portions of the attenuator would be present (Figure 13). SS312 carries the downstream portion of the attenuator, encompassing Stems III and IV. SS350, 361, and 370 carry increasingly larger portions of the upstream part of the attenuator region. The data from these strains are listed in Table 10.

The data from SS312 show that, despite the loss of Stems I and II, only a small decrease in attenuator activity occurs. The portion of the attenuator downstream of C-69, containing Stems III and IV, is therefore sufficient for the majority of attenutaor activity, with the upstream portions not playing an essential role. These data also suggest that no terminator lies in the Stem I/Stem II region, a model that is supported by the data from SS350, 361, and 370 (Table 10). These constructs, which are missing Stems III and IV, showed no attenuator-mediated decrease in expression, and therefore no evidence of a transcriptional terminator. They also showed that Stems III and IV cannot both be deleted without complete loss of function. Thus, these data and those from the stem-loop deletions indicate that a portion of the attenuator downstream of Stem III must be present for the attenuator to function. It is interesting to note that the expression in SS350, 361, and 370 is actually higher than the promoter control, SS36. The presence of only the upstream region of the attenuator (or the lack of Stems III and IV) may have changed the stability of the mRNA or activity of the upstream promoter. On the other hand, this region may encode an unmapped promoter that was responsible for the increase in activity. This issue will be addressed in the section entitled **The Search for a Promoter in the Attenuator Region**.

REGULATION OF THE *PLSX* ATTENUATOR

The purpose of the experiments described below was to determine if and how the *plsX* attenuator regulates expression of downstream genes. The activities of some attenuators are affected by transcription and/or translation. The binding of a ribosome to the mRNA of the *ampC* attenuator alters the termination frequency of the attenuator (84).

Ribosome binding also plays a role in the *trp* (52) and *pyrBI* (53) attenuators of *E. coli,* with termination frequency affected by the coupling of transcription and translation. Other attenuators respond to specific cellular needs. The *rpoBC, trp, pyrBI,* and *pheS* attenuators of *E. coli* and the *tyrS* attenuator of *B. subtilis* all respond to a depletion of the enzymes encoded by downstream genes or a depletion of the products of those enzymes. Since a phospholipid synthetic gene, *plsX,* and three fatty acid biosynthetic genes lie downstream of the *plsX* attenuator, the effect of fatty acid depletion on attenuator activity was tested.

Instead of fatty acid synthesis, the attenuator may be controlled in the same way membrane synthesis is regulated. One mechanism of regulation involves the protein/lipid ratio of the membrane. Overexpression of ATP synthase (55), glycerol-P acyltransferase (56), or fumarate reductase (54) causes an increase in the production of membrane without a change in protein/lipid ratio. An experiment was conducted to determine if activity of the *plsX* attenuator is altered by the perturberation of lipid synthesis occuring during overproduction of fumarate reductase.

Both the *trp* attenuator of *B. subtilis* (52) and the *bgl* attenuator of *E. coli* (86) are directly controlled by binding of specific proteins to attenuator mRNA. To determine if PlsX directly or indirectly affects the *plsX* attenuator, activity of the attenuator was tested in *plsX*$^+$ and *plsX50* strains. To examine the possiblity that a protein other then PlsX may specifically bind the *plsX* attenuator, a titration experiment involving attenuator mRNA was performed.

Growth temperature also affects the regulation of membrane synthesis, with the levels of short-chain fatty acids and unsaturated fatty acids increasing at lower temperatures (1). To determine if the *plsX* attenuator is affected by temperature, the attenuator activity was assessed during growth at various temperatures.

The Effect of Translational Initiation on *plsX* Attenuator Activity

To determine the effect of ribosome binding and translational initiation on gene expression, two attenuator mutations were used. The transcriptional fusion in SS194 carries mutations that eliminate the ribosome binding site and replace the *plsX* initiation codon with a termination codon (Figure 14). These changes should prevent binding of ribosomes to the attenuator mRNA. On the other hand, SS196 carries an altered attenuator with a ribosome binding site more similar to the consensus Shine-Dalgarno sequence and a mutation that changes the UUG *plsX* start codon to AUG. These changes are expected to greatly increase frequency of translational initiation at this site (124-126). The β-galactosidase activities of these strains were measured and the results are listed in Figure 14.

It is clear that the mutation which increases the frequency of translation initiation in the attenuator region resulted in an increase in expression. This change could be due to either an increase in translational initiation or a change in attenuator secondary structure. More importantly, the elimination of ribosome binding had no apparent effect on attenuator activity. This result is not suprising. Translational initiation at the wild-type *plsX* Shine-Dalgarno sequence is probably so poor that ribosomes rarely occupy the

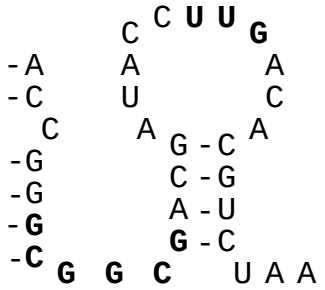

Strain	Shine-Dalgarno Region	Initiation Codon	β-Galactosidase Activity (M.U.)	Percent Expression
SS36	--------	---	810 +/- 51	----
SS77 (wt)	GCGGCG	UUG	240 +/- 19	30%
SS194	GACGUG	UAG	230 +/- 14	28%
SS196	GGGAGG	AUG	430 +/- 22	53%

Figure 7. Translational Initation and Activity of the *plsX* Attenuator
The locations of the putative ribosome binding site and the **UUG** start codon are shown in bold on the predicted structure for the 3' end of the *plsX* mRNA. (Only Stem II is shown). Cultures were grown at 37°C in LB. The strains and mutations are as follows: SS194, C-50A, G-51C, C-53T, T-64A; SS196, C-50G, G-52A, C-53G, T-63A.

attenuator region and, therefore, changes that eliminate translation probably do not dramatically decrease ribosome binding.

The Effect of Expression of a Cytoplasmic Thioesterase on *plsX* Attenuator Activity

Cho and Cronan recently engineered an altered thioesterase I gene, *'tesA*, that encodes a thioesterase lacking its signal sequence. The protein is consequently not exported from the cell (110,127). In the cytoplasm, the 'TesA protein cleaves the fatty acyl group from fatty acyl-ACP, destroying large amounts of this essential biomolecule. Since fatty acyl are not esterified to ACP, but instead excreted into the medium in large quantities, expression of 'TesA forces the cell to produce much more acyl-ACP than usual. A plasmid expressing *'tesA* under control of the *araB* promoter, pHC122, was used to determine if *plsX* attenuator activity is affected by increasing the production of fatty acids. Expression of *'tesA* was induced by the addition of arabinose. The vector for pHC122, pBAD22, was used as a control. Strains carrying P_{N25} transcriptional fusions, SS36 and SS77, and *rpmF-plsX-fab* promoter transcriptional fusions, SS90 and SS144, were used. 'TesA and β-galactosidase activities were measured and the results are listed in Table 11.

These data show that pHC122 increased thioesterase activity at least 7.5-fold under these conditions. The strains that carried the *'tesA* plasmid grew more slowly in medium containing arabinose than in medium lacking this inducer, providing further evidence of overexpression (data not shown). Production of 'TesA did not appear to have

Table 11. The Effect of Expression of *'tesA* on *plsX* Attenuator Activity
Cultures were grown at 37°C in M9 minimal medium containing, 0.4% glucose, 0.4% succinate, 1% casamino acids, 0.005% thiamine, 1 mM $MgSO_4$, 0.1 mM $CaCl_2$, ampicillin and 0.4% arabinose. Thioesterase and β-galactosidase activities were expressed as Units per milligram of cellular protein (U/mg).

Strain (promoter in *lacZ* fusion)	Thioesterase Activity (U/mg)	β-galactosidase Activity (U/mg)	Percent Expression
SS36 pBAD22 (P_{N25})	11 ± 3	3000 ± 252	--------
SS77 pBAD22 (P_{N25})	16 ± 2.4	840 ± 64	28
SS36 pHC122 (P_{N25})	280 ± 10	3300 ± 288	--------
SS77 pHC122 (P_{N25})	120 ± 3	850 ± 61	26
SS90 pBAD22 (P_{1-3})	4.6 ± 0.7	5400 ± 452	--------
SS144 pBAD22 (P_{1-3})	5 ± 1.5	1430 ± 21	26
SS90 pHC122 (P_{1-3})	61 ± 4.9	6500 ± 521	--------
SS144 pHC122 (P_{1-3})	100 ± 8.6	1500 ± 102	23

any effect on attenuator activity. However, the activity of the operon promoters increased slightly upon *tesA* induction. This suggests the promoters may be positively affected by increased cellular demand for fatty acyl-ACP.

The Effect of Fumarate Reductase Overexpression on Activity of the *plsX* Attenuator

Overexpression of the membrane-bound fumarate reductase causes a change in membrane morphology (54). The cell responds to an increase in protein concentration in the membrane by also increasing lipid levels. This maintains a constant membrane protein/lipid ratio, but it also increases membrane content of the cell and the membrane consequently becomes excessively large and heavily folded. The regulatory mechanism responsible for this effect is not understood. To overexpress fumarate reductase in strains containing the P_{N25}-*lacZ* and P_{N25}-attenuator-*lacZ* fusions, pFRD84 (112) was used. Lemire and coworkers reported that cells carrying this plasmid overexpress all four subunits of fumarate reductase when grown anaerobically on glycerol-fumarate medium (112). The control plasmid used in this experiment was pBR322, the parent plasmid of pFRD84. The P_{N25} fusion strains carrying either pBR322 or pFRD84 were grown as described above and the membrane fraction analyzed on an SDS-polyacylamide gel. Unfortunately, no overexpression of fumarate reductase proteins was seen (data not shown). Since no effect on attenuator activity was seen in the strains expressing the altered thioesterase, it appeared unlikely that regulation of the attenuator was related to lipid synthesis. Further efforts to overexpress fumarate reductase were therefore not made.

The Effect of PlsX on *plsX* Attenuator Activity

Since PlsX has no known function, experiments were conducted to determine if the protein has any direct or indirect affect on *plsX* attenuator activity. Strains were

Table 12. The Effect of PlsX on *plsX* Attenuator Activity

Cultures were grown at 37°C in LB.

Strain	Fusion	Relevent Genotype	β-Galactosidase Activity (U/mg)	Percent Expression
SS36X50	P_{N25}-*lacZ*	*plsX50*	3400 ± 155	--------
SS77X50	P_{N25}-att-*lacZ*	*plsX50*	1500 ± 198	44
SS36Xwt	P_{N25}-*lacZ*	*plsX*$^+$	3400 ± 479	--------
SS77Xwt	P_{N25}-att-*lacZ*	*plsX*$^+$	1500 ± 113	44

constructed that contained the P_{N25} fusions with or without the attenuator and either the *plsX50* mutation or *plsX*$^+$ on the chromosome. SS36X50 and SS77X50 carry the *plsX50* frame-shift mutation and cannot produce PlsX, while SS36Xwt and SS77Xwt are isogenic except they are *plsX*$^+$. These strains are derivatives of MC4100. The β-galactosidase activities of these strains was measured and the results are listed in Table 12.

This experiment yielded surprising results. Though there was no difference in activity between the wild-type *plsX* strain and *plsX50* strain, the percent expression in both strains appears to be higher than in previous experiments. When derivatives of the wild-type TL504 strain were analyzed, the attenuator fusion always produced 25-30% of the activity of the control fusion. However, MC4100 derivatives were used in this experiment and the expression was raised to 44%. This change in activity may be due to a mapped (or unmapped) mutation in MC4100. An experiment designed to investigate this possibility is described below.

The Effect of *relA* Expression on Activity of the *plsX* Attenutor

MC4100 is *relA*, and the strains used in previous experiments, derivatives of TL504, are *relA*$^+$. The *relA* gene encodes ppGpp synthetase I (38), which produces guanosine 3', 5'-bispyrophosphate (ppGpp). This effector molecule is thought to bind directly to RNA polymerase (47), and cause transcriptional pausing (43,44), thereby increasing the coupling of transcription and translation (45,46). A change in the degree of coupling changes the termination frequency of the *pheS* (69,70), *trp* (52), and *pyrBI* (53) attenuators of *E. coli.* To determine if ppGpp accounted for the difference in attenuator activities between MC4100 and TL504 derivatives, a plasmid carrying *relA* downstream of the IPTG-inducible *tac* promoter was used to complement the *relA* deficiency of MC4100 deriviatives. The wild-type *relA* gene is present on pALS10. A plasmid serving as a negative control, pALS14, encodes a truncated, inactive derivative of *relA* (108). The P_{N25}-*lacZ* or P_{N25}-attenuator-*lacZ* transcriptional fusion was inserted into the chromosome of MC4100, forming SS36X$^+$ and SS77X$^+$, respectively. Since MC4100 is *relA*, only SS36X$^+$(pALS10) and SS77X$^+$(pALS10) express ppGpp synthetase I upon induction by IPTG. Experimentation revealed that growth of pALS10 strains was severely inhibited in media containing 0.8 μM IPTG. This growth inhibition strongly suggested the expression of active ppGpp synthetase I. To maintain approximately the same growth rates, a concentration of 0.6 μM IPTG was used. The β-galactosidase activities of strains SS36X$^+$(pALS10), SS77X$^+$(pALS10),

Table 13. The Effect of *relA* Expression on Activity of the *plsX* Attenuator
Cultures were grown at 37°C in LB with ampicillin and 0.6 μM IPTG.

Strain	Fusion	Plasmid Gene	β-Galactosidase Activity (U/mg)	Percent Expression
SS36X$^+$(pALS10)	P_{N25}-*lacZ*	*relA*	2500 ± 122	--------
SS77X$^+$(pALS10)	P_{N25}-att-*lacZ*	*relA*	1028 ± 5	41
SS36X$^+$(pALS14)	P_{N25}-*lacZ*	control	1710 ± 25	--------
SS77X$^+$(pALS14)	P_{N25}-att-*lacZ*	control	670 ± 20	39

Table 14. The Effect of Growth Temperature on *plsX* Attenuator Activity
Cultures were grown in LB to stationary phase overnight. The cultures were then diluted into LB, grown to log phase, and assayed for β-galactosidase activity. Both the overnight culture and the dilution were grown at the same temperature, either 28 or 42°C. Also included in this table is the data for cultures grown at 37°C originally seen in Figure 7.

Strain	Fusion	Temperature (°C)	β-galactosidase Activity (U/mg)	Percent Expression
SS36	P_{N25}-*lacZ*	28	4800 ± 463	--------
SS77	P_{N25}-att-*lacZ*	28	2240 ± 97	47
SS36	P_{N25}-*lacZ*	37	2800 ± 259	--------
SS77	P_{N25}-att-*lacZ*	37	740 ± 43	26
SS36	P_{N25}-*lacZ*	42	3400 ± 320	--------
SS77	P_{N25}-att-*lacZ*	42	700 ± 104	21
SS90	$P_{1,2,3}$-*lacZ*	28	18000 ± 1064	--------
SS144	$P_{1,2,3}$-att-*lacZ*	28	8800 ± 930	49
SS90	$P_{1,2,3}$-*lacZ*	37	6900 ± 717	--------
SS144	$P_{1,2,3}$-att-*lacZ*	37	1800 ± 319	26
SS90	$P_{1,2,3}$-*lacZ*	42	4000 ± 283	--------
SS144	$P_{1,2,3}$-att-*lacZ*	42	800 ± 68	20

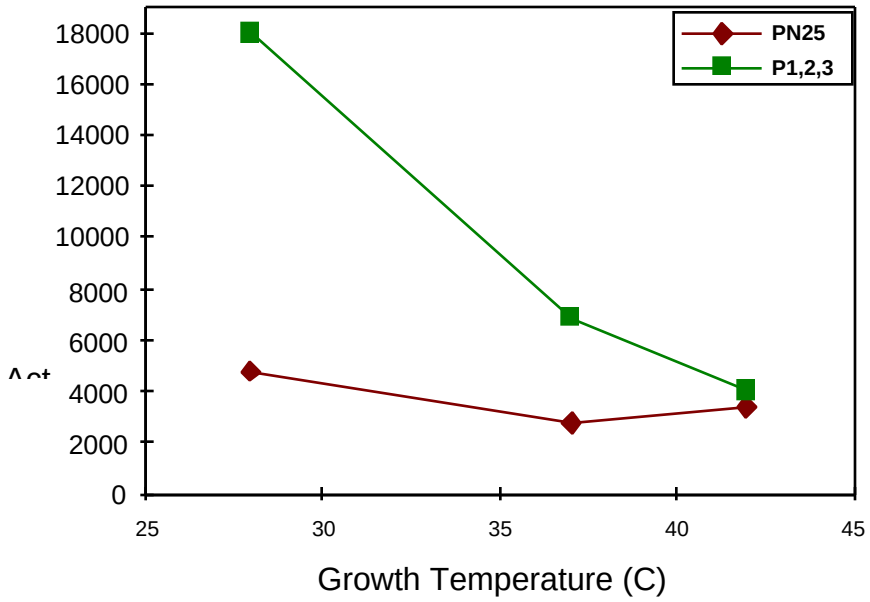

Figure 8. The Effect of Growth Temperature on Promoter Activity of P_{N25} (SS36) and on Promoter Activity of the region of the *rpmF-plsX-fab* operon containing P_1, P_2, and P_3 (SS90).

Above is a graph of a portion of the data from Table 14. Squares denote data from SS90 and diamonds denote data from SS36.

SS36X$^+$(pALS14), and SS77X$^+$(pALS14) were measured and the results are listed in Table 13.

With only a slight difference in percent expression between the pALS10 strains and pALS14 strains, these data show the attenuator is not affected by expression of *relA*. The percent expression in these MC4100 derivatives was also similar to the other MC4100-derived strains. This experiment shows again that attenuator activity is different in MC4100 but that this difference is not due to *relA*.

The Effect of Temperature on *plsX* Attenuator Activity

Membrane lipid composition changes with environmental temperature; the levels of short-chain and unsaturated fatty acids increase as temperature decreases (1). Since little is known about the molecular mechanism of this regulation, it is conceivable that regulated expression of the *rpmF-plsX-fab* operon plays a role. To determine if attenuator activity (and transcriptional expression of *plsX*) is affected by growth temperature, cultures of strains carrying the P_{N25} or $P_{1,2,3}$ fusions with or without the attenuator were grown at either 28 or 42°C and the β-galactosidase activities of these cultures measured. The results are listed in Table 14.

The data in Table 14 reveal two mechanisms of regulation of the *rpmF-plsX-fab* operon. The first concerns promoter activity of the region containing P_1, P_2, and P_3. Expression of β-galactosidase in this strain increased 4.5-fold when the growth

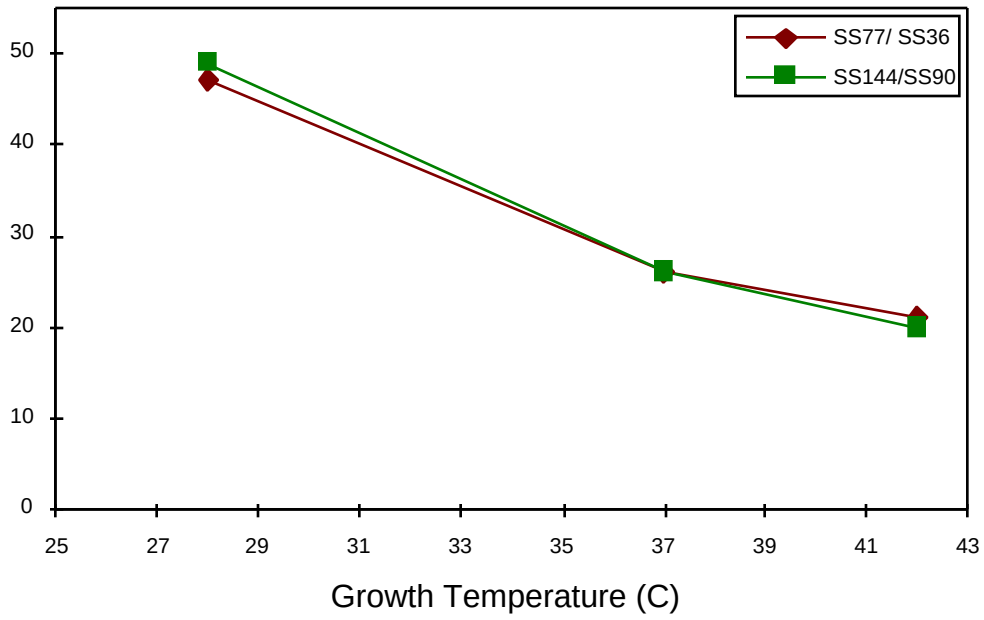

Figure 9. The Effect of Growth Temperature on *plsX* Attenuator Activity
Above is a graph of a portion of the data from Table 14. Squares denote data from strains SS90 and SS144 and diamonds denote data from SS36 and SS77.

temperature was decreased from 42 to 28°C (Figure 15). The other mechanism relates to the activity of the attenuator; it may also be regulated with growth temperature. A 2.2-fold increase in percent expression was seen when the growth temperature was lowered from 42 to 28°C (Figure 16).

Possible Mechanisms of Temperature Regulation of *plsX* Attenuator Activity

It is conceivable that the results from the temperature-dependence study were due to activation of a promoter that lies in the attenuator region. The presence of a promoter regulated with growth temperature could account for the increase in β-galactosidase expression of the two Promoter-attenuator-*lacZ* fusions seen in Table 14. To examine this possibility, the attenuator region was tested for the presence of a promoter.

On the other hand, the attenuator may decrease the expression of the downstream genes by terminating transcription or destabilizing the mRNA or by a combination of these two factors. If termination or destabilization is taking place, these are not necessarily affected by temperature, but rather could be influenced by changes in upstream promoter activity or in growth rate. Upstream promoter activity affects the *rpoBC* attenuator of *E. coli*, with an increase in promoter activity mediating an increase in termination frequency at the attenuator (75,128). Since temperature had a dramatic effect on the activity of the operon promoters, and a lesser effect on the activity of P_{N25} (Figure 15), experiments were performed to determine if the change in attenuator activity

seen in the temperature-dependence study was the result of promoter activity-mediated regulation. The *ampC* attenuator of *E. coli* is regulated with growth rate, with termination frequency decreasing as growth rate increases (84). Since cultures at 28°C grow more slowly than cultures at 42°C, additional experiments were performed to determine if the *plsX* attenuator is regulated not with temperature but rather with growth rate.

As stated above, the decrease in expression of genes downsteam of the attenuator may be due to transcriptional termination and/or mRNA degradation mediated by the attenuator mRNA. To determine if either or both of these are true, experiments were performed using a transcriptional fusion encoding an RNase III cleavage site immediately upstream of *lacZ.* This design ensures that the full length transcript is cleaved between the attenuator and *lacZ* region soon after synthesis (129,130). The attenuator mRNA will therefore be unable to mediate degradation of the *lacZ* transcript. These constructs therefore should allow measurement of the effect of transcriptional termination on *lacZ* expression.

The final topic that will be addressed concerns attenuator binding proteins. The mRNA of the *trp* attenuator of *B. subtilis* is bound by TRAP (52) and the mRNA of the *bgl* attenuator of *E. coli* is bound by BglG (86). Both TRAP and BglG are attenuator-binding proteins, and in both cases they alter the termination frequency of a specific attenuator by binding the mRNA. To test for the presence of a *plsX* attenuator-binding protein, a titration experiment similar that done by Shimotsu and Henner (131) was performed. The effect of the overproduction of *plsX* attenuator mRNA on attenuator activity was measured.

The Search for a Promoter in the Attenuator Region

The data in Table 14 show that the β-galactosidase activity of the strains carrying promoter-attenuator-*lacZ* fusions (SS77 and SS144) increased as growth temperature decreased. To determine if a temperature-dependent promoter in the attenuator region caused this, pSS421 was made. This plasmid contains the attenuator region fused to *lacZ* in a derivative of pRS415 (Table 4). (No known promoter lies upstream of the attenuator is this construct.) Cultures of TL504 (Δ*lacZ*) carrying this plasmid were grown at 28 and 42°C and assayed for β-galactosidase activity (Table 15).

Simons and coworkers report that the β-galactosidase activity of strains carrying the parent vector of pSS421, pRS415, is approximately 50 U/mg. Since these data show that the presence of the attenuator region does not increase promoter activity, it was concluded that the attenuator region has little or no promoter activity at either 28 or 42°C. In addition, the highest activity seen here is at least 15-fold lower than the activities of strains from the temperature-dependence studies (Table 14). The increase in apparent promoter activity at 28°C of strains carrying promoter-attenuator-*lacZ* fusions is therefore not due to activation of a promoter within the attenuator region.

The Effect of Upstream Promoter Activity on *plsX* Attenuator Activity

The termination frequency of an attenuator upstream of *rpoBC* of *E. coli* increases as the level of upstream promoter activity increases (75,128). Since the promoter activity of both P_{N25} and the operon promoters was higher at 28°C versus 42°C, the following experiment was conducted to determine if the change in *plsX* attenuator activity in

Table 15. The Abscence of Promoter Activity in the *plsX* Attenuator
Cultures were grown at 28 or 42°C in LB with ampicillin.

Strain	Temperature (°C)	β-Galactosidase Activity (U/mg)
pSS421 in TL504	28	41 ± 3.4
pSS421 in TL504	42	34 ± 4.4

Table 16. The Effect of Upstream Promoter Activity on *plsX* Attenuator Activity
Cultures were grown in LB supplemented with 30 to 60 ng/mL of tetracycline. Each concentration of tetracycline produced two different levels of promoter activity because the dilutions of tetracycline into LB were made on two different days, and therefore slightly different tetracyline concentrations resulted. TetR is so sensitive to tetracycline levels that different levels of derepression resulted from the nearly identical levels of the inducer. Since the same dilution of LB + tetracyline was used for both the SS36R and SS77R cultures, the same level of tetracyline was present in both cultures, and the results of this experiment are reliable.

Strain	Tetracycline (ng/ml)	β-galactosidase Activity (U/mg)	Percent Expression
SS36R	30	95 ± 4.1	--------
SS77R	30	19.5 ± 0.4	21
SS36R	30	125 ± 1	--------
SS77R	30	30 ± 2.4	24
SS36R	45	420 ± 32	--------
SS77R	45	100 ± 6.4	24
SS36R	45	1150 ± 24	--------
SS77R	45	300 ± 10	26
SS36R	60	1400 ± 154	--------
SS77R	60	314 ± 5	22
SS36R	60	2380 ± 35	--------
SS77R	60	600 ± 19	25

cultures grown at 28 and 42°C was actually mediated by the change in upstream promoter activity.

The strains SS36R and SS77R were constructed to allow the induction of various levels of promoter activity (Table 16). These strains carry P_{N25} transcriptional fusions, and also express TetR, the repressor that negatively controls transcription from P_{N25}. In

the absence of tetracycline, TetR binds to P_{N25}, decreasing promoter activity (107). Upon the addition of sub-bacteriostatic levels of tetracycline, various levels of derepression can be achieved. For this study, tetracycline concentrations of 30 to 60

Table 17. The Effect of Growth Rate on *plsX* Attenuator Activity in P_{N25} Fusions
Cultures of these strains were grown in "Rich" medium (AB salts, 0.1% glucose, 0.5% casamino acids, 0.001% tryptophan, 0.005% thiamine), "Glucose" medium (AB salts, 0.2% glucose, 0.005% thiamine), or "Glycerol" medium (AB salts, 0.4% glycerol, 0.001% tryptophan, 0.005% thiamine) at 37°C. Growth rate is expressed in doublings per hour (μ).

Strain	Medium	Growth Rate (μ)	β-Galactosidase Activity (U/mg)	Percent Expression
SS36(P_{N25}-*lacZ*)	Rich	1.0	2800 ± 259	--------
SS77(P_{N25}-att-*lacZ*)	Rich	1.0	740 ± 43	26
SS36(P_{N25}-*lacZ*)	Glucose	0.79	2400 ± 226	--------
SS77(P_{N25}-att-*lacZ*)	Glucose	0.79	530 ± 30	22
SS36(P_{N25}-*lacZ*)	Glycerol	0.45	2800 ± 203	--------
SS77(P_{N25}-att-*lacZ*)	Glycerol	0.45	690 ± 41	25

ng/mL were used. The β-galactosidase activity of the strain carrying the control promoter-*lacZ* fusion (SS36R) ranged from 95 to 2380 U/mg (Table 16).

The results that although promoter activity increased over a 25-fold range, the activity of the attenuator changed little. The *plsX* attenuator therefore does not appear to be affected by upstream promoter activity.

The Effect of Growth Rate on *plsX* Attenuator Activity

Temperature had a slight effect on the growth rate of cultures used in the temperature-dependence study; the 42°C cultures grew more rapidly than the 28°C cultures. To determine if the change in attenuator activity was actually due to the difference in growth rate, the effect of growth rate on attenuator activity was measured. Cultures of strains carrying the P_{N25} fusions with or without the attenuator were grown in three different media, each medium allowing for growth at a different rate, and the β-galactosidase activities of these strains were determined (Table 17). Cultures of strains carrying the $P_{1,2,3}$ fusions were grown in two different media, allowing for growth at two different rates, and the β-galactosidase activities of these strains are listed in Table 18.

The data from the P_{N25} fusions show no apparent correlation between growth rate and attenuator activity. The three media used provided a 2-fold increase in growth rate with no significant change in promoter or attenuator activity. Likewise, the data from the $P_{1,2,3}$ fusions show no difference in attenuator activity over a 4-fold range in growth rate. Importantly, these growth rate changes are far more extreme that those seen in the temperature-dependence studies. The *plsX* attenuator is therefore not affected by growth rate.

Table 18. The Effect of Growth Rate on *plsX* Attenuator Activity in Operon Promoter Fusions

Cultures of these strains were grown in "Fast" (90% AB salts, 0.1% glucose, 0.5% casamino acids, 0.001% tryptophan, 0.005% thiamine, 10% LB) or "Slow" (AB salts, 0.4% sodium succinate, 0.005% thiamine) medium at 37°C. Growth rate is expressed in doublings per hour (μ).

Strain	Medium	Growth Rate (μ)	β-Galactosidase Activity (U/mg)	Percent Expression
SS90($P_{1,2,3}$-*lacZ)*	Fast	1.1	6900 ± 717	--------
SS144($P_{1,2,3}$-att-*lacZ)*	Fast	1.1	1800 ± 319	26
SS90($P_{1,2,3}$-*lacZ)*	Slow	0.26	4400 ± 609	--------
SS144($P_{1,2,3}$-att-*lacZ)*	Slow	0.26	1110 ± 89	25

Contributions to *plsX* Attenuator Activity: Transcriptional Termination versus mRNA Instability

Up to this point, all constructs used in this study have been traditional transcriptional fusions. The transcript from the promoter-attenuator-*lacZ* fusion encodes both the attenuator and the *lacZ* gene. In such constructs, expression of β-galactosidase will be affected if the attenuator region causes the transcript to be unstable. In order to determine if the attenuator decreases expression of downstream genes by making the transcript unstable, in addition to attenuating transcription, strains SS333 and SS410 were made. SS333 and SS410 are TL504 derivatives carrying single-copies of either P_{N25}-*lacZ* or P_{N25}-attenuator-*lacZ* transcriptional fusions, respectively. In addition, each

construct encodes an RNase III cleavage site immediately upstream of the *lacZ* gene. RNase III cleaves these sites soon after mRNA synthesis (129,130), separating the portion of the transcript that encodes the attenuator from that which encodes *lacZ.* This cleavage is expected to minimize any effect the attenuator mRNA may have on the stability of the *lacZ* transcript. SS333 and SS410 therefore allow termination frequency alone to be quantitated.

These strains were also used to investigate the mechanism of temperature-dependent regulation of the attenuator. Cultures grown at 28 and 42°C revealed whether temperature-dependent regulation is due to a change in termination frequency or a change in transcript stability (Table 19).

The data in Table 19 shed light on both the *plsX* attenuator mechanism and temperature-dependent regulation. At 28°C, the effect of the attenuator is the same in the constructs both with and without the RNase III site. The attenuator activity, at this temperature, is therefore mainly due to transcriptional termination and not mRNA instability. However, at 42°C, the strains carrying fusions with the RNase III site had a 2-fold higher percent expression than strains carrying fusions without the RNase III site. The constructs without the RNase III site, which encode RNAs that may be more vunerable to degradation, have a decreased level of expression at this temperature. It therefore appears that an increase in temperature from 28 to 42°C is followed by a 2-fold decrease in attenuator transcript stability. The effect of temperature on transcriptional

Table 19. The Effect of Growth Temperature on *plsX* Attenuator-Mediated Transcriptional Termination and mRNA Stablility

Cultures of these strains were grown at 28, 37, or 42°C in LB.

Strain	Temperature (°C)	β-Galactosidase Activity (U/mg)	Percent Expression
SS36 (no RNase III site)	28	4800 ± 463	--------
SS77 (no RNase III site)	28	2240 ± 97	47
SS36 (no RNase III site)	37	2800 ± 259	-------
SS77 (no RNase III site)	37	740 ± 43	26
SS36 (no RNase III site)	42	3400 ± 320	--------
SS77 (no RNase III site)	42	700 ± 104	21
SS333 (RNase III site)	28	9000 ± 1195	--------
SS410 (RNase III site)	28	4400 ± 239	49
SS333 (RNase III site)	37	5800 ± 240	--------
SS410 (RNase III site)	37	2300 ± 67	40
SS333 (RNase III site)	42	4900 ± 126	--------
SS410 (RNase III site)	42	2040 ± 79	42

termination can be seen by comparing the results for cultures of SS333 and SS410 grown at 28 and 42°C. A slight decrease in expression (from 49 to 42%) is seen, but no dramatic effect on termination is evident.

The Effect of Overproduction of *plsX* Attenuator Transcript on Activity of the Attenuator

Experiments in the previous sections demonstrate that the *plsX* attenuator affects the expression of downstream genes. The activities of the *trp* attenutor of *B. subtilis* (52) and the *bgl* attenuator of *E. coli* (86) are both regulated by specific binding protiens. To determine if a binding protein specific for the *plsX* attenuator might exist, a titration experiment similar to that done by Shimotsu and Henner (131) was performed. In their work, Shimotsu and Henner demonstrated expression of *trp* attenuator mRNA from a high-copy plasmid altered expression of the *trp* operon. These results suggested that an attenuator-binding protein may alter the termination frequency of the *trp* attenuator. Under normal conditions, the binding protein interacts with the attenuator mRNA, affecting the frequency of termination at the attenuator. When attenuator mRNA was overexpressed, the protein bound to the attenuator mRNAs transcribed from the plasmid instead of to the *trp* operon transcripts, and the frequency of termination at the attenuator was affected. To determine if a *plsX* attenuator-binding protein exists, strains were constructed that carry both a plasmid that overexpresses the *plsX* attenuator transcript and a transcriptional fusion that monitors the effect of the overexpression on attenuator activity.

Table 20. The Effect of Overproduction of the *plsX* Attenuator Transcript on Activity of the Attenuator

Cultures of these strains were grown overnight at 37°C in LB supplemented with ampicillin, spectinomycin, and 1 mM IPTG. The overnight cultures were then diluted in to the same media, grown to log phase, and assayed for β-galactosidase activity. All strains also carried pMS421, a pSC101 derivative carrying *lacI*^{q}.

Strain	Transcript Expressed	β-galactosidase Activity (U/mg)	Percent Expression
SS36 (pSS160)	control	4200 ± 582	--------
SS77 (pSS160)	control	1100 ± 102	26
SS36 (pSS161)	attenuator	3800 ± 309	--------
SS77 (pSS161)	attenuator	1100 ± 162	29
SS90 (pSS160)	control	8200 ± 510	--------
SS144 (pSS160)	control	2400± 131	29
SS90 (pSS161)	attenuator	8000 ± 728	--------
SS144 (pSS161)	attenuator	2200 ± 142	28

Overproduction of attenuator mRNA was achieved using pSS161. This plasmid contains the IPTG-inducible P_{lacUV5} followed by the *plsX* attenuator. A control plasmid, pSS160, was also used. Here, P_{lacUV5} promotes transcription of essentially the same transcript, sans the attenuator. Strains carrying the P_{N25} or $P_{1,2,3}$ fusions were transformed with either pSS160 or pSS161, allowing the effect of expression of the attenuator transcript to be monitored. Also present in these strains is pMS421, a low copy number plasmid carrying *lacI*^{q}. Expression of *lacI*^{q} leads to the repression of P_{lacUV5} and therefore decreases the expression of either the control or the attenuator transcript. IPTG (1 mM) was added to the cultures in order to derepress P_{lacUV5}, allowing expression of the attenuator transcript (Table 20).

The data listed in Table 20 show the percent expression is nearly the same whether or not the attenuator transcript is overexpressed. Therefore, overexpression of attenuator mRNA appears to have no effect on activity of the chromosome-borne attenuator and no evidence of a *plsX* attenuator-binding protein is seen. Results from the SS90 derivatives also show that overexpression of attenuator mRNA has no effect on activity of the promoters upstream of *rpmF*.

CHAPTER 4: DISCUSSION

Structural and functional characteristics of a transcriptional attenuator in the *rpmF-plsX-fab* operon of *E. coli* are described in this work. The attenuator was localized to a 200 bp region downstream of *rpmF* at the 5' end of the *plsX* reading frame. Analysis of the secondary structure of the attenuator mRNA has lead to a model that includes four stem-loop structures within the 150 nt upstream of the mapped 3' endpoints. Mutational analysis showed that all four stem-loops play a role in attenuator activity. Several experiments were performed regarding regulation of the attenuator and the attenuator's mechanism of controlling downstream gene expression. Changes in translational initiation, the amount of the PlsX protein, ppGpp concentration, rate of lipid synthesis, growth rate, and upstream promoter activity all appear to have no effect on attenuator activity. Interestingly, growth temperature appears to have an effect on both attenuator activity and the activity of one or all of the promoters upstream of *rpmF* and *plsX*. Growth temperature-regulation of attenuator activity is apparently mediated by a change in stability of the mRNA.

LOCALIZATION OF THE *PLSX* ATTENUATOR

Quantification of activity of the *plsX* attenuator was established by comparison of strains carrying the $P_{1,2,3}$-attenuator-*lacZ* or $P_{1,2,3}$-*lacZ* fusions (Figure 7). These strains carry a fragment from the operon spanning from either 711 to 1770 or from 711 to 1965. A similar experiment using strains with P_{N25} fusions (Figure 7) demonstrated that none of the region upstream of 1770 is required for wild-type attenuator activity. With a growth temperature of 37°C, the attenuator reduces transcriptional expression of the downstream gene four-fold, to 26% of the level found in the fusion without the attenuator.

These experiments do not address the mechanism of the attenuator. Transcriptional expression of downstream genes could be decreased by attenuator-mediated transcriptional termination. The presence of a stem-loop structure six nucleotides upstream of the mapped 3' endpoint supports this theory. On the other hand, the RNA of the attenuator region may also mediate the cleavage or degradation of downstream mRNA. This issue will be discussed below.

ANALYSIS OF THE *PLSX* ATTENUATOR SECONDARY STRUCTURE

Probing with various RNases yielded information used to propose a model of the secondary structure of the attenuator mRNA (Figure 9). This model contains four stem-loop structures. The mFOLD program predicted Stems I, III, and IV to be the most stable, with free energies of -24.1, -15.5, and -18.5 kcals/mole, respectively. The UUG start codon of *plsX* located in the loop region of Stem II, which is predicted to have a free energy of only -2.1 kcal/mole. Interestingly, Stems III and IV lie in tandem, with no single-stranded region between them. The most contradictory data in this analysis involved the form of Stem II and the unstructured region between Stems II and III. The ds-specific RNase V1 cleaved heavily at sites on the loop of Stem II and lightly at several sites in the single-stranded region downstream (Figure 9). As stated above, RNase V1 cleaves not only in double-stranded regions but at stacked helical residues as well (122,123); this may explain the results.

Two additional scenerios also seem possible. Though the model in Figure 9 is presented in a 2-dimensional form, the mRNA almost definitely does not lie flat and portions of the mRNA may interact with one another. The regions of the transcript that are proposed to be single-stranded may in fact participate in this more complex structure, and this could account for the RNase V1 cleavage sites. It is also possible that the model proposed in Figure 9 represents only the predominant form. As seen in Figure 6, the portion of the attenuator in the vicinity of Stem II could exist in several alternative structures. The region may transiently exist in these alternate forms, with stems and loops in different locations, accounting for the contradictory cleavage data.

MUTATIONAL ANALYSIS OF THE *PLSX* ATTENUATOR

The *plsX50* mutation is a one base-pair deletion within the attenuator region that creates a frameshift early in the reading frame of the gene (10). Strains carrying both this mutation and *plsB26* are auxotrophic for glycerol-P. It is conceivable that *plsX50* exerts its phenotype effect by decreasing expression of the downstream *fab* gene cluster. Experiments described above show that the *plsX50* mutation (ΔT-79, Figure 10) changes the activity of the attenuator, increasing percent expression from 30 to 48%. This mutation can therefore only increase the level of transcripts encoding the downstream genes involved in fatty acid synthesis, *fabH, fabD, fabG,* and *acpP*.

Other site-directed and random mutations were used to determine the importance of each portion of the attenuator region. Of six mutations affecting Stem I that were characterized, three altered the sequence of the bottom portion of the stem. Both the ΔT5-T16 deletion (Figure 12, Table 9) and the G-47T mutation (Figure 10, Table 7) appeared to slightly decrease the expression of the downstream gene. On the other hand, introduction of the C-50T mutation into the attenuator increased expression nearly 2-fold (SS239, Figure 10, Table 7). The one deletion of the top portion of Stem I, ΔT16-A37 (SS261, Figure 12, Table 9), also increased expression greater than 2-fold. Two mutations in the attenuator region were characterized that affected both the top and bottom portion of the first stem. The mutation in SS250, three base-pair changes, had a dramatic effect, increasing expression nearly 2-fold (Figure 11, Table 8). The deletion of all of Stem I (and Stem II) caused a less extreme effect, a slight increase in expression is observed (SS312, Figure 13, Table 10). Overall, mutations in either the top or bottom of Stem I do not affect expression in a predictable manner; some increase expression while others decrease it. The only conclusion that can be drawn is that all of Stem I is required for wild-type attenuator activity, but that the deletion of the stem does not eliminate the ability of the attenuator to decrease expression of downstream genes.

Several mutations were made in Stem II and the region downstream of it, which is predicted to be unstructured (Figure 9). The point mutations in SS243, SS231, SS198 (Figure 10, Table 7), and multiple substitutions in SS262 (Figure 11, Table 8) all increase expression over the wild-type attenuator level. Notably, deletion of both Stems I and II leads to only a slight increase in percent expression. Since only a slight effect from this mutation is seen, it can be concluded that, while Stem II (like Stem I) need not be present for the attenuator to decrease expression of downstream genes, activity is slightly altered by mutations in this portion of the attenuator.

Stems III and IV (Figure 9) are interesting both because of their proximity both to the 3' end of the mRNA and to each other. The traditional view of terminators would suggest that one or both of these stems are involved in any transcription termination occuring at the uridine-rich region downstream of them (77). The mutations in SS263 and SS264 tell a different story (Figure 12, Table 9). Apparently, either stem can be deleted with little effect on attenuator activity. However, if both stems and the region downstream are deleted (SS370, Figure 13, Table 10), the attenuator-mediated decrease in downstream gene expression is lost. It therefore appears that a portion of the attenuator that is essential for activity lies between Stem III and the end of the attenuator.

REGULATION OF THE *PLSX* ATTENUATOR

Various possible modes of regulation of the attenuator were tested. The effects of translational initiation, coupling of transcription and translation, an increased rate of lipid synthesis, the absence of PlsX, the expression of *relA*, growth rate, upstream promoter activity, and growth temperature were all evaluated. The mechanism by which the attenuator decreases gene expression is also discussed below.

The effect of translational initiation on attenuator activity was determined by constructing and assaying two strains, each carrying different mutations in the attenuator region. One has mutations that should eliminate ribosome binding, while the other has mutations predicted to increase translational initiation (Figure 14). The results show that an increase in expression could be obtained by altering the ribosome binding site such that translational initiation is increased, though it can not be said whether this is due to the increase in ribosome binding or another effect of the sequence change. More conclusive data was gathered from the construct in which the Shine-Dalgarno site has been eliminated. This change has no effect on attenuator activity, suggesting that translational initiation plays no role in regulation of the activity of the attenuator *in vivo* under the rapid growth conditions employed.

Expression of an altered thioesterase was used to evaluate the effect of an increased rate of lipid synthesis on attenuator activity. Although no dramatic change in attenuator activity was produced, the promoter activity of a fragment containing the operon promoters appeared to be affected (Table 11). The promoter activity of this fragment increased by about 20% when the 'TesA protein was expressed. This suggests that one or more of these promoters may respond to a cellular depletion of fatty acyl-ACP. To further investigate this observation, transcriptional fusions using each of the three promoters could be made and tested in strains carrying the *'tesA* plasmid.

Binding proteins affect the activities of specific attenuators by binding to attenuator mRNA (52). A titration experiment was used to look for evidence of a *plsX* attenuator-binding protein (Table 20). Though no evidence for a binding protein was found, abundant, nonspecific proteins in the cell that could not be titrated off may in fact be involved in control of attenuator activity.

To determine if the PlsX protein has a direct or indirect role in altering attenuator activity, two sets of strains that are isogenic (except for *plsX*) were constructed. Though attenuator activity was the same in both the *plsX*$^+$ and *plsX50* strains, surprising results were seen. In these strains, derivatives of MC4100, the attenuator does not decrease

expression of the downstream gene to the degree it does in TL504, an MG1655 derivitive (Table 12). There must therefore be some difference in these strains that affects attenuator activity. One difference between MG1655 and MC4100 is *relA*, the gene that encodes ppGpp synthetase I. MG1655 is wild-type for this gene, while MC4100 carries the *relA1* allele and does not express active protein. The attenuator activity was tested in MC4100 strains carrying a plasmid-borne copy of the *relA* gene (Table 13). These results show that the attenuator is not effected by *relA* expression and that some other difference between MC4100 and MG1655 must be responsible for the change in attenuator activity.

The most interesting data were gathered upon testing the temperature-dependence of the attenuator (Table 14). The *rpmF-plsX-fab* operon appears to be regulated with temperature in at least two ways. The activity of the operon promoters (SS90) increases 4.5-fold as the temperature is decreased from 42 to 28°C (Figure 15). One could argue that the decrease in growth rate that accompanies the decrease in growth temperature is actually responsible for the change in promoter activity. This suggestion is not supported by data gathered in the growth rate-dependence experiment. Data in Table 19 show that promoter activity actually decreases as the growth rate decreases, the opposite of the effect seen in the temperature-dependence studies. One could also argue that the increase in β-galactosidase expression at lower temperatures is due to an increase in *lacZ* transcript stability at 28°C or due to some other general metabolic change that causes an increase in the activities of all promoters. If either of these were true, the same increase in promoter activity should be seen with all promoters. The P_{N25} promoter of SS36, however, increases by only 40% as the temperature decreases to 28°C (Table 14, Figure 15). Therefore, it appears that one or more of the promoters upstream of *rpmF* and *plsX* are regulated in a temperature-dependent manner.

To determine which promoter(s) are responsible for the change in expression, each of the promoters should be tested for temperature-dependence by constructing separate transcriptional fusions with each of them. Determining the mechanism of this regulation, however, would be far more difficult. Although no cold-shock specific sigma factor has been found, many proteins appear to be expressed at higher levels after a drop in temperature, including CsdA (132), NusA, IF2, polynucleotide phosphorylase, and both CspA and CspB, from the CspA family of cold-shock proteins (reviewed in ref. 133). Interestingly, both CspA and B are transcriptionally and translationally induced with cold-shock (134), but the specific mechanisms controlling temperature-dependent transcription are not understood.

The *plsX* attenuator also appears to alter the expression of downstream genes in accordance with growth temperature. The attenuator allowed at least 2-fold more expression at 28°C as compared with 42°C (Table 14, Figure 16). One could suggest that this difference in *lacZ* expression was due to a difference in RNA stability at 28°C. Since the transcript from the attenuator fusion is not the same length as that from the the control fusion, a change in RNase activity may effect the relative degradation rates of the two transcripts. The change in relative degradation rates could then alter the relative levels of β-galactosidase expression, and it would appear that the attenuator had mediated a change in expression. If this were true, a change in the size or sequence of the transcript upstream of the *lacZ* coding region should eliminate the temperature-dependent effect. The results in Table 14 argue that this theory is probably false. The constructs made with

P_{N25} and with the operon promoters both showed the same temperature effect, despite the fact that the operon promoter fusion produces transcripts at least 450 nts longer than the P_{N25} fusion.

Since an increase in promoter activity accompanied the change in attenuator activity, the argument could be made that the change in attenuator activity was in fact mediated by the increase in promoter activity. The results in Table 16 show that a change in promoter activity did not affect attenuator function. These data are not absolutely conclusive, however, because the promoter activities seen in Table 16 are all below those seen in the growth temperature study (Table 14). One could argue that the attenuator only responds to promoter activity above a minimum strength. A closer examination of the data from the temperature-dependence study, however, shows that promoter strength clearly does not affect attenuator function. With growth at 37°C, the percent expression is the same for both the P_{N25} fusions and the operon promoter fusions, despite the 2.5-fold difference in promoter activities.

Though growth of cultures at different temperatures led to slightly different growth rates, the change in attenuator activity cannot be attributed to a change in growth rate. The growth rate-dependence data in Tables 18 and 19 demonstrate that the attenuators in both the P_{N25} and operon promoter constructs are uneffected by 2- or 4-fold changes in growth rate, respectively. Since these growth changes are far more extreme than those seen in the temperature-dependence experiment (data not shown), it seems very unlikely that growth rate has any effect on attenuator activity.

The experiments relating to growth temperature and attenuator activity also show that one or more of the promoters upstream of *rpmF* is regulated with growth temperature. Though, as mentioned above, growth rate is effected by temperature, the change in promoter activity cannot be attributed to differences in growth rate. If the increase in promoter activity was due to the decrease in growth rate that followed the decrease in temperature, any decline in growth rate would lead to a increase in promoter activity. The results in Table 18 show that the opposite occurs. Promoter activity decreases following a decline in growth rate.

Although these results do show that transcriptional expression of *plsX* is regulated with growth temperature, no experiments presented here demonstrate that the level of the PlsX protein is affected by growth temperature. The effect of temperature on production of PlsX can be measured in two ways. A strain carrying a *plsX-lacZ* translational fusion can be constructed and the effect of temperature on β-galactosidase activity determined. On the other hand, western blot analysis can be performed on extracts from cultures grown at different temperatures.

CONTRIBUTIONS TO ACTIVITY OF THE *PLSX* ATTENUATOR: TRANSCRIPTIONAL TERMINATION VERSUS MESSENGER RNA INSTABILITY

The *plsX* attenuator could decrease expression of downstream genes by terminating transcription or by mediating the degradation of the transcript, or by a combination of these mechanisms. Transcriptional fusions that contain the RNase III site allowed the attenuator portion of the transcript and the *lacZ* transcript to be separated

soon after synthesis (129,130). The cleavage by RNase III should prevent the attenuator transcript from affecting the stability of the *lacZ* transcript. This permits the frequency of termination at the attenuator to be measured, and thus the role mRNA stability plays in attenuator activity was indirectly determined. The results in Table 19 show that the attenuator mediates both termination and mRNA instability. The data for the cultures grown at 28°C reveal that the attenuator does not mediate transcript instability at this temperature but that attenuator termination reduces expression 2-fold. The results from cultures grown at 37 or 42°C show evidence of both termination and message instability. These data demonstrate that, at this higher temperature, the transcript downstream of the attenuator is destabilized, reducing expression 2-fold. Comparing the termination frequency at 28 and 42°C (the data for SS333 and SS410), reveals that there is little difference in termination at the different temperatures. It therefore appears that, although termination does take place, the temperature-dependent expression mediated by the attenuator is due to a change in mRNA stability.

The regulation of attenuator activity may be related to cold-shock, and specifically, to the major cold-shock protein, CspA (reviewed in ref. 133). Expression of this protein is induced 200-fold following a shift from 37°C to 10°C (135,136) and recent work shows CspA functions as an RNA chaperone (137). Jiang and co-workers report that CspA binds to its own mRNA, in an untranslated region predicted to form an extensive secondary structure. The protein is proposed to function as an RNA chaperone, interacting with RNA and preventing the formation of secondary structures at low temperatures. The results reported here suggest the activity of CspA may be related to the *plsX* attenuator. Binding of CspA, along with the RNA helicase activity of CsdA (132), may destablize the secondary structure of the attenuator at low temperatures. If the *plsX* attenuator secondary structure mediates degradation of the transcript, binding of CspA and CsdA may increase mRNA stability and thereby increase the expression of genes downstream of the attenuator in a temperature-dependent manner.

Since the attenuator seems to function both to destabilize downstream mRNA and also to terminate transcription, one cannot help but wonder which portions of the attenuator are involved in each activity. Also, for all nucleotides or structures involved in transcript stability, there may be some that are needed for temperature regulation while others are not. The mutational analysis used constructs that do not contain an RNase III site and, therefore, the effect of the mutation on either transcriptional termination, mRNA stability, or both cannot be determined. More could be learned about the regulation and the activities of the attenuator by inserting an RNase III site into the constructs containing mutations. The effects of the mutations on temperature-dependent regulation, termination frequency, and transcript stability could then be measured.

POTENTIAL ACTIVITIES OF THE PLSX PROTEIN

The results in this work shed some light on the role of the PlsX protein. Only one clue to the specific function of PlsX has been previously reported. Strains that carry both the *plsX50* mutation and *plsB26*, a mutation in the gene for glycerol-P acyltransferase, are auxotrophic for glycerol-P (10). (Strains with only *plsB26* do not have this phenotype.) The *plsB26*-encoded acyltransferase is Km-defective; the enzyme has a 10-fold lower affinity for glycerol-P and may also have a lower affinity for fatty acyl-ACP (36). This information suggests that PlsX may function to increase cellular levels of glycerol-P or

fatty acyl-ACP, allowing the cell to overcome the challenge the altered acyltransferase presents. On the other hand, PlsX may function as a facilitator for the acyltransferase, shuttling specific acyl-ACP molecules to the acyltransferase for incorporation into 1-acylglycerol-P (Figure 4). In this model, PlsX would decrease the Km of the acyltransferase for the shuttled acyl group. Similarly, PlsX could act as an acyltransferase that only uses specific acyl-ACPs as substrates.

The work presented here shows that transcriptional expression of *plsX* is dramatically increased with a decrease in growth temperature, both through a 4.5-fold change in promoter activity and a 2-fold change in attenuator-mediated transcript stability. This 9-fold increase in expression of *plsX* strongly suggests that the function of PlsX relates to the temperature-dependent changes in membrane composition. Since higher glycerol-P levels are not expected to be required at lower temperatures, PlsX activity is probably not directed at increasing levels of glycerol-P. Likewise, higher levels of fatty acids should not be required, though greater amounts of certain types of fatty acids would be needed. Since the concentrations of short-chain and unsaturated fatty acids in the membrane rise with a drop in temperature, PlsX could play a role in the synthesis of these types of fatty acids. In this model, the absence of PlsX would dramatically decrease the rate of synthesis of short-chain and unsaturated fatty acids, affecting the total supply of fatty acids. Strains with both *plsB26* and *plsX50* would therefore be unable to produce sufficient amounts of 1-acylglycerol-P, due to the defective acyltransferase and an inadequent level of fatty acids. The *plsB26, plsX50* strain could survive, however, if the other substrate for the acyltransferase, glycerol-P, were present at a sufficiently high concentration.

Another possible role for PlsX revolves around the incorporation of specific fatty acids into membrane phospholipids. Synthesizing or otherwise obtaining short-chain and unsaturated fatty acids would definitely be required to change the membrane composition, but these fatty acids also must become part of a phospholipid molecule. PlsX may act to facilitate the incorporation of short-chain and unsaturated fatty acyl-ACP molecules into phospholipids by shuttling them to the acyltransferase for incorporation into 1-acylglycerol-P. In this model, the absence of PlsX would severely decrease the ability of the cell to use short-chain and unsaturated fatty acids as substrates for the acyltransferase reaction. This impairment, along with the Km-defective, *plsB26*-encoded acyltransferase, would inhibit the acyltransferase reaction to such an extent that an exceptionally high level of the other substrate, glycerol-P, would be needed for survival. PlsX may also be a an acyltransferase specific for short-chain and unsaturated fatty acyl-ACPs. Strains carrying both plsB26 and plsX50 would require glycerol-P because they express only one Km-defective acyltransferase.

The first step to discovering which, if any, of these models is true would be to determine if PlsX is needed for temperature-dependent regulation of membrane composition. Cultures of *plsX*$^+$ or *plsX50* strains could be grown at 28 and 42°C, and an analysis of the fatty acid composition of each of the four cultures should reveal if PlsX affects membrane composition at either of the temperatures. If PlsX proves to play a role in regulating membrane composition, the specific biochemical activity would need to be found. As stated above, PlsX may function to alter the rate of synthesis of short-chain and unsaturated fatty acids. The function of PlsX could be tested using an *in vitro* fatty acid synthesis system (18,20,25) that either included or excluded PlsX. Analysis of the products of this system would reveal if PlsX induces the production of a greater amount

of short-chain or unsaturated fatty acids. On the other hand, PlsX may facilitate the use of short-chain and unsaturated fatty acids by the *plsB*-encoded acyltransferase. This could be tested using an *in vitro* acyltransferase assay. The assay environment would provide an excess of two or more types of acyl-ACPs for the *plsB*-encoded acyltransferase, and experiments would be done with and without PlsX. The effect of the protein could then be determined by analyzing the levels of the different types of fatty acids that had been incorporated into the products. An assay for PlsX acyltransferase activity could be done the same way, with the *plsB*-encoded acyltransferase excluded.

LITERATURE CITED

1. Cronan, J. E., Jr. and C. O. Rock. 1996. Biosynthesis of membrane lipids. In *Escherichia coli* and *Salmonella.* Cellular and Molecular Biology. F. C. Neidhardt, R. Curtiss, J. L. Ingraham, E. C. C. Lin, K. B. Low, B. Magasanik, W. S. Reznikoff, M. Riley, M. Schaechter, and H. E. Umbarger, editors. ASM Press, Washington, D.C. pp. 612-636.

2. Raetz, C. R. H. and W. Dowhan. 1990. Biosynthesis and function of phospholipids in *Escherichia coli. J. Biol. Chem.* 265:1235-1238.

3. Rock, C. O. and S. Jackowski. 1982. Regulation of phospholipid synthesis in *Escherichia coli*: Composition of the acyl-acyl carrier protein pool *in vivo. J. Biol. Chem.* 257:10759-10765.

4. Rock, C. O. and J. E. Cronan, Jr. 1996. *Escherichia coli* as a model for the regulation of dissociable (type II) fatty acid biosynthesis. *Biochim. Biophys. Acta Lipids Lipid Metab.* 1302:1-16.

5. Podkovyrov, S. and T. J. Larson. 1995. Lipid biosynthetic genes and a ribosomal protein gene are cotranscribed. *FEBS Lett.* 368:429-431.

6. Podkovyrov, S. Unpublished results.

7. Oh, W. and T. J. Larson. 1992. Physical locations of genes in the *rne (ams)-rpmF-plsX-fab* region of the *Escherichia coli* K-12 chromosome. *J. Bacteriol.* 174:7873-7874.

8. Oh, W. 1992. Characterization of an operon containing a ribosomal protein gene and lipid biosynthetic genes in *Escherichia coli* K-12. Ph.D. Dissertation. Virginia Polytechnic Institute and State University, Blacksburg, VA

9. Tanaka, Y., A. Tsujimura, N. Fujita, S. Isono, and K. Isono. 1989. Cloning and analysis of an *Escherichia coli* operon containing the *rpmF* gene for ribosomal protein L32 and the gene for a 30-kilodalton protein. *J. Bacteriol.* 171:5707-5712.

10. Larson, T. J., D. N. Ludtke, and R. M. Bell. 1984. *sn*-Glycerol-3-phosphate auxotrophy of *plsB* strains of *Escherichia coli*: evidence that a second mutation, *plsX*, is required. *J. Bacteriol.* 160:711-717.

11. Tsay, J.-T., W. Oh, T. J. Larson, S. Jackowski, and C. O. Rock. 1992. Isolation and characterization of the beta-ketoacyl-acyl carrier protein synthase III gene (*fabH*) from *Escherichia coli* K-12. *J. Biol. Chem.* 267:6807-6814.

12. Magnuson, K., W. Oh, T. J. Larson, and J. E. Cronan, Jr. 1992. Cloning and nucleotide sequence of the *fabD* gene encoding malonyl coenzyme A-acyl carrier protein transacylase of *Escherichia coli*. *FEBS Lett.* 299:262-266.

13. Rawlings, M. and J. E. Cronan, Jr. 1992. The gene encoding *Escherichia coli* acyl carrier protein lies within a cluster of fatty acid biosynthetic genes. *J. Biol. Chem.* 267:5751-5754.

14. Zhang, Y. and J. E. Cronan, Jr.. 1996. Polar allele duplication for transcriptional analysis of consecutive essential genes: Application to a cluster of *Escherichia coli* fatty acid biosynthetic genes. *J. Bacteriol.* 178:3614-3620.

15. Magnuson, K., M. Rawlings Carey, and J. E. Cronan, Jr. 1995. The putative *fabJ* gene of *Escherichia coli* fatty acid synthesis is the *fabF* gene. *J. Bacteriol.* 177:3593-3595.

16. Li, S.-J. and J. E. Cronan, Jr. 1992. The genes encoding the biotin carboxylase subunit of *Escherichia coli* acetyl-CoA carboxylase. *J. Biol. Chem.* 267:855-863.

17. Li, S.-J. and J. E. Cronan, Jr. 1992. The genes encoding the two carboxyltransferase subunits of *Escherichia coli* acetyl-CoA carboxylase. *J. Biol. Chem.* 267:16841-16847.

18. Heath, R. J. and C. O. Rock. 1996. Inhibition of β-ketoacyl-acyl carrier protein synthase III (FabH) by acyl-acyl carrier protein in *Escherichia coli*. *J. Biol. Chem.* 271:10996-11000.

19. Mohan, S., T. M. Kelly, S. S. Eveland, C. R. H. Raetz, and M. S. Anderson. 1994. An *Escherichia coli* gene (*FabZ*) encoding (3*R*)-hydroxymyristoyl acyl carrier protein dehydrase. Relation to *fabA* and suppression of mutations in lipid A biosynthesis. *J. Biol. Chem.* 269:32896-32903.

20. Heath, R. J. and C. O. Rock. 1996. Roles of the FabA and FabZ β- hydroxyacyl-acyl carrier protein dehydratases in *Escherichia coli* fatty acid biosynthesis. *J. Biol. Chem.* 271:27795-27801.

21. Bergler, H., P. Wallner, A. Ebeling, B. Leitinger, S. Fuchsbichler, H. Aschauer, G. Kollenz, G. Hogenauer, and F. Turnowsky. 1994. Protein EnvM is the NADH-dependent enoyl-ACP reductase (FabI) of *Escherichia coli*. *J. Biol. Chem.* 269:5493-5496.

22. Garwin, J. L., A. L. Klages, and J. E. Cronan, Jr. 1980. Structural, enzymatic, and genetic studies of β-ketoacyl-acyl carrier protein synthases I and II of *Escherichia coli*. *J. Biol. Chem.* 255:11949-11956.

23. Gellmann, E. P. and J. E. Cronan, Jr. 1972. Mutant of *Escherichia coli* deficient in the synthesis of *cis*-vaccenic acid. *J. Bacteriol.* 112:381-387.

24. Garwin, J. L., A. L. Klages, and J. E. Cronan, Jr. 1980. β-ketoacyl-acyl carrier protein synthase II of *Escherichia coli*: Evidence for functions in thermal regulation of fatty acid synthesis. *J. Biol. Chem.* 255:3263-3265.

25. Heath, R. J. and C. O. Rock. 1996. Regulation of fatty acid elongation and initiation by acyl-acyl carrier protein in *Escherichia coli*. *J. Biol. Chem.* 271:1833-1836.

26. Clark, D. P. and J. E. Cronan, Jr. 1996. Two carbon compounds of fatty acids as carbon sources. In *Escherichia coli* and *Salmonella*: Cellular and Molecular Biology. F. C. Neidhardt, R. Curtiss, J. L. Ingraham, E. C. C. Lin, K. B. Low, B. Magasanik, W. S. Reznikoff, M. Riley, M. Schaechter, and H. E. Umbarger, editors. American Society for Microbiology, Washington, D. C. pp. 343-357.

27. DiRusso, C. C., A. K. Metzger, and T. L. Heimert. 1993. Regulation of transcription of genes required for fatty acid biosynthesis in *Escherichia coli* by FadR. *Mol. Microbiol.* 7:311-322.

28. Marr, A. G. and J. L. Ingraham. 1962. Effect of temperature on the composition of fatty acids in *Escherichia coli*. *J. Bacteriol.* 84:1260-1267.

29. De Mendoza, D., A. Klages Ulrich, and J. E. Cronan, Jr. 1983. Thermal regulation of membrane fluidity in *Escherichia coli.* Effects of overproduction of β-ketoacyl-acyl carrier protein I. *J. Biol. Chem.* 250:2098-2101.

30. Ulrich, A. K., D. De Mendoza, J. L. Garwin, and J. E. Cronan, Jr. 1983. Genetic and biochemical analyses of *Escherichia coli* mutants altered in the temperature-dependent regulation of membrane lipid composition. *J. Bacteriol.* 154:221-230.

31. Magnuson, K., S. Jackowski, C. O. Rock, and J. E. Cronan, Jr. 1993. Regulation of fatty acid biosynthesis in *Escherichia coli*. *Microbiol. Rev.* 57:522-542.

32. Cronan, J. E., Jr. 1975. Thermal regulation of the membrane lipid composition of *Escherichia coli.* Evidence for the direct control of fatty acid biosynthesis. *J. Biol. Chem.* 250:7074-7077.

33. Sinensky, M. 1971. Temperature control of phospholipid biosynthesis in *Escherichia coli*. *J. Bacteriol.* 106:449-455.

34. Raetz, C. R. H. 1996. Bacterial lipopolysaccharides: a remarkable family of bioactive macroamphiphiles. In *Escherichia coli* and *Salmonella.* Cellular and Molecular Biology. F. C. Neidhardt, R. Curtiss, J. L. Ingraham, E. C. C. Lin, K. B. Low, B. Magasanik, W. S. Reznikoff, M. Riley, M. Schaechter, and H. E. Umbarger, editors. ASM Press, Washington,D.C. pp. 1035-1063.

35. Coleman, J. 1992. Characterization of the *Escherichia coli* gene for 1-acyl-*sn*-glycerol-3-phosphate acyltransferase (*plsC*). *Mol. Gen. Genet.* 232:295-303.

36. Bell, R. M. 1974. Mutants of *Escherichia coli* defective in membrane phospholipid synthesis. Macromolecular synthesis in an *sn*-glycerol-3-phosphate acyltransferase Km mutant. *J. Bacteriol.* 117:1065-1076.

37. Cashel, M., D. R. Gentry, V. J. Hernandez, and D. Vinella. 1996. The stringent response. In *Escherichia coli* and *Salmonella*: Cellular and Molecular Biology. F. C. Neidhardt, R. Curtiss, J. L. Ingraham, E. C. C. Lin, K. B. Low, B. Magasanik, W. S. Reznikoff, M. Riley, M. Schaechter, and H. E. Umbarger, editors. American Society for Microbiology, Washington, D.C. pp. 1458-1496.

38. Metzger, S., I. B. Dror, E. Aizenman, G. Schreiber, M. Toone, J. B. Friesen, and M. Cashel. 1988. The nucleotide sequence and characterization of the *relA* gene of *Escherichia coli*. *J. Biol. Chem.* 263:15699-15704.

39. Xiao, H., M. Kalman, K. Ikehara, S. Zemel, G. Glaser, and M. Cashel. 1991. Residual guanosine 3',5'-bispyrophosphate synthetic activity of *relA* null mutants can be eliminated by *spoT* null mutations. *J. Biol. Chem.* 266:5980-5990.

40. Hernandez, V. J. and H. Bremer. 1991. *Escherichia coli* ppGpp synthetase II activity requires *spoT*. *J. Biol. Chem.* 266:5991-5999.

41. Gentry, D. R., V. J. Hernandez, L. H. Nguyen, D. B. Jensen, and M. Cashel. 1993. Synthesis of the stationary phase sigma factor σ^S is positively regulated by ppGpp. *J. Bacteriol.* 175:7982-7989.

42. Tedin, K. and H. Bremer. 1992. Toxic effects of high levels of ppGpp in *Escherichia coli* are relieved by *rpoB* mutations. *J. Biol. Chem.* 267:2337-2344.

43. Hernandez, V. J. and H. Bremer. 1993. Characterization of RNA and DNA synthesis in *Escherichia coli* strains devoid of ppGpp. *J. Biol. Chem.* 268:10851-10862.

44. Kingston, R. E., W. C. Nierman, and M. J. Chamberlin. 1991. A direct effect of guanosine tetraphosphate on pausing of *Escherichia coli* RNA polymerase during RNA chain elongation. *J. Biol. Chem.* 256:2787-2797.

45. Vogel, U., M. A. Sorensen, S. Pedersen, K. F. Jensen, and M. Kilstrup. 1992. Decreasing transcription elongation rate in *Escherichia coli* exposed to amino acid starvation. *Mol. Microbiol.* 6:2243-2251.

46. Vogel, U. and K. F. Jensen. 1994. Effects of guanosine 3'5'-bispyrophosphate on rate of transcription elongation in isoleucine-starved *Escherichia coli*. *J. Biol. Chem.* 269:16236-16241.

47. Vinella, D. and R. D'Ari. 1994. Thermoinducible filamentation in *Escherichia coli* due to an altered RNA polymerase β subunit is supressed by high levels of ppGpp. *J. Bacteriol.* 176:966-972.

48. Gaal, T. and R. L. Gourse. 1990. Guanosine 3'-diphosphate 5'-diphosphate is not required for growth rate-dependent control of rRNA synthesis in *Escherichia coli*. *Proc. Natl. Acad. Sci. U. S. A.* 87:5533-5537.

49. Josaitis, C. A., T. Gaal, and R. L. Gourse. 1995. Stringent control and growth rate-dependent control have nonidentical promoter sequence requirements. *Proc. Natl. Acad. Sci. U. S. A.* 92:1117-1121.

50. Heath, R. J., S. Jackowski, and C. O. Rock. 1994. Guanosine tetraphosphate inhibition of fatty acid and phospholipid synthesis in *Escherichia coli* is relieved by overexpression of glycerol-3-phosphate acyltransferase (*plsB*). *J. Biol. Chem.* 269:26584-26590.

51. Li, S.-J. and J. E. Cronan, Jr. 1993. Growth rate regulation of *Escherichia coli* acetyl coenzyme A carboxylase, which catalyzes the first committed step of lipid biosynthesis. *J. Bacteriol.* 175:332-340.

52. Landick, R., C. L. Turnbough, Jr., and C. Yanofsky. 1996. Transcription attenuation. In *Escherichia coli* and *Salmonella*: Cellular and Molecular Biology. F. C. Neidhardt, R. Curtiss, J. L. Ingraham, E. C. C. Lin, K. B. Low, B. Magasanik, W. S. Reznikoff, M. Riley, M. Schaechter, and H. E. Umbarger, editors. American Society for Microbiology, Washington, D.C. pp. 1263-1286.

53. Donahue, J. P. and C. L. Turnbough, Jr. 1994. Nucleotide-specific transcriptional pausing in the *pyrBI* leader region of *Escherichia coli* K-12. *J. Biol. Chem.* 269:18185-18191.

54. Weiner, J. H., B. D. Lemire, M. L. Elmes, R. D. Bradley, and D. G. Scraba. 1984. Overproduction of fumarate reductase in *Escherchia coli* induces a novel intracellular lipid-protein organelle. *J. Bacteriol.* 158:590-596.

55. Von Meyenburg, K., B. B. Jorgensen, and B. Reurs. 1984. Physiological and morphological effect of overproduction of membrane-bound ATP synthase in *Escherichia coli* K-12. *EMBO J.* 3:1791-1797.

56. Wilkenson, W. O., J. P. Walsh, J. M. Corless, and R. M. Bell. 1986. Crystalline arrays of the *Escherchia coli sn*-glycerol-3- phosphate acyltransferase intergral membrane protein. *J. Biol. Chem.* 261:9951-9958.

57. Podkovyrov, S. M. and T. J. Larson. 1996. Identification of promoter and stringent regulation of transcription of the *fabH, fabD* and *fabG* genes encoding fatty acid biosynthetic enzymes of *Escherichia coli*. *Nucleic Acids Res.* 24:1747-1752.

58. Chang, S.-I. and G. G. Hammes. 1989. Homology analysis of the protein sequences of fatty acid synthases from chicken liver, fat mammary gland, and yeast. *Proc. Natl. Acad. Sci. U. S. A.* 86:8373-8376.

59. Carty, S. M., A. Colbeau, P. M. Vignais, and T. J. Larson. 1994. Identification of the *rpmF-plsX-fabH* genes of *Rhodobactercapsulatus*. *FEMS Microbiol. Lett.* 118:227-232.

60. Kaneko, T., S. Sato, H. Kotani, and *et al.* 1996. Sequence analysis of the genome of the unicellular cyanobacterium *Synechocystis* sp. strain PCC6803. II. Sequence determination of the entire genome and assignment of potential protein-coding regions. *DNA Res.* 3:109-136.

61. Morbidoni, H. R., D. De Mendoza, and J. E. Cronan, Jr. 1996. *Bacillus subtilis* acyl carrier protein is encoded in a cluster of lipid biosynthesis genes. *J. Bacteriol.* 178:4794-4800.

62. Fraser, C. M., J. D. Gocayne, O. White, M. D. Adams, R. A. Clayton, R. D. Fleischmann, C. J. Bult, A. R. Kerlavage, G. Sutton, J. M. Kelley, J. L. Fritchman, J. F. Weidman, K. V. Small, M. Sandusky, J. Fuhrmann, D. Nguyen, T. R. Utterback, D. M. Saudek, C. A. Phillips, J. M. Merrick, J.-F. Tomb, B. A. Dougherty, K. F. Bott, P.-C. Hu, T. S. Lucier, S. N. Peterson, H. O. Smith, C. A. Hutchison,III, and J. C. Venter. 1995. The minimal gene complement of *Mycoplasma genitalium*. *Science* 270:397-403.

63. Himmelreich, R., H. Hilbert, H. Plagens, E. Pirkl, B.-C. Li, and R. Herrmann. 1996. Complete sequence analysis of the genome of bacterium *Mycoplasma pneumoniae*. *Nucleic Acids Res.* 24:4420-4449.

64. Narumi, I., H. Watanabe, A. Hossain, A. Tanaka, and S. Kitayma. 1995. Molecular cloning and nucleotide sequence of radiation-inducible catalase gene form radio-resistant bacterium, *Deinococcus radiodurans*. DDBJ Accession Number D63898.

65. Fleischmann, R. D., M. D. Adams, O. White, R. A. Clayton, E. F. Kirkness, A. R. Kerlavage, C. J. Bult, J.-F. Tomb, B. A. Dougherty, J. M. Merrick, K. McKenney, G. Sutton, W. FitzHugh, C. Fields, J. D. Gocayne, J. Scott, R. Shirley, L.-I. Liu, A. Glodek, J. M. Kelley, J. F. Weidman, C. A. Phillips, T. Spriggs, E. Hedblom, M. D. Cotton, T. R. Utterback, M. C. Hanna, D. T. Nguyen, D. M. Saudek, R. C. Brandon, L. D. Fine, J. L. Fritchman, J. L. Fuhrmann, N. S. M. Geoghagen, C. L. Gnehm, L. A. McDonald, K. V. Small, C. M. Fraser, H. O. Smith, and J. C. Venter. 1995. Whole-genome random sequencing and assembly of *Haemophilus influenzae* Rd. *Science* 269:496-512.

66. Gourse, R. L., T. Gaal, M. S. Bartlett, J. A. Appleman, and W. Ross. 1996. rRNA transcription and growth rate-dependent regulation of ribosome synthesis in *Escherichia coli*. *Annu. Rev. Microbiol.* 50:645-677.

67. Burton, Z. F., C. A. Gross, K. F. Watanabe, and R. R. Burgess. 1983. The operon that encodes sigma subunit of RNA polymerase also encodes ribsomal protein S21 and DNA primase in *Escherichia coli* K-12. *Cell* 32:335-349.

68. Keener, J. and M. Nomura. 1996. Regulation of ribosome synthesis. In *Escherchia coli* and *Salmonella*: Cellular and Molecular Biology. F. C. Neidhardt, R. Curtiss, J. L. Ingraham, E. C. C. Lin, K. B. Low, B. Magasanik, W. S. Reznikoff, M. Riley, M. Schaechter, and H. E. Umbarger, editors. American Society for Microbiology, Washington, D.C. pp. 1417-1431.

69. Lesage, P., H.-N. Truong, M. Graffe, J. Dondon, and M. Springer. 1990. Translated translational operator in *Escherichia coli* autoregulation in the *infC-rpmI-rplT* operon. *J. Mol. Biol.* 213:465-474.

70. Fayat, G., J.-F. Mayaux, C. Sacerdot, M. Fromant, M. Springer, M. Grunberg-Manago, and S. Blanquet. 1983. *Escherichia coli* phenylalanyl-tRNA synthetase operon region. *J. Mol. Biol.* 171:239-261.

71. Lupski, J. R. and G. N. Godson. 1989. DNA->DNA, and DNA->RNA->Protein: Orchestration by a single complex operon. *Bioessays* 10:152-157.

72. Lupski, J. R., A. A. Ruiz, and G. N. Godson. 1984. Promotion, termination, and anti-termination in the *rpsU-dnaG-rpoD* Macromolecular Synthesis Operon of *Escherichia coli* K-12. *Mol.Gen. Genet.* 195:391-401.

73. Yanik, V. and G. N. Godson. 1993. Selective decay of *Escherichia coli dnaG* messenger RNA is initiated by RNase E. *J. Biol. Chem.* 268:13253-13260.

74. Downing, W. and P. P. Dennis. 1991. RNA polymerase activity may regulate transcription initiation and attenuation in the *rplKAJLrpoBC* operon in *Escherchia coli*. *J. Biol. Chem.* 266:1304-1311.

75. Dykxhoorn, D. M., R. St.Pierre, and T. Linn. 1996. Synthesis of the β and β' subunits of *Escherichia coli* RNA polymerase is autogenously regulated in vivo by both transcriptional and translational mechanisms. *Mol. Microbiol.* 19:483-493.

76. Linn, T. and J. Greenblatt. 1992. The NusA and NusG proteins of *Escherichia coli* increase the *in vitro* readthrough of a transcriptional attenuator preceding the β subunit of RNA polymerase. *J. Biol. Chem.* 267:1449-1454.

77. Richardson, J. P. and J. Greenblatt. 1996. Controls of RNA chain elongation and termination. In *Escherichia coli* and *Salmonella*: Cellular and Molecular Biology. F. C. Neidhardt, R. Curtiss, J. L. Ingraham, E. C. C. Lin, K. B. Low, B. Magasanik, W. S. Reznikoff, M. Riley, M. Schaechter, and H. E. Umbarger, editors. American Society for Microbiology, Washingtion, D.C. pp. 822-847.

78. Law, L. F., J. W. Roberts, and R. Wu. 1983. RNA polymerase pausing and the transcript release at the lambda tR1 terminator. *J. Biol. Chem.* 258:9391-9397.

79. Lowery, C. and J. P. Richardson. 1977. Characterization of the nucleoside triphosphate phosphohydrase (ATPase) activity of RNA synthesis termination factor rho. I: Enzymatic properties and effects of inhibitors. *J. Biol. Chem.* 252:1375-1380.

80. Lowery, C. and J. P. Richardson. 1977. Characterization of the nucleoside triphosphate phosphohydrase (ATPase) activity of RNA synthesis termination

factor rho. II: influence of synthetic RNA homopolymers and random copolymers on the reaction. *J. Biol. Chem.* 252:1381-1385.

81. Brennan, C. A., A. J. Dombroski, and T. Platt. 1987. Transcription termination factor rho is an RNA-DNA helicase. *Cell* 48:945-952.

82. Fisher, R. F. and C. Yanofsky. 1983. A complementary oligomer releases a transcript pause complex. *J. Biol. Chem.* 258:9208-9212.

83. Martin, F. H. and I. Tinoco, Jr. 1980. DNA-RNA hybrid duplexes containing oligo (dA:rU) sequences are exceptionally unstable and may facillitate termination of transcription. *Nucleic Acids Res.* 8:2295-2299.

84. Jaurin, B., T. Grundstrom, T. Edlund, and S. Normark. 1981. The *Escherichia coli* β-lactamase attenuator mediates growth rate-dependent regulation. *Nature* 290:221-225.

85. Otridge, J. and P. Gollnick. 1993. MtrB from *Bacillius subtilis* binds specifically to *trp* leader RNA in a tryptophan-dependent manner. *Proc. Natl. Acad. Sci. U. S. A.* 90:128-132.

86. Amster-Choder, O. and A. Wright. 1990. Regulation of a transcriptional antiterminator in *Escherichia coli* by phosphorylation *in vivo*. *Science* 249:540-542.

87. Henkin, T. M. 1994. tRNA-directed transcription antitermination. *Mol. Microbiol.* 13:381-387.

88. Grundy, F. J., S. M. Rollins, and T. M. Henkin. 1994. Interaction between the acceptor stem tRNA and the T-box stimulates antitermination in the *Bacillius subtilis tyrS* gene: A new role for the discriminator base. *J. Bacteriol.* 176:4518-4526.

89. Silhavy, T. J., M. L. Berman, and L. W. Enquist. 1984. Experiments with Gene Fusions. Cold Spring Harbor Laboratory, Cold Spring Harbor, NY. 217 pp.

90. Spencer, M. E. and J. R. Guest. 1974. Proteins of the inner membrane of *Escherichia coli*: Changes in composition associated with anaerobic growth and fumarate reductase amber mutation. *J. Bacteriol.* 117:954-959.

91. Sambrook, J., E. F. Fritsch, and T. Maniatis. 1989. Molecular Cloning. A Laboratory Manual. Cold Spring Harbor Laboratory, Cold Spring Harbor, NY. p. A1

92. Kunkel, T. A., J. D. Roberts, and R. A. Zakour. 1987. Rapid and efficient mutagenesis without phenotypic selection. *Methods Enzymol.* 154:368-382.

93. Metcalf, W. W. and B. L. Wanner. 1991. Involvement of the *Escherichia coli phn* (*psiD*) gene cluster in assimilation of phosphorus in the form of phosphonates, phosphite, P_i esters and P_i. *J. Bacteriol.* 173:587-600.

94. Podkovyrov, S. M. and T. J. Larson. 1995. A new vector-host system for construction of *lacZ* transcriptional fusions where only low-level gene expression is desirable. *Gene* 156:151-152.

95. Yanisch-Perron, C., J. Vieira, and J. Messing. 1985. Improved M13 phage cloning vectors and host strains: Nucleotide sequence of the M13mp18 and pUC19 vectors. *Gene* 33:103-119.

96. Liss, L. R. 1987. New M13 host, DH5aF' competent cells. *Focus* 3:13-14.

97. Guyer, M. S., R. R. Read, T. A. Steitz, and K. B. Low. 1980. Identification of a sex-factor-affinity site in *Escherichia coli* as $\gamma\ \delta$. *Cold Spring Harbor Symp. Quant. Biol.* 45:135-140.

98. Jensen, K. F. 1993. The *Escherichia coli* K-12 "wild-type" W3110 and MG1655 have an *rph* frameshift mutation that leads to pyrimidine starvation due to low *pyrE* expression levels. *J. Bacteriol.* 175:3401-3407.

99. Casadaban, M. J. 1976. Transposition and fusion of the *lac* genes to selected promoters in *Escherichia coli* using bacteriophage lambda and Mu. *J. Mol. Biol.* 104:541-555.

100. Schweizer, H. and W. Boos. 1983. Transfer of the Δ*(argF-lac)U169* mutation between *Escherichia coli* strains by selection for a closely linked Tn*10* insertion. *Mol. Gen. Genet.* 192:293-294.

101. Silhavy, T. J., M. L. Berman, and L. W. Enquist. 1984. Experiments with Gene Fusions. Cold Spring Harbor Laboratory, Cold Spring Harbor, NY. pp. 89

102. Sambrook, J., E. F. Fritsch, and T. Maniatis. 1989. Molecular Cloning. A Laboratory Manual. Cold Spring Harbor Laboratory, Cold Spring Harbor, NY. pp. 1.74

103. Maniatis, T., E. F. Fritsch, and J. Sambrook. 1982. Molecular Cloning. Cold Spring Harbor Laboratory, Cold Spring Harbor, NY. pp. 90

104. Simons, R. W., F. Houman, and N. Kleckner. 1987. Improved single and multicopy *lac*-based cloning vectors for protein and operon fusions. *Gene* 53:85-96.

105. Sambrook, J., E. F. Fritsch, and T. Maniatis. 1989. Molecular Cloning. A Laboratory Manual. Cold Spring Harbor Laboratory, Cold Spring Harbor, NY. pp. 6.9

106. Sanger, F., S. Nicklen, and A. R. Coulson. 1977. DNA sequencing with chain-termination inhibitors. *Proc. Natl. Acad. Sci. U. S. A.* 74:5463-5467.

107. Deuschle, U., W. Kammerer, R. Gentz, and H. Bujard. 1986. Promoters of *Escherichia coli*: a hierarchy of in vivo strength indicates alternate structures. *EMBO J.* 5:2987-2994.

108. Svitil, A. L., M. Cashel, and J. W. Zyskind. 1993. Guanosine tetraphosphate inhibits protein synthesis *in vivo*. A possible protective mechanism for starvation stress in *Escherichia coli*. *J. Biol. Chem.* 268:2307-2311.

109. Guzman, L.-M., D. Belin, M. J. Carson, and J. Beckwith. 1995. Tight regulation, modulation, and high level expression by vectors containing the arabinose P_{BAD} promoter. *J. Bacteriol.* 177:4121-4130.

110. Cho, H. and J. E. Cronan,Jr. 1995. Defective export of a periplasmic enzyme disrupts regulation of fatty acid synthesis. *J. Biol. Chem.* 270:4216-4219.

111. Bolivar, F., R. L. Rodriquez, P. J. Greene, M. C. Betlach, H. L. Heyneker, and H. W. Boyer. 1977. Construction and characterization of new cloning vehicles. II. A multipurpose cloning system. *Gene* 2:95-113.

112. Lemire, B. D., J. J. Robinson, and J. H. Weiner. 1982. Identification of membrane anchor polypeptides of *Escherichia coli* fumarate reductase. *J. Bacteriol.* 152:1126-1131.

113. Linn, T. and R. St.Pierre. 1990. Improved vector system for constructing transcriptional fusions that ensures independent translation of *lacZ*. *J. Bacteriol.* 172:1077-1084.

114. Waldburger, C. and M. M. Susskind. 1994. Probing the informational content of *Escherichia coli* σ^{70} region 2.3 by combinatorial cassette mutagenesis. *J. Mol. Biol.* 235:1489-1500.

115. T. Sitz. Personal communication. 1996.

116. Leung, D., E. Chen, and D. V. Goeddel. 1983. A method for random mutagenesis of a defined DNA segment using a modified polymerase chain reaction. *Technique* 1:11-15.

117. Laemmli, U. 1970. Cleavage of structural proteins during the assembly of the head of bacteriophage T4. *Nature* 227:680-685.

118. Bradford, M. M. 1976. A rapid and sensitive method for the quantitation of microgram quantities of protein utilizing the principle of protein-dye binding. *Anal. Biochem.* 72:248-254.

119. Barnes, J. , E.M. 1975. Long-chain fatty acyl thioesterases I and II from *Escherichia coli*. *Methods Enzymol.* 35:102-109.

120. Miller, J. H. 1972. Experiments in Molecular Genetics. Cold Spring Harbor Laboratory, Cold Spring Harbor, N.Y.

121. Giacomini, A., V. Corich, F. J. Ollero, A. Squartini, and M. P. Nuti. 1992. Experimental conditions may affect reproducibility of the β-galactosidase assay. *FEMS Microbiol. Lett.* 100:87-90.

122. Lockard, R. E. and A. Kumar. 1981. Mapping tRNA structure in solution using double-stranded-specific ribonuclease V1 from cobra venom. *Nucleic Acids Res.* 9:5125-5140.

123. Lowman, H. B. and D. E. Draper. 1986. On the recognition of helical RNA by cobra venom V1 nuclease. *J. Biol. Chem.* 269:5396-5403.

124. Ringquist, S., S. Shinedling, D. Barrick, L. Green, J. Binkley, G. D. Stormo, and L. Gold. 1992. Translation initiation in *Escherichia coli*: sequences within the ribosome-binding site. *Mol. Microbiol.* 6:1219-1229.

125. Sussman, J. K., E. L. Simons, and R. W. Simons. 1996. *Escherichia coli* translation initiation factor 3 discriminates the initiation codon *in vivo*. *Mol. Microbiol.* 21:347-360.

126. Farwell, M. A., M. W. Roberts, and J. C. Rabinowitz. 1992. The effect of ribosomal protein S1 from *Escherichia coli* and *Micrococcus luteus* on protein synthesis *in vitro* by *E. coli* and *Bacillus subtilis*. *Mol. Microbiol.* 6:3375-3383.

127. Cronan, J. E., Jr. 1997. In vivo evidence that acyl coenzyme A regulates DNA binding by the *Escherichia coli* FadR global transcription factor. *J. Bacteriol.* 179:1819-1823.

128. Steward, K. L. and T. Linn. 1992. Transcription frequency modulates the efficiency of an attenuator preceding the *rpoBC* RNA polymerase genes of *Escherichia coli*. *Nucleic Acids Res.* 20:4773-4779.

129. King, T. C., R. Sireschmukh, and D. Schlessinger. 1986. Nucleolytic processing of ribonucleic transcripts in prokaryotes. *Microbiol. Rev.* 50:428-451.

130. Robertson, H. D. 1982. *Escherichia coli* ribonuclease III cleavage sites. *Cell* 30:669-672.

131. Shimotsu, H. and D. J. Henner. 1984. Characterization of the *Bacillus subtilis* tryptophan promoter region. *Proc. Natl. Acad. Sci.U. S. A.* 81:6315-6319.

132. Jones, P. G., M. Mitta, Y. Kim, W. Jiang, and M. Inouye. 1996. Cold shock induces a major ribosomal-associated protein that unwinds double-stranded RNA in *Escherichia coli. Proc. Natl. Acad. Sci. U. S. A.* 93:76-80.

133. Jones, P. G. and M. Inouye. 1994. The cold-shock response--a hot topic. *Mol. Microbiol.* 12:811-818.

134. Lee, S. J., A. Xie, W. Jiang, J. P. Etchegaray, P. G. Jones, and M. Inouye. 1994. Family of the major cold-shock protein, CspA (CS7.4), of *Escherichia coli,* whose members show a high sequence similarity with the eukaryotic T-box binding proteins. *Mol. Microbiol.* 11:833-839.

135. Jones, P. G., R. A. Van Bogelen, and F. C. Neidhardt. 1987. Induction of proteins in response to low temperatures in *Escherichia coli. J. Bacteriol.* 169:2092-2095.

136. Goldstein, J., N. S. Pollitt, and M. Inouye. 1990. Major cold-shock protein of *Escherichia coli. Proc. Natl. Acad. Sci. U. S. A.* 87:283-287.

137. Jiang, W. N., Y. Hou, and M. Inouye. 1997. CspA, the major cold- shock protein of *Escherichia coli*, is an RNA chaperone. *J. Biol. Chem.* 272:196-202.

VITA

Steven P.Solow

Steven Solow was born in Boston, MA on July 26, 1970. He received a B. A. in Chemistry with a Specialization in Biochemistry from the Univerisity of Virginia in 1992. After completing a three month internship at Biotechnology Research Institute in Bethesda, MD, he entered the graduate program of the Department of Biochemistry at Virginia Polytechnic Institute and State University. Working under Dr. Timothy J. Larson, he received a Ph.D. in April of 1997.